The final report on the growth and dynamics of *Ensis directus* in the near coastal zone off Egmond, in relation to environmental conditions in 2011-2012.

Rob Witbaard, Gerard Duineveld, Magda Bergman

NIOZ report 2013-2
NIOZ, Postbus 59, 1790AB Den Burg Texel, Nederland

Commissioned by:
Foundation La Mer
Postbus 474
2800 AL Gouda

Colophon

Report number:	NIOZ report 2013-2.
Published by:	Foundation La Mer.
Referentienummer	LM-006588.
Date:	2 April 2013.
Authors:	R. Witbaard, G.Duineveld, M.Bergman.
Title:	The final report on the growth and dynamics of *Ensis directus* in the near coastal zone off Egmond, in relation to environmental conditions in 2011-2012.
Project name:	La Mer long Deploy.
Commissioned by:	Foundation La Mer Postbus 474 2800 AL Gouda.
Programme:	Monitoring and Evaluation Programme Sand mining RWS LaMER, part B5-2 of the evaluation programme Sand mining (Ellerbroek e.a. 2008). Monitoring and Evaluation Programme Sand mining Sand engine.
Partners	Foundation La Mer Rijkswaterstaat Project realization Sand engine.
Supervised by:	Marcel Rozemeijer (IMARES) Saa H. Kabuta (RWS-WD) John de Ronde (Deltares) Johan de Kok (Deltares) Rik Duijts (RWS-DNZ) Sarah Marx (RWS-WD).
Executed by:	NIOZ Netherlands Institute for Sea Research Landsdiep 4 1797 SZ Den Hoorn (Texel) Nederland.

Tasks:	
Analyses & Reporting	Rob Witbaard, Gerard Duineveld, Magda Bergman.
Lab work organization	Rob Witbaard, Magda Bergman.
Logistics	Rob Witbaard, Magda Bergman.
Lab Work	Hans Witte, Evaline van Weerlee, Joost van der Hoek.
Field work	Crew Terschelling, Crew Pelagia, Crew Navicula, Rob Witbaard, Gerard Duineveld, Magda Bergman, Hans Witte, Job ten Horn, Evaline van Weerlee, Carola van der Hout, Selma Ubbels, Charlotte Soul, Joost van der Hoek, Roald ter Heide.
Project management	Rob Witbaard, Magda Bergman.

To be quoted as: Witbaard R., G.C.A. Duineveld & M. Bergman (2013). The final report on the growth and dynamics of *Ensis directus* in the near coastal zone off Egmond, in relation to environmental conditions in 2011-2012. NIOZ report 2013-2, 79pp.

CONTENTS

1 INTRODUCTION

1.1 Background

Continuous efforts to protect the Dutch coastline from erosion require large amounts of sand to be annually supplied onto the coastline (year 2010: > 12 million M³). Traditionally sand is supplied on to the beaches but since 1997 beach nourishment is alternated with underwater replenishment at the shoreface. With latter method large amounts of sand are dumped in front of the beach. Apart from the fact that this method is logistically less complex, it also aims at a promotion of the natural processes to reinforce the beach and dunes.

In the meantime a large portion of the coastal zone has been designated as an area of conservation in the framework of inter- and national agreements (NATURA 2000, Natuurbeschermingswet, http://www.noordzeenatura2000.nl/), because of its ecological value for birds and fish. Especially the abundant bivalves form a basic food source of overwintering birds. Over the past 15 years, a doubling has taken place in the total standing stock of bivalves in the Dutch coastal zone. While in the 1990's, *Spisula subtruncata* was the most abundant species occurring in dense aggregations, nowadays the invasive American razor shell, *Ensis directus*, dominates the biomass (Figure 1)(Goudswaard et al, 2011).

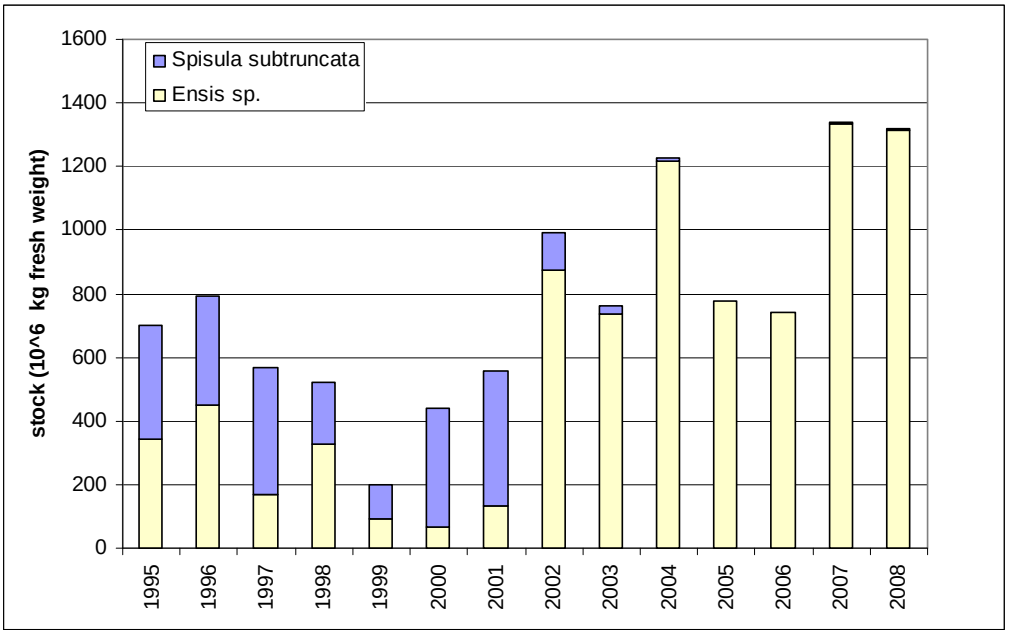

Figure 1. Standing stock of *Spisula subtruncata* and *Ensis directus* in the Dutch coastal waters in the period 1995-2008 (not published data IMARES) based on yearly stock assessments with modified hydraulic dredge or trawled dredge; sampling efficiency for *E. directus* is estimated at 50%) (Craeymeersch,Perdon,Goudswaard, unpublished)

The presently known standing stock of *Ensis directus* is substantially higher than previously reported estimates of bivalve biomass. Because *E. directus* rapidly retracts itself deep in the sediment, accurate density estimates are difficult. Moreover a significant number of *E. directus* lives in the shallow shoreface at depths which are difficult to access with ships which can use gear to sample this species quantitatively. Densities are, therefore, likely even higher (Figure 2).

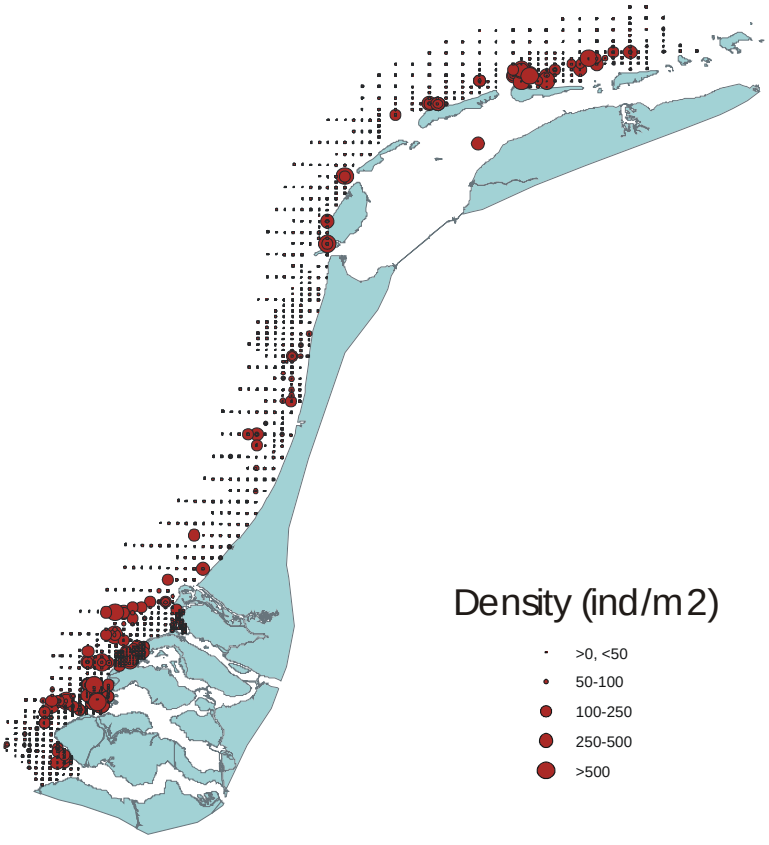

Figure 2 Spatial distribution and density (ind/m²) of *Ensis spp*. in the Dutch coastal waters in the period 1995-2008 (not published data IMARES) based on yearly stock assessments with modified hydraulic dredge or trawled dredge; densities not corrected for 50% sampling efficiency) (Craeymeersch, Perdon, Goudswaard, unpublished).

Shoreface depostion of sand can directly harm bottom organisms that are normally dependent on contact with the overlying water (worms, bivalves) though some species survive burial to some extent (polychaete *Lanice*). With the sand, a small percentage of silt is released. Percentages silt in sediment off the coast vary between 0 and ~4%. Tides transport this material and thereby potentially cause an effect over a larger area than the dumping plot (e.g. van Duin e.a., 2007). This in contrast to underwater shoreface replenishements which is likely to have a significant effect on a local scale because of burial and smothering of the original bottom surface with it's fauna.

1.2 Questions

In chapter 6 of the evaluation program of the MER (Ellerbroek et al, 2008) several knowledge gaps which were identified and outlined. These deal with the distribution of SPM (Suspended matter), negative "Far field" effects of increased SPM concentrations on primary production and effects of the increase of SPM in relation to natural conditions as well as its effect on the disturbance of spatial and temporal distribution of species.
In more detail the Monitoring programme RWS LaMER research program focuses on:

(1) What are the effects of the reduced food conditions on the growth of *E. directus*
(2) When does food limitation occur as a result of these changed conditions?

Many filter-feeding invertebrates (bivalves and polychaetes) show a depressed filtration activity and growth rate in the presence of large concentrations of suspended silt (Wilber & Clarke 2001,

Archambault et al 2004). The bivalve species inhabiting the Dutch coastal zone (e.g. *Ensis directus*, *Macoma baltica*, *Tellina tenuis*) have to cope with natural high concentrations of silt. Longshore SPM transport in a narrow strip along the Dutch coast (Anonymous, 2002) is estimated to be in the order of 10 to 20 million tons per year (Van Alphen, 1990; De Kok, 2004) but this is most likely an underestimate. Nevertheless, preliminary laboratory experiments showed that *Ensis directus* show depressed clearance rates under high silt concentrations (>200mg/l) (Witbaard & Kamermans 2011).

Thus, as *Ensis directus* nowadays plays an important ecological role in the coastal "protected" zone more insight into determinants of the feeding behaviour and growth of this species is especially important to assess and validate effects of increased SPM concentrations caused by shoreface and beach nourishment or sand extraction elsewhere.
To obtain such insights, we deployed a measurement platform (lander) at 10m water depth off Egmond equipped with a sensor package (Turbidity, Chlorophyll, Temperature, Salinity, Current) and a monitor recording the gape of multiple individuals of two bivalve species (*Ensis directus*, *Mytilus edulis*). More specifically we asked the following questions in this particular study:

1. What is the natural variation in silt concentrations close to the seabed
2. What is the forcing factor of this variation (erosion, advection, season)
3. Is the valve gape of *Ensis directus* related to the silt concentration and how (linear, stepwise) if not which other factors control the gape of *Ensis*.
4. Describe the growth of Ensis *directus* in terms of DEB variables.
5. What factors correlate the best with DEB growth variables of *Ensis directus*

The research and results presented here consists of two parts. One part deals with assessment of natural variation in environmental conditions close to the seafloor continuously measured with abovementioned autonomous measurement (lander) platform. The other part deals with *in situ* sampling of the local *Ensis directus* population with the aim to follow timing of growth, reproduction and follow population development.
In the end, the data obtained from this field monitoring off shore Egmond (2010, 2011 and 2012) will be used to develop, calibrate and validate a DEB (Dynamic Energy Budget) model for *E. directus* (Wijsman e.a., 2011, Kamermans e.a. 2011, Cardoso e.a. 2011, Cardoso e.a., 2006, Cardoso e.a. 2009, Schellekens & Witbaard, 2012).
As a next step, the coupling of the DEB model with the Delft 3D (e.g. Schellekens 2012) water quality model will provide a useful management tool to assess the effects of beach nourishments and sand extraction on the level of individual organisms and populations and the potential effects on secondary production by *Ensis directus*. This latter work has been presented by Schellekens and Witbaard (2012).

This research represents the results of section B5-2 of the evaluation programme of Ellerbroek e.a. (2008). The Monitoring and Evaluation Programme Sand mining Sand engine participates in this programme to fulfil their monitoring requirements on monitoring the impact of sand mining on silt and the impact of extra silt and reduced food conditions on the growth of *E. directus.* The literature mentioned in this report by far not covers all aspects of the research field, nor does this report give a literature review. Because of time limitations, we focussed on the presentation and interpretation of the results obtained exclusively within the project itself.

2 METHODS

2.1 Lander Deployments

At about one kilometer off the coast of Egmond a lander platform was placed at a depth of 11 meter Figure 3, table 1).

Table 1. Positions of and around the central lander position at where boxcore samples are taken to follow the seasonal development of sediment grain size and to follow the wax and wane of the local *Ensis directus* population.

station	gr min dec min N	gr min dec min E	gr dec gr N	gr dec gr E
LNE (Lander North East)	52° 38.28'	4° 36.356'	52.6380°	4.605933°
LSE (Lander South East)	52° 38.216'	4° 36.380'	52.6369°	4.606333°
LSW (Lander South West)	52° 38.22'	4° 36.22'	52.6370°	4.603667°
LNW (Lander North West)	52° 38.281'	4° 36.22'	52.6380°	4.603667°
Lander	52° 38.249'	4° 36.294'	52.63748°	4.6049°

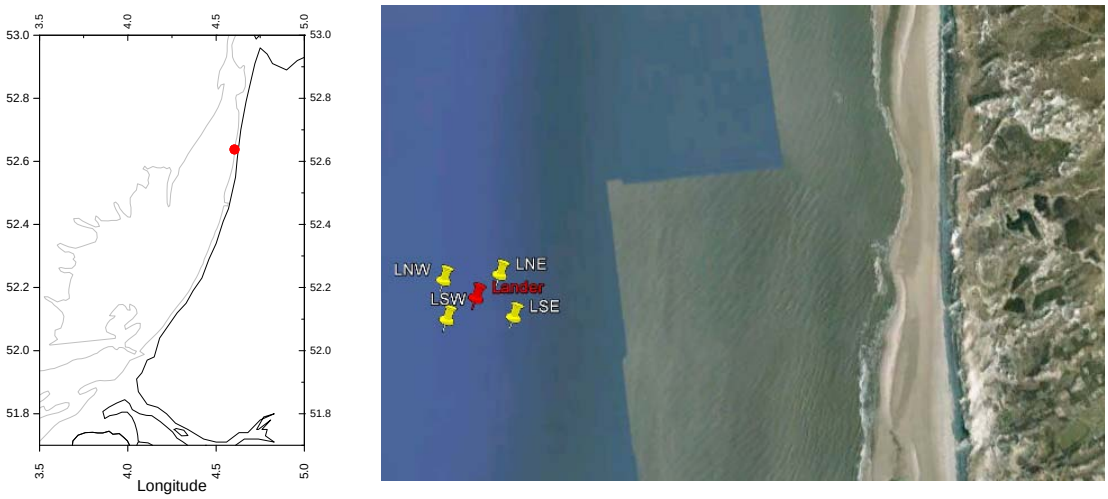

Figure 3. Position of the lander and the four surrounding stations off the coast of Egmond. The distance of the location is about 1 km from the coast. The left panel gives the position (red dot) in relation to the coast of the provinces of North- and South Holland.

The lander platform consists of an triangular aluminium frame (Height Width: 2 x 2 m) with a series ballast weights (total 500 kg) fixed onto the lower support that stands on the seafloor. In this way the center of gravity is lowered as much as possible preventing the platform from falling over during storms. On top of the platform is a pop-up system with a 50-m rope connected to 40 kg floatation. The pop-up is triggered from the surface by 2 acoustic releasers (http://www.ixsea.com/). The platform carries 1 closeable mesocosm. This mesocosm is opened (and closed) by means of sliding top valves activated with hydraulics. The hydraulics are operated by an ALTRAP pump (Figure 4).

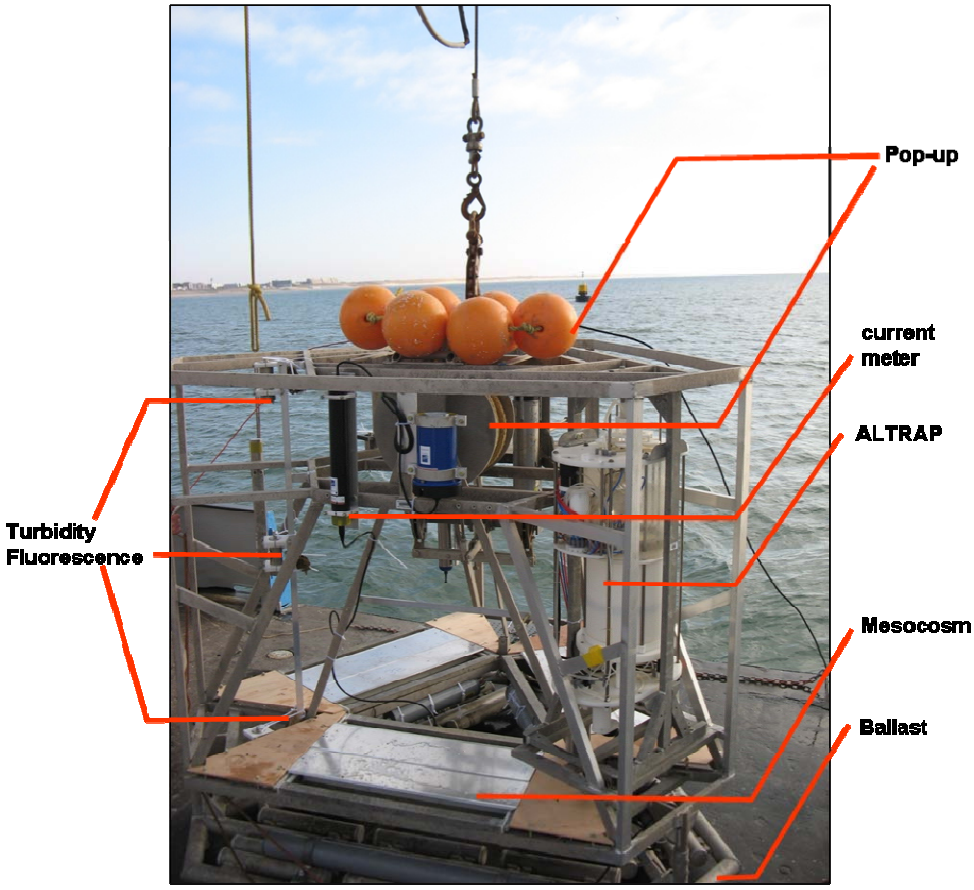

Figure 4. Overview of one the lander frames used in the environmental monitoring off the coast of Egmond in 2011.

Before deployment of the lander, the mesocosms are closed this to prevent sediment to be washed out from the containers carrying live *Ensis directus*. At the planned end of the deployment the mesocosm is kept open as sediment loss at this moment is not important as valve gape monitoring will be stopped once the lander comes on deck.

The platform carried 2 gape monitors. Each monitor is simultaneously measuring the gape of 7 bivalves with a frequency of 1/60 Hz (T=0.016 $s^{-1)}$. The gape size is measured by means of the inductive current generated through a pair of micro-coils which are glued to the valves (Figure 5). One gape monitor was connected to 7 Mussels (*Mytilus edulis*) that were attached to the underside of a PVC plate. The PVC plate was bolted onto the platform at 30 cm above the sediment. The second gape monitor was connected to 7 specimens of *Ensis directus* that were contained in sand filled cylinders in one of the mesocosms (Figure 6). Both gape monitors had one blank sensor to be used as a control signal.

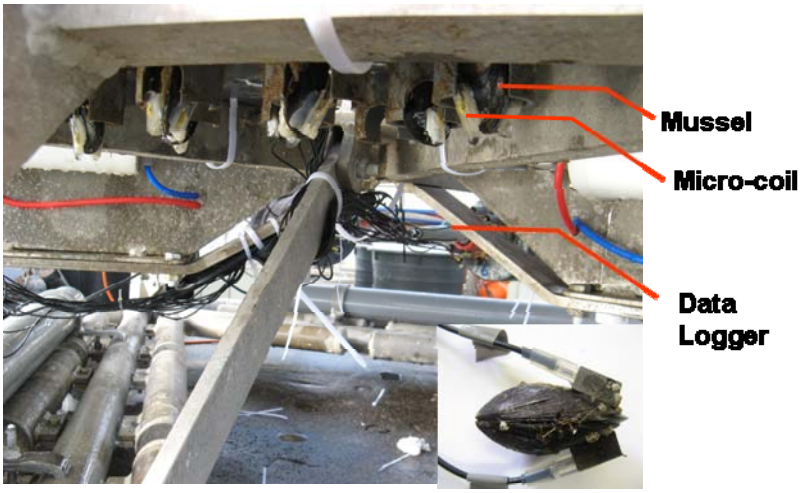

Figure 5. Detail picture of the valve monitor with attached mussels, hanging at 30 cm above the seafloor. Mussels pointing down wards in half open cups in which they can attach themselves.

Figure 6. Placement of sediment cores with live *Ensis directus* connected to a valve monitor in one of the trays which are mounted on the lander.

The lander platform was furthermore equipped with a series of sensors measuring the following physical parameters: current, temperature, salinity, turbidity and fluorescence. Current speed and direction (3D) were measured every 10 min at 140 cm above the bottom with a NORTEK Aquadopp Doppler current meter. This instrument also yielded a record of the acoustic backscatter. Temperature and Salinity were measured every 10 min with a pumped version of the Seabird SM37 CTD system (http://www.seabird.com/). The CTD sensors are protected from effects of fouling by the presence of a TBT impregnated plastic ring inside the dead volume of the pump.

In addition to the NORTEK Aquadopp current meter a NORTEK Vektor current meter (http://www.nortek-as.com/) was mounted at the lander at a height of 30 cm above the bottom. Every 10 minutes this instruments made high frequency burst measurements during 2 minutes with a frequency of 1/sec. Deltares takes care of detailed analyses of these Vektor data. Sensor “glasses” from both the Vektor and Aquadopp current meters were protected against fouling by applying a light veneer of udder ointment.

Turbidity and fluorescence were measured optically at four heights above the bottom, i.e. 30, 80, 140 and 200 cm, using ALEC Compact-CLW’s (http://ocean.jfe-advantech.co.jp) with wipers

to keep fouling under control. The measurement at the lowest height (30cm) was done with the infinity version of the instrument as it can deal with higher turbidity. The wiped versions appeared all to be crucial for obtaining optic records in coastal environments with heavy fouling. All Alec sensors have been calibrated in the lab over a range of local SPM and Chlorophyll concentrations. In this report we refer to the material being measured as turbidity as SPM. The fluorescent part of it, and simultaneously measured is referred to as Chlorophyll or Chl-a. During three deployment periods (May 3-31, June24-July12, Oct 25-Jan 11.) Deltares placed a LISST 100 (http://www.sequoiasci.com/) upon the lander frame to measure the particle size distribution of suspended material.

The platform was launched on 22/Feb/2011 with the RV Terschelling (RWS) (Figure 7). The position of the platform was marked by two buoys protecting it from trawling activity. In table 2 an overview of the deployment and retrieval dates is given.

Table 2. Deployment periods and dates of lander service as well as the used ships

Deployment nr/period	Date	Ship
1 week 08	22/02/2011	Terschelling
2 week 14	07/04/2011	Terschelling
3 week 18	03/05/2011	Terschelling
4 week 22	31/05/2011	Terschelling
5 week 25	24/06/2011	Pelagia
6 week 28	12/07/2011	Terschelling
7 week 31	02/08/2011	Terschelling
8 week 34	23/08/2011	Terschelling
9 week 39	27-28/09/2011	Terschelling/Pelagia
10 week 43	25/10/2011	Terschelling
11 week 02	11/01/2012	Terschelling
12 week 09	29/02/2012	Terschelling
13 week 13	27/03/2012	Terschelling
14 week 18	02/05/2012	Terschelling
15 week 21	24/05/2012	Terschelling
16 week 25	18/06/2012	Pelagia
17 week 30	26-27/07/2012	Terschelling//Navicula
18 week 41	08/10/2012	Terschelling
19 week 47	24/11/2012	Pelagia

Figure 7. Deployment of one of the lander platforms off the coast of Egmond.

In spring and autumn the platform is retrieved for maintenance and data collection every 5th or 6th week. During the summer the platform is retrieved every third week to prevent problems and minimize the effects of fouling by barnacles and other epifaunal organisms. For most of these 1 day maintenance cruises the RWS ship Terschelling has been used. This with the exception of two times when RV Pelagia or RV Navicula had been used for these operations (See table 2).

2.2 Valvometry

During every deployment period two valve monitors were mounted on the lander frame. The first valve monitor hosted 7 live mussels (*Mytilus edulis*) (Figure 5), the second valve monitor hosted 7 *Ensis directus* (Figure 6). The average start size of the mussels was 39 mm and the size of the *Ensis directus* used was approximately 115 mm. Of each bivalve the valves were attached to sensors on basis of which the relative gape distance could be measured and monitored. Measurement frequency in both instances was 1/minute (T=0.016). Of each valve monitor the 8th channel was used as control on the electronics, i.e. no bivalve was attached. The experimental *Mytilus edulis* were hang in cavities at the underside of a pvc plate which on its turn was mounted on the lander. This was done to prevent the accumulation of sedimenting mud and sand which could smother the animals. The *Ensis directus* were placed in pvc tubes which were hosted in a tray like construction. During deployment of the lander this tray was closed with a lid which would open at a pre-programmed time i.e. once the lander was on the seafloor. This was done to prevent that the substratum in the tubes which hosted the animals was being washed out. The height at which both valve monitors were placed on to the lander was within the measuring range of the lowest placed turbidity sensor, i.e. 30-45 cm. As far as possible, the same animals were used again in following deployment periods.

2.3 Boxcore sampling

During each service operation two boxcore samples at each of the four corner locations around the (central) lander platform position were taken (see table 1; LSE, LSW, LNE, LNW). If the

boxcore sample was of sufficient quality a subcore for sediment grain size analyses was preserved. These samples have been split into two layers of 5 cm height and kept frozen until freeze dried. The remainder of the boxcore was sieved over a 1 mm screen and the live *Ensis directus* were collected and stored for size measurements and ash free dry weight (AFDW) determination. In this way a time series of the growth and population development of the local *Ensis directus* stock is obtained on basis of population averages.
In addition to these samples additional boxcores were taken to collect at least 50 *Ensis directus* individuals for determination of the seasonal change in gonado-somatic index and change in glycogen and energy reserve content (caloric content). On board all samples were stored refrigerated. In the analyses of shell growth, data collected during the pilot study in 2010 and those collected during cruises for the MEDUSA project since 2009 were used as well.

2.4 Lab procedures

2.4.1 Sediment grain size analyses.

A Beckman Coulter LS 13 320 (https://www.beckmancoulter.com) has been used for the sediment grain size analyses of samples collected at each of the four sampling stations. The apparatus works according to the principle of laser diffraction. The range of grain sizes which can be measured runs from 0.4 to 2000 µm in 132 size bins.
Analyses were performed on untreated samples which implies that before analyses, the samples were only freeze dried. Thus none of the samples were treated with acid nor oxidized with H_2O_2. Samples neither underwent a ultrasonic treatment. This to obtain individual (natural) particles without breaking them into the units from which they are composed.
The freeze dried sample was homogenized and a subsample was taken for the actual analyses. This subsample was sieved over a 2 mm screen to remove large particles. The subsample was transferred into a measurement tube and water was added. This sample was shaken for 30 seconds to obtain a sediment water suspension. This material was used for the ultimate grainsize determination. In case the sample contained too much fine material which caused obscuration, the analyses was repeated with a smaller subsample. From the results the median grain size and vol % particles <64µm are presented. Only the top 5 cm layer of the samples has been analysed.

2.5 Population development and average individual growth.

To determine seasonality of shell growth, tissue growth and gonad development the *Ensis directus* population around the lander was followed by collecting the living animals from (additional) boxcore samples taken at the four stations around the lander taken at each of sampling dates. All living animals were routinely measured with digital callipers. Three measurements were made, length, width and thickness. Together with these size measurements the ash free dry weight (AFDW) was determined in the lab. For this, the soft tissue was removed, dried at 60°C until constant weight and then incinerated at 540°C during 4 hours. The weight difference of dry weight and ash-weight is the ash free dry weight.

2.5.1 Weights-Gonado somatic index.

In addition to above sampling extra individuals were collected. In the lab a selection of 50 individual of different size classes from the entire size range was made. From these animals the

shell size (length, width and thickness) were measured as well as their wet weights. There after gonads were separated from the somatic tissue and after drying both fractions were incinerated to obtain the ash free dry weights of both types of tissue separately. These weights were used to calculate the contribution of the gonadal mass in the total weight of the animals. Based on these determinations and the collection of data over the seasons, the change in gonadal mass over the season could be determined.

2.5.2 Glycogen analyses / Caloric content.

On each sampling date 10 living animals were taken. Soft tissue was removed from the shell and frozen at -80°C. After freezing the tissue was freeze dried. Before analyses the freeze dried samples were homogenized and grinded until a fine powder was left. This material was split into two fractions. One fraction to be used for the glycogen content and the other fraction for energy content in a bomb calorie analyzer. This means that for most animals collected for above purposes both the caloric content as well as the glycogen content could be determined. For samples which had been collected before 2011 these analyses were not performed.

2.5.3 Caloric content.

Caloric content has been measured with a C2000 IKA bomb calorimeter (www.ika.com). From the homogenized sample ~0.5 gram of material is pelleted. This pelleted material is burned completely in an oxygen atmosphere at a pressure of 30 bar. The heat produced is determined and a measure for the energy content of the sample. The energy released by the combustion is recalculated to energy content per gram sample. The energy content of the sample depends on the composition of the sample (relative amounts carbohydrates, fat and proteins). Thus if there are seasonal variations in the body composition of the animal tissues, they can be observed as seasonal variations in the caloric content of the combusted tissues.

2.5.4 Glycogen content.

Glycogen content has been determined according to the method of Keppler and Decker originally published in 1970 and adjusted in 1974 (Keppler & Decker, 1970; 1974). It is an enzymatic/colourographic method. Glycogen present in the sample is first hydrolyzed to glucose. This glucose is enzymatically transformed into glucose-6-P-dehydrogenase into 6-fosfogluconolacton. In this reaction NADPH is formed which is spectro photometrically determined at a wavelength of 340 nm. A calibration line was used to recalculate the observed extinction values into concentrations. Analyses took place in batches of 20 samples. The calibration line was determined on basis of pure mussel tissue glycogen. Average sample weight for each determination was approximately 40 mg.

3 RESULTS.

3.1 Population development *Ensis directus*

For the period between 10/03/2010 up to 24/11/2012 the mean density of *Ensis directus* around the lander is 200 individuals/m². If only the 2011 and 2012 data are used, the average density is 140 individuals/m². The variation between samples taken at different sites, stations and dates is large (Table 3). The average densities at the southern stations (LSW and LSE) are higher than at the northern stations.

Table 3. The average densities per station (n/m²) and sampling date are given. The average density at the southern station differs significantly from both northern station (LNW –LNE). (Tukey HSD pairwise comparison, $p<0.05$). Letter codes refer to sampling locations around lander. LNW=lander North West, LSW=Lander South West, LNE=Lander North East, LSE=Lander south East. Avg=Average, Stdev=Standard deviation.

Date	LNE	LNW	LSW	LSE	Avg	Stdev
10/03/2010	525	243	614	499	470	159
06/04/2010	371	397	704	602	518	161
26/04/2010	282	550	371	358	390	114
15/07/2010	166	461	128	166	230	155
12/08/2010	179	346	525	218	317	156
31/08/2010	294	333	166	384	294	93
13/09/2010	166	154	179	333	208	84
13/10/2010	128	154	243	410	234	127
29/10/2010	64	205	218	192	170	71
23/12/2010	77	269	410	269	256	137
22/02/2011	122	147	582	442	323	226
07/04/2011	179	237	314	320	262	67
03/05/2011	64	109	70	109	88	24
31/05/2011	429	77	314	224	261	149
24/06/2011	64	141	83	147	109	41
12/07/2011	173	77	243	166	165	68
02/08/2011	102	134	525	186	237	195
23/08/2011	211	186	186	147	182	26
28/09/2011	122	154	307	186	192	81
25/10/2011	70	134	64	77	86	32
11/01/2012	128	70	122	147	117	33
29/02/2012	86	86	128	73	93	24
27/03/2012	78	83	102	141	101	28
02/05/2012	37	38	93	81	62	29
24/05/2012	58	38	109	38	61	33
18/06/2012	64	51	64	32	53	15
26/07/2012	26	26	77	64	48	26
09/10/2012	45	26	147	102	80	55
24/11/2012	102	115	32	70	80	136
Avg	152	174	246	213		
Stdev	124	134	189	148		

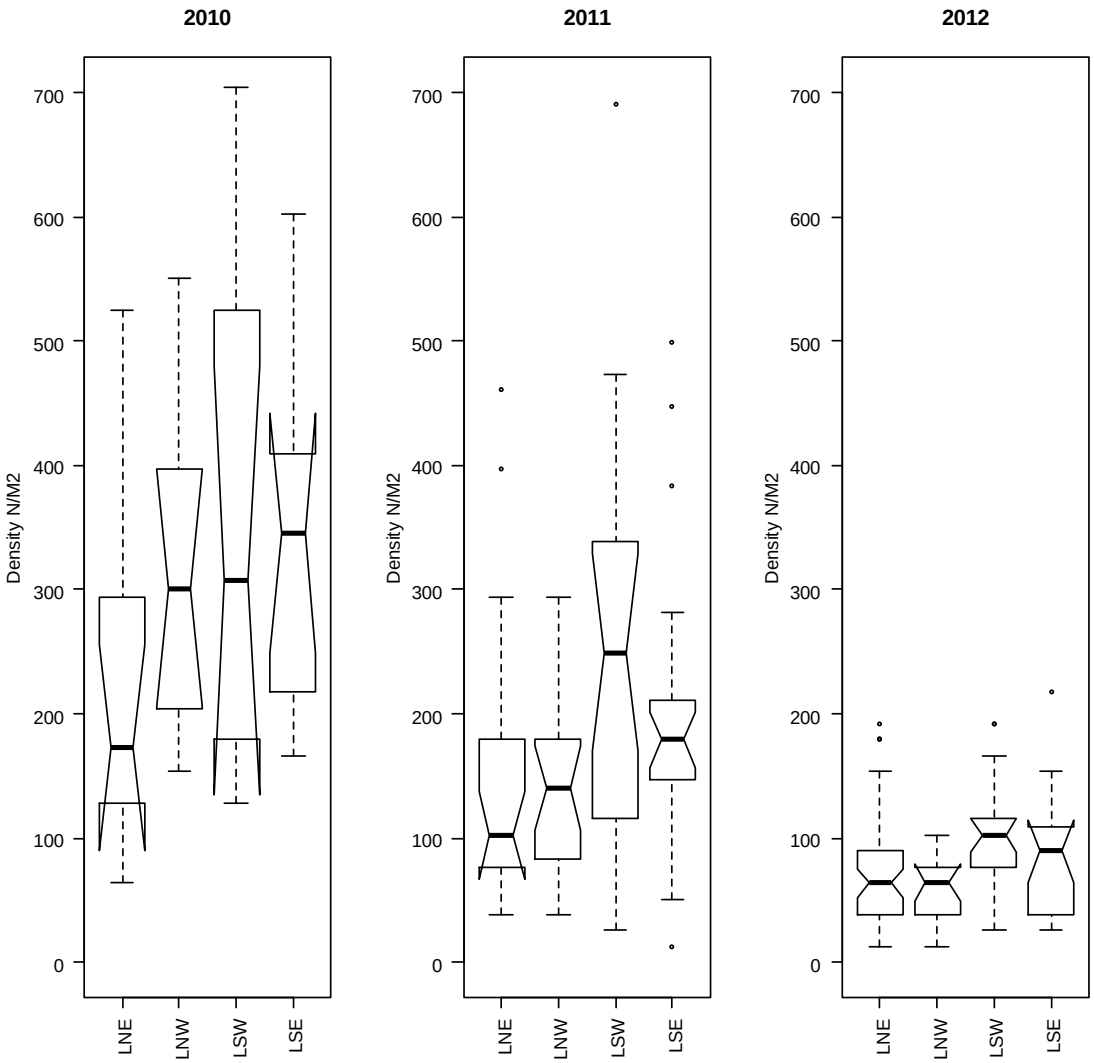

Figure 8. Notched Box and whisker plot of the densities of *Ensis directus* at the four stations around the lander position given by year. Non overlapping notches implies that there is a statistical significant difference in density. The figure illustrates the steady population decline of the local patch, without new cohorts settling.

To get a better insight in the variability of the density estimates, we changed the qualitative collection of animals to be used for condition parameters into a quantitative sampling in 2012. The animals collected for gonad determination, glycogen and caloric content determination were kept separate by boxcore to enable the estimation of average density with standard deviation of the densities on basis of a large number of boxcores from the same site. The results of this quantitative sampling (which is a subset of the results as given in (Table 3) are given in Table 4. Calculation of the Morisita's index of dispersion (Young & Young, 1998) over these series of boxcore samples gives values for the index which are smaller than those expected in case *Ensis directus* is distributed clumped. This finding suggests that this species is randomly to evenly distributed in the area and that the boxcore samples give reliable estimates of the local densities of *Ensis directus* in the area of study. On basis of the decrease in average density between March 2010 and Oktober 2012 the survival is estimated at 17%, i.e. 50% when recalculated over an annual time basis (Figure 9).

Table 4. Average density and standard deviation of *Ensis directus* in the area around the lander, measured on a large number of boxcore samples.

Date	Average density (n/m²)	Stdev	Number of boxcores
29/02/2012	91	47	10
27/03/2012	80	49	18
02/05/2012	60	48	16
24/05/2012	50	36	23
18/06/2012	58	39	24
26/07/2012	53	41	25
09/10/2012	67	42	15

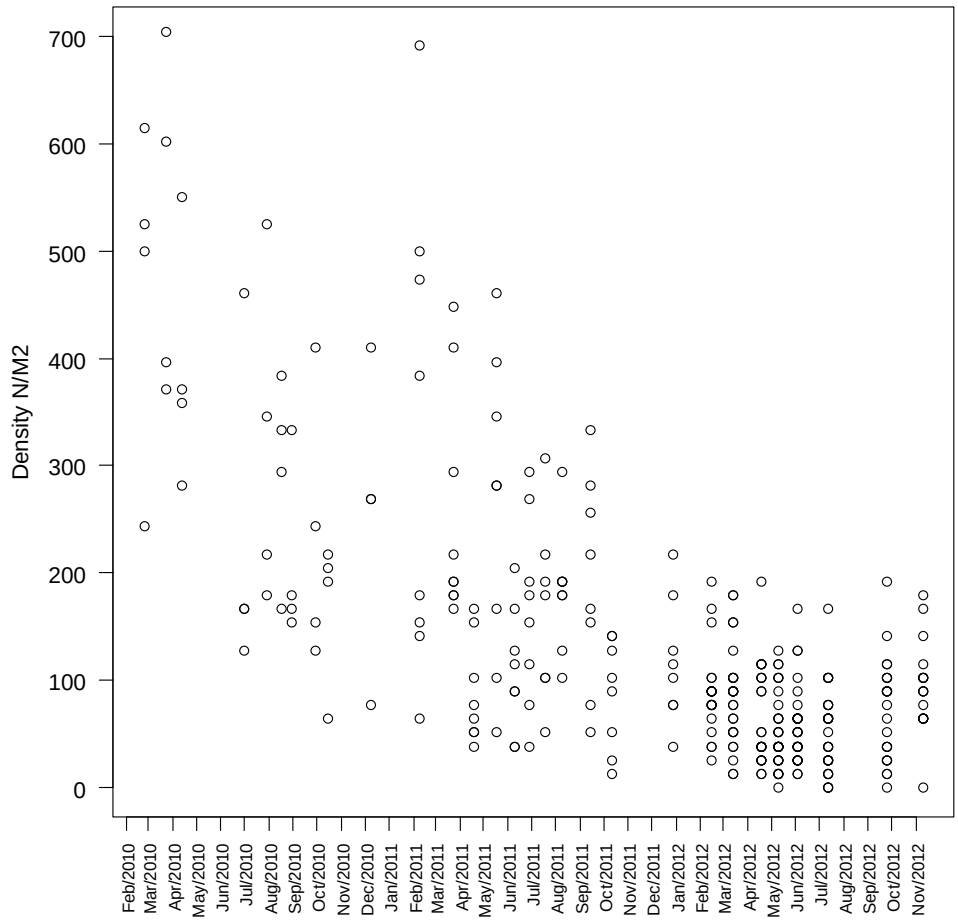

Figure 9. Densities of *Ensis directus* over time sampled at the locations around the lander (LSE, LSW, LNW, LNE).

This density difference between the two northern and the two southern locations (Figure 8) coincides with a small size difference between stations. This is illustrated in the notched box and whisker plots (Figure 10) which illustrates this size difference as non overlapping notches between the subsequent stations. When all samples at each of the four stations are pooled over all years the difference in shell lengths is non significant. If shell lengths are compared for only

the year 2010 shell lengths between station LSW and LNW differ from each other (Tukey HSD, p=0.02). In 2011 both southern stations differ from the northern stations although the difference for the combination LSE_LNW is only marginally. In 2012 the significance of above differences had gone. Although these observed size differences suggest that there are small spatial scaled differences in growth rates, they are not taken into account in the further analyses as none of the (a)biotic measurements were measured at that scale and given the dynamics of the processes taking place in the water phase it is unlikely that there will be differences in these characteristics (Salinity, Temperature, Current regime, Primary production) on this small scale. Hence the data obtained from the four locations have been interpreted as being the average response of the *Ensis directus* population around the lander location.

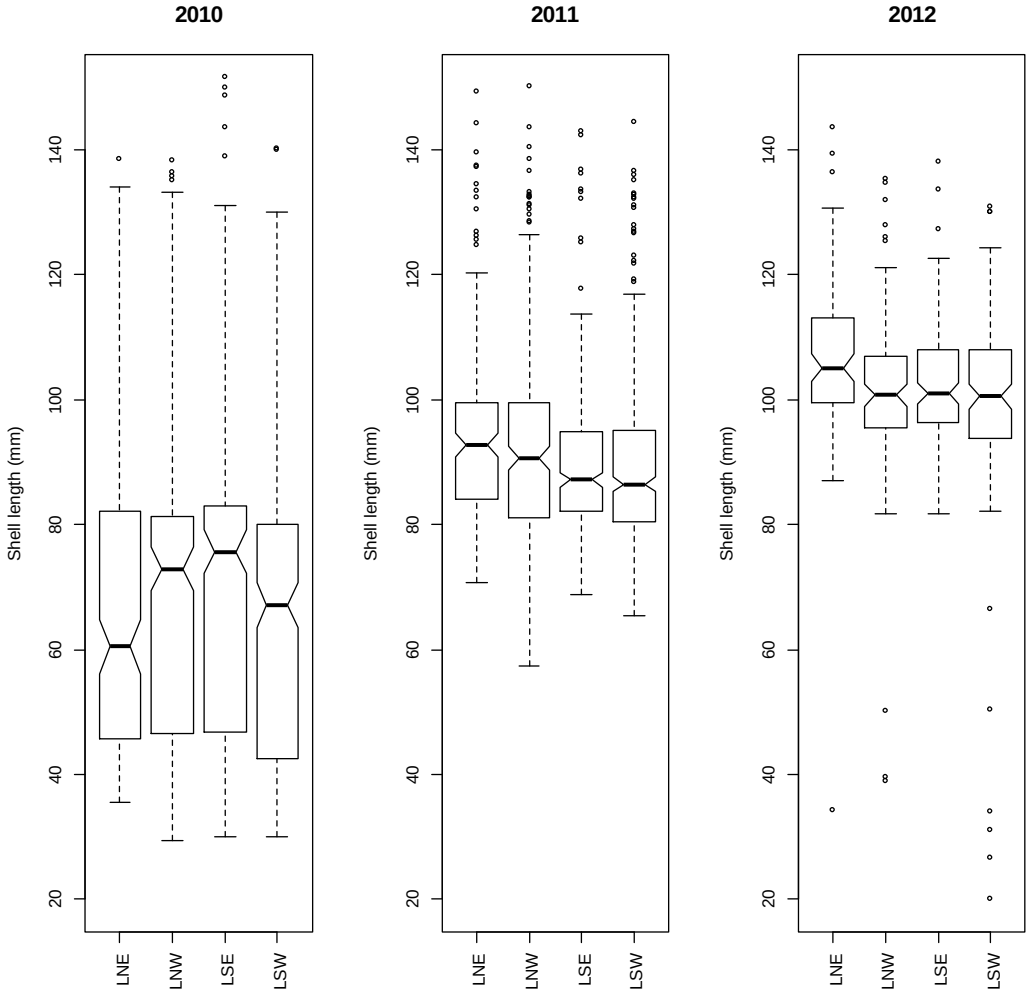

Figure 10. Boxplot of the shell lengths of *Ensis directus* collected around the lander in the three years of sampling.

Over the period that the population was sampled, shell size roughly increased from 45 mm to around 100mm length (Figure 11). Initially there was a bimodal size distribution in 2010. Later this bimodality got lost as depicted in Figure 12. In the end of 2012 low numbers of newly settled individuals appear. The temporal evolution of the shell size distribution around the lander for the year 2011 and 2012 is given in Figure 13

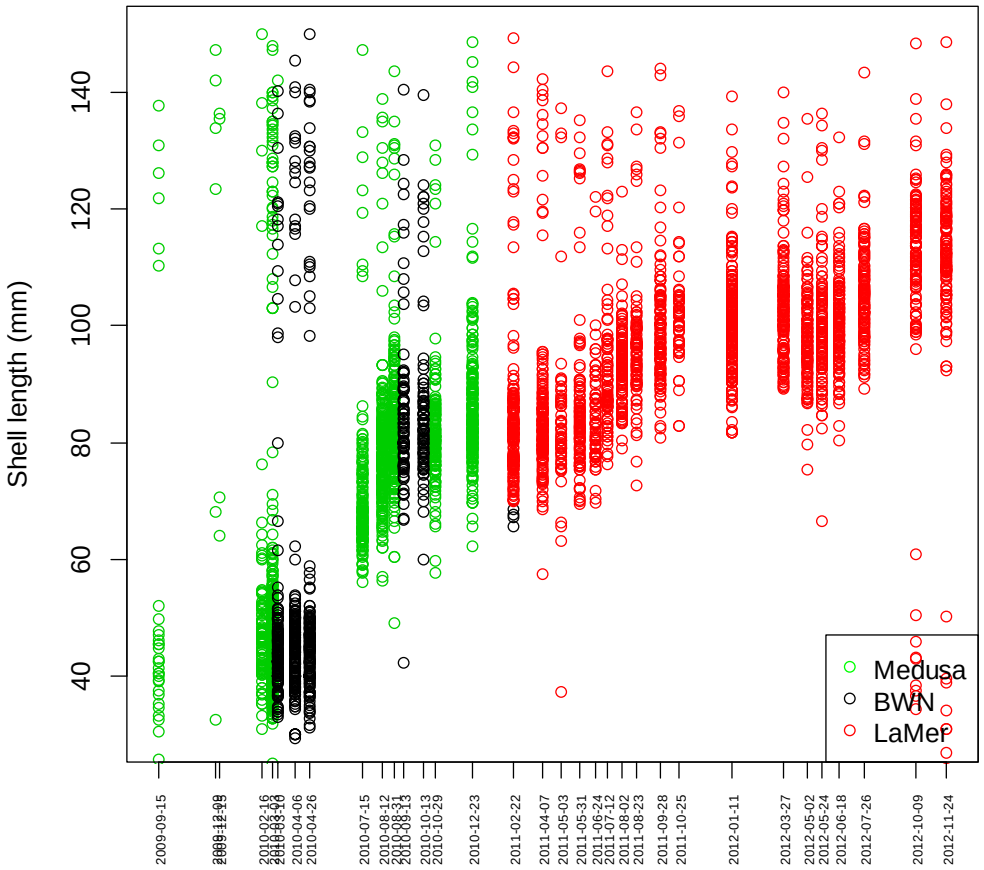

Figure 11. Shell size measurements of *Ensis directus* taken from boxcores in the area since September 2009. Data collected in three different research programs are indicated by colour. The samples were collected around the lander (2010-2012) and along a transect perpendicular to the coast (2009-2010). The LaMer study and the Medusa study were both financed by RWS and LaMer. The BWN study was embedded within Ecoshape a consortium of private dredging companies, research institutes and the national government.

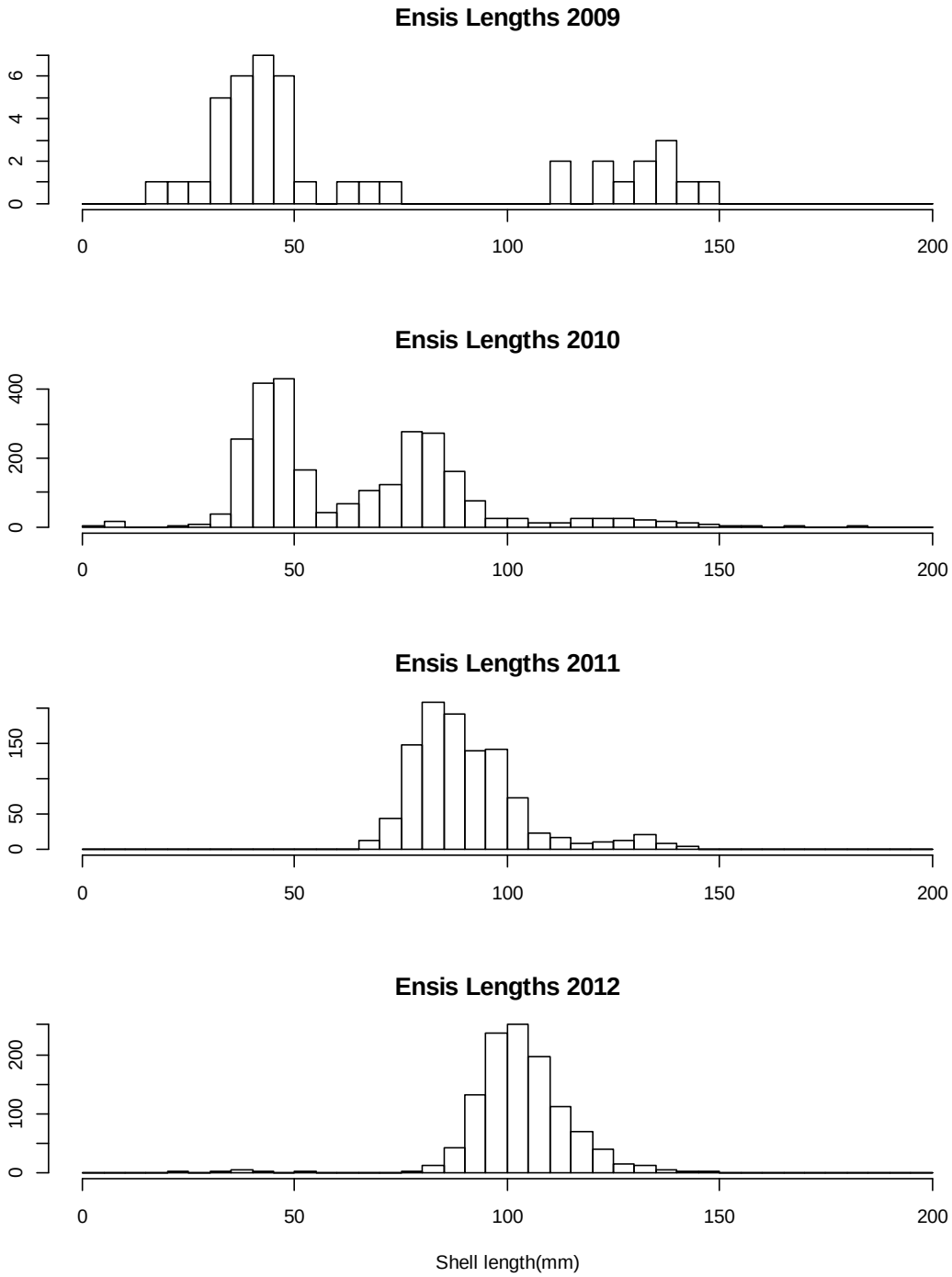

Figure 12. The average size distribution of *Ensis directus* collected around the lander location for each year separated. Samples originate from the four stations around the lander (LSW,LNW,LSE,LNE).

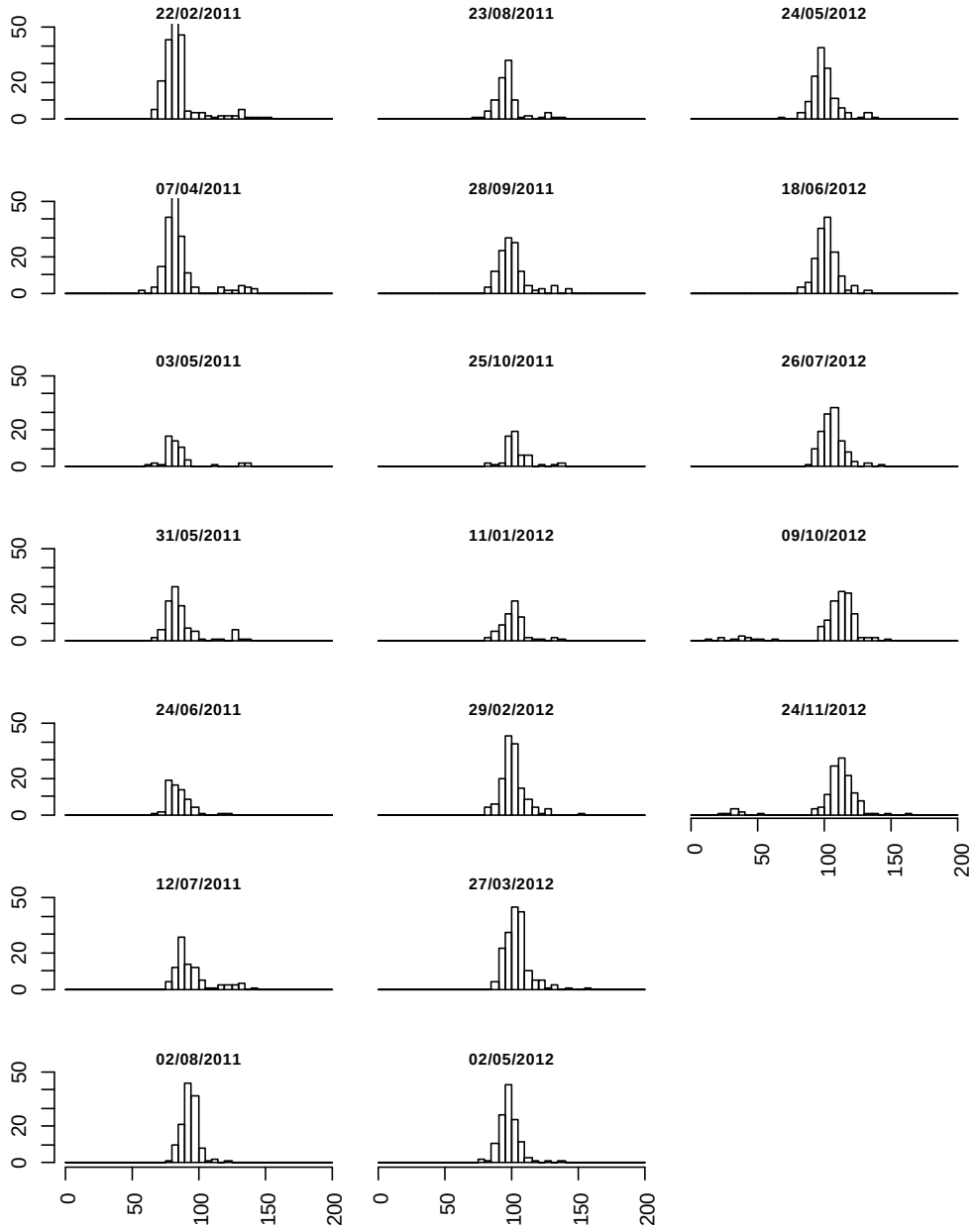

Figure 13. Size distribution of *Ensis directus* derived from samples which were pooled by collection date and location (Station). During the last two collection dates (09/10/12 and 24/11/12) low numbers of newly settled animals were found.

The pooled collection of samples (Figure 13) taken around the lander at each sampling occasion (n=8) is used to estimate shell growth over time in the field.

On basis of the average shell sizes per sample per location per date, shell growth rates could be estimated from the change in average length divided by the time (days) passed by. This shows (Figure 14) that maximum shell growth rates are about 0.3 mm/day and that these maximum rates are achieved in the summer months only. The trend of decreasing growth rates with time is caused by the fact that as the animals get bigger, their growth rates decrease. Although the model fit is significant the amount of explained deviance is small and analyses of the fit suggest that the model can be improved, i.e. residuals are not entirely normal distributed and still show a weak trend when plotted against the fitted values. One of the problems with the data is that

due to size dependent mortality (observation while sampling) average sizes sometimes tend to decrease, leading to negative shell growth rates.

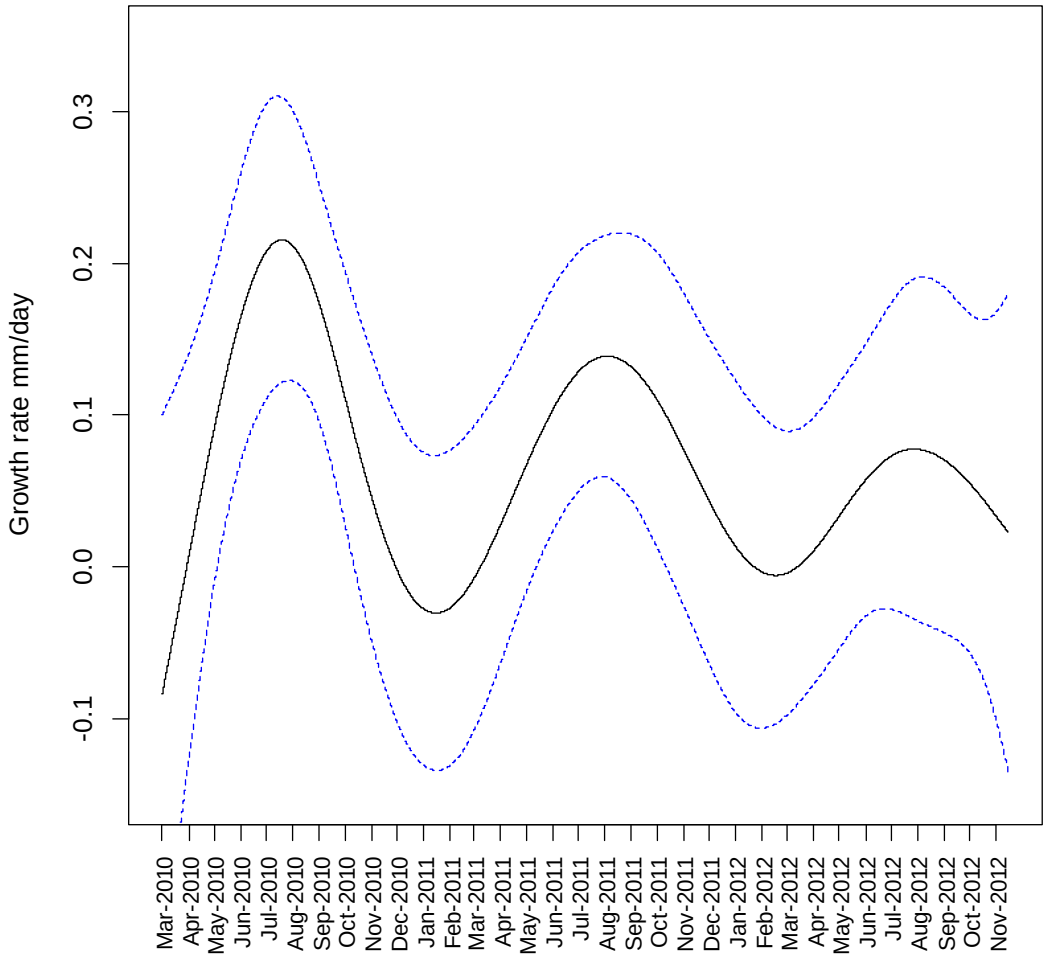

Figure 14. Shell growth (mm/day) at the stations around the lander, located off the coast of Egmond. Black line GAM estimate of shell growth (mm/day), blue dotted lines are the 2.5 percent significance levels around the estimate. The fitted smoother function (black line) is significant at p=0.03.

3.2 Weight and Condition and gonad development

3.2.1 Weight and condition

For each sampling date and from a subset of animals (50) the ash free dry weights (AFDW) of the somatic and gonadal tissues were determined separately. Plotting these (Figure 15) data shows that there is a strong seasonal trend in the development of both. The increase in the AFDW mainly takes place in spring. Because AFDW is linked to shell size (Figure 17) the seasonal change in condition index (Figure 16) might give a better estimate of the temporal evolution of tissue weights which is independent of shell size.

This shows that there is an increase of the condition index between April and June. The increase is greatest in spring. The best condition is found in the summer months. After mid July condition indices decrease. In Figure 15 the percentage of gonad tissue of the total ash free dry weight is given together with the total AFDW. The largest percentage of gonads was found in the beginning of May when 90 % of the dissected specimens had developed gonads and could be sexed (Figure 18). At the end of May the numbers of animals which could be sexed had decreased to about 50 %. This suggest that spawning takes place in May

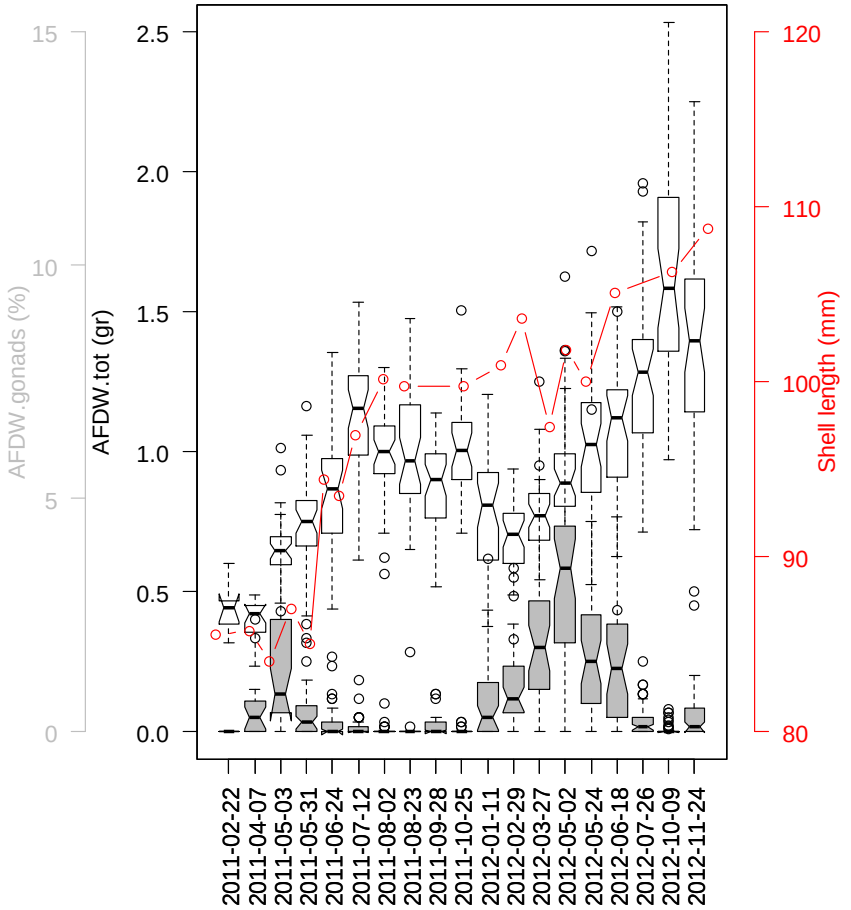

Figure 15. Plot of the AFDW (gram) and percentage gonadal tissue and shell lengths between February 2011 and July 2012.

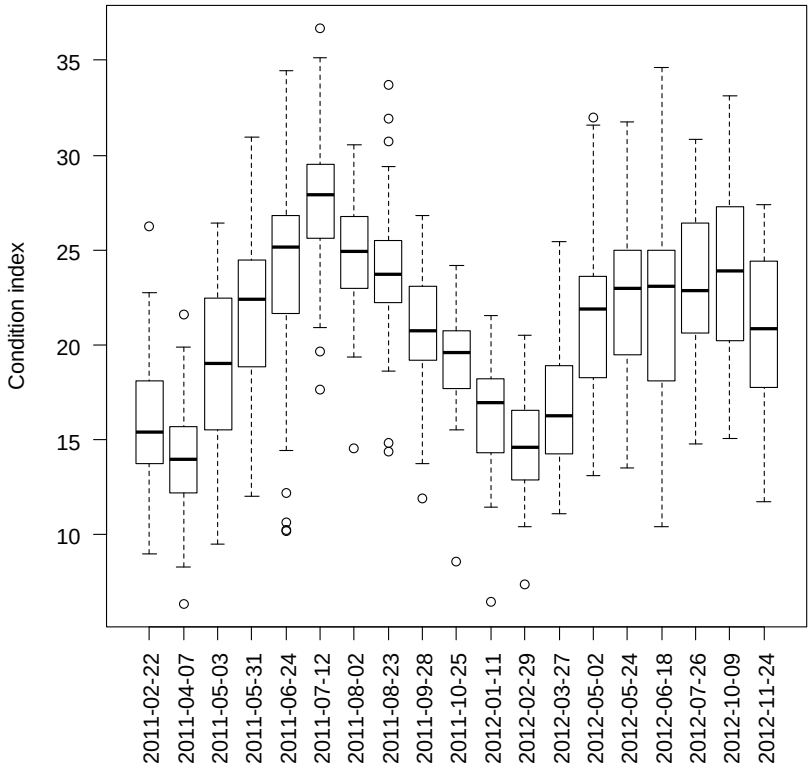

Figure 16. Boxplot of the condition indices of animals collected around the lander station in 2011 and 2012.

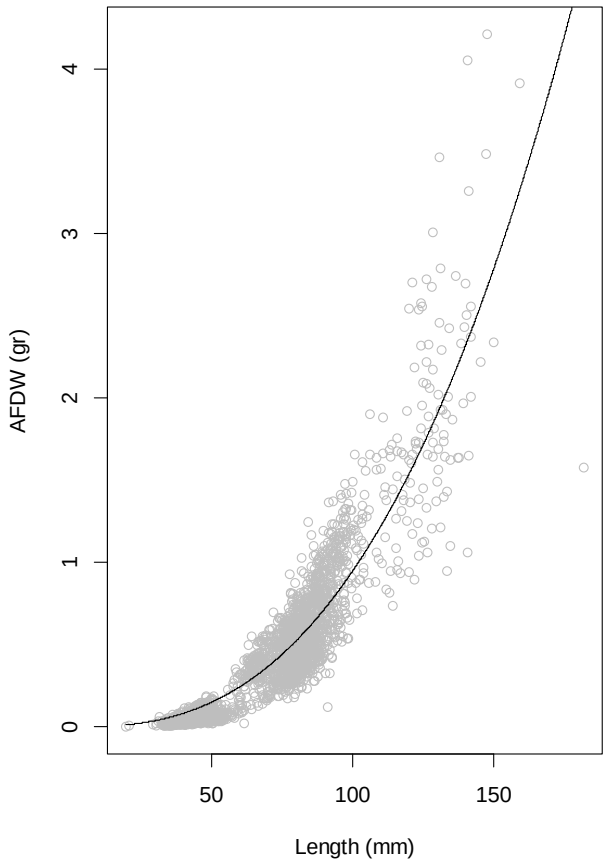

Figure 17. Length-AFDW relationship for *Ensis directus* irrespective of time of sampling. Regression of the form ; $AFDW=4.467e\text{-}6*Length^{2,66.}$ $p_a<0.001$, $p_b<0.001$

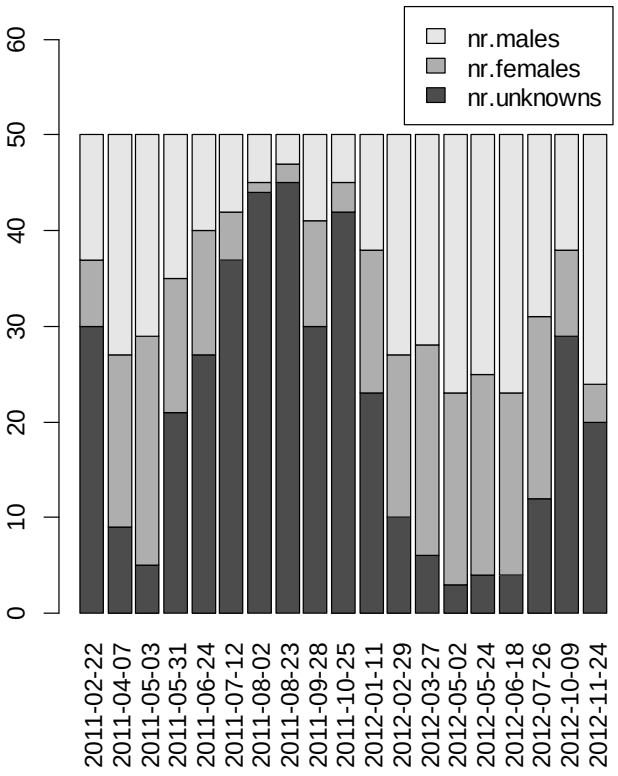

Figure 18. Percentage of animals by sex. Animals which had ripe or partially ripe gonads could be sexed. The figure shows that the number of animals which could be sexed is maximal in the beginning of May

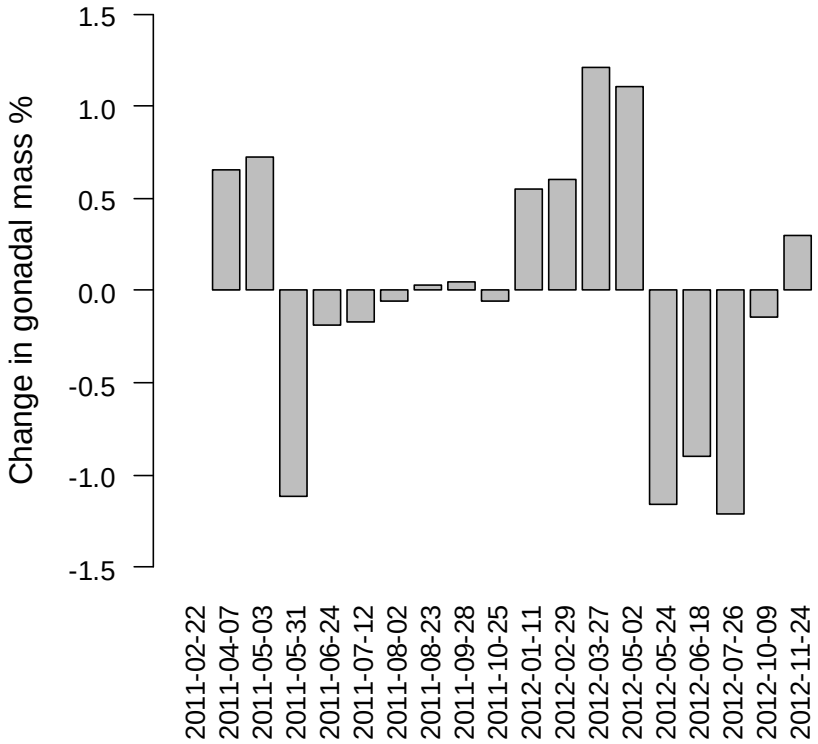

Figure 19. Change in the gonadal mass over time. Loss of gonadal tissue is observed for the period between the end of May and July which indicates spawning.

Figure 19 shows that largest loss of spawning mass is between May and July. In 2011 the period of loss of gonadal tissue is much more confined than in 2012. This might have to do with interannual variability of the environmental conditions as well as with an effect of animals which are bigger and more aged in 2012, when compared to 2011. The data clearly suggest that development of gonadal tissue starts in autumn and winter and actually precedes the phytoplankton bloom which peaks in May. In the months just before spawning (Feb-April) the percentage of gonadal mass depends on animal size. Larger specimens tend to have a large amount of gonadal tissue relative to total body mass.

3.2.2 Caloric values.

While glycogen content specifically yields information about stored energy reserves in the hepatopancreas and in muscle tissue, the caloric content gives a more overall view of the energy content of each animal, derived from proteins, fats and carbohydrates together which not necessarily represent stored reserves. Analyses were performed on ~0.5 gram homogenized grinded and freeze dried tissue. During the process we discovered that intermixed anorganic parts (sand in the stomach) contributed significantly to the large variance of the caloric contents. Later on this has been corrected. Nevertheless we remain with a large scatter in energy content but despite this scatter the data show a seasonal pattern (Figure 20). In the autumn and winter months the caloric content is at minimum and in early spring it rapidly

increases. This is visible in both sampling years. The maximum range between maximum and minimum caloric content is approximately 400 cal/gram. Lowest caloric contents are always found in the autumn period. Maximum values are found in the spring bloom period until late in summer (August). This suggests that the composition of the tissue changes such that the energy content per unit tissue decreases in autumn and winter. This is supported by the other measurements of conditional parameters.

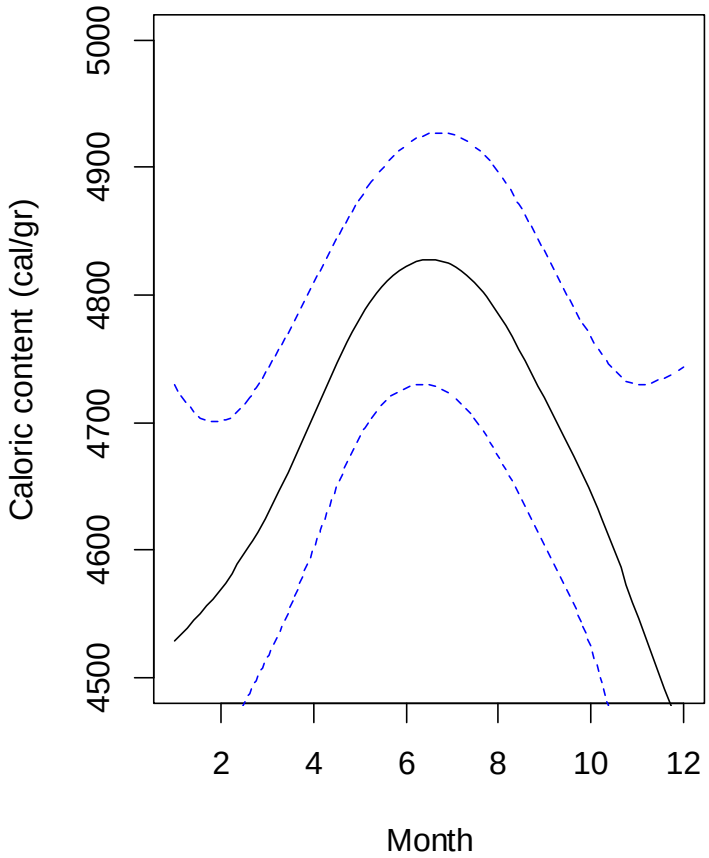

Figure 20. Gam model describing the caloric content per gram freeze dried tissue. In both years the caloric content peaks in spring-summer. Due to the large spread in caloric content between animals the model has a poor fit, but still is significant. (P=0.005)

3.2.3 Glycogen Content.

Figure 21 shows the seasonal variation in the percentage of glycogen. Maximum glycogen tissue concentrations are found in the summer months, minima are found in the winter months. In the spring period there is a rapid increase in the amount of glycogen suggesting that the animals profit from the freshly produced organic spring bloom material. The maximum glycogen tissue content which is found in June-July never surpass 10%. For the 2011 data it is obvious that the amount of glycogen rapidly decreases at the end of summer. Minima (0-1%) are found between November and March. Sample size per collection date is too small to see if there are relationships with shell size. There is however a significant relation between the average glycogen content and the average condition index (explained variance 76%), $p<0.05$.

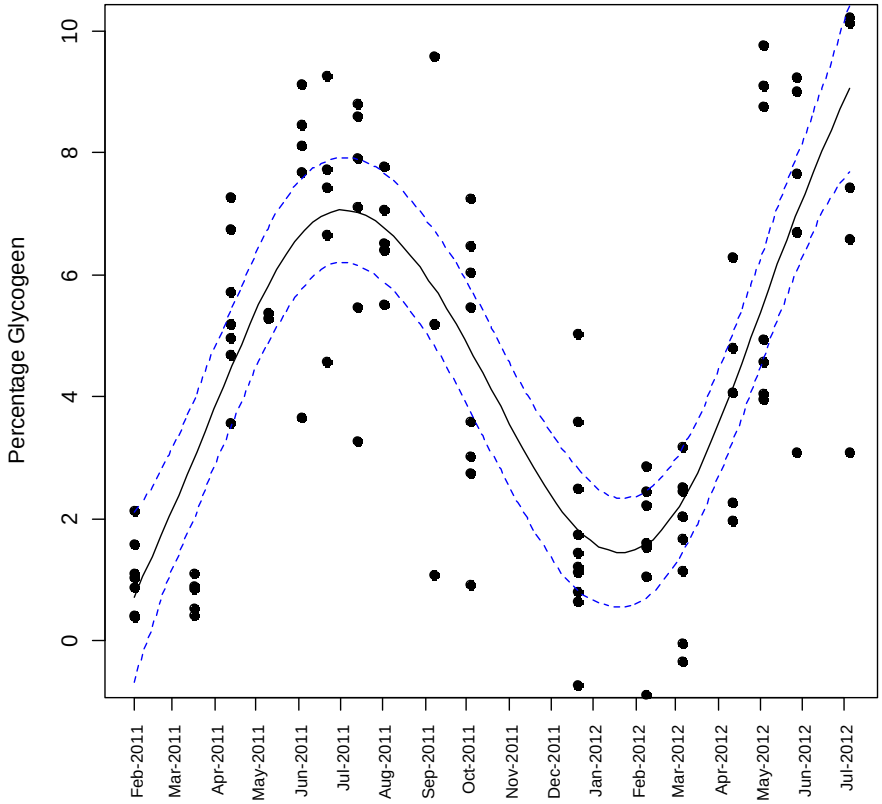

Figure 21. Gam fit of the percentage of glycogen in homogenized freeze dried tissue, significant at $p<0.001$. Explained deviance 53 %.

This strong relationship shows that the determination of the condition index based on shell size and AFDW is a good predictor of the energy reserves stored within the animal. To get a quick overview of these relationships between the various measured attributes of *Ensis directus* a pair plot is given in Figure 22. This pairplot shows that the correlation of the average glycogen content is strongly related ($R=0.88, p<0.01$) to the average condition index and that the caloric content is related to the percentage of gonads ($R=0.56$ $p<0.05$).

The glycogen determination and the determinations of the caloric content were performed on the same set of animals. This made it possible to look at the interrelationship between condition index, caloric content and percentage of glycogen on basis of measurements on individual specimens (Figure 22) and thus give more detail. From this figure it readily becomes clear that also caloric content and percentage glycogen are linked but like in the analyses of the population averages, condition index is a better estimator for percentage of glycogen than for the caloric content.

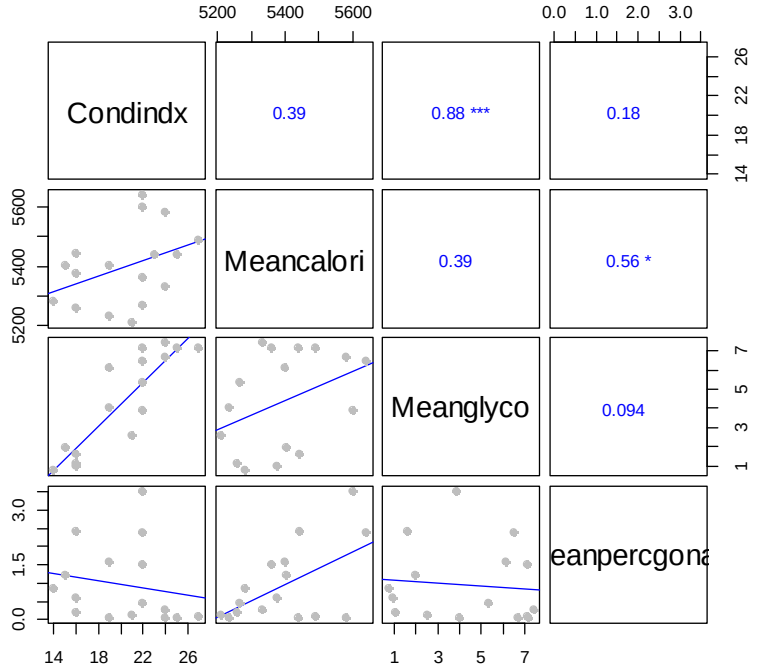

Figure 22. Pair plot of the (population) average attributes of *Ensis directus* (=average over animals on a single measurement date) measured in the samples taken at each sampling date, with in the upper panel the correlation coefficients of the depicted relationships.The lower panel (below the diagonal) gives the relation between the variables together with a linear regression. The upper panel gives the associated absolute correlation coefficients and significance level (*P<0.05; **p<0.01;***p<0.001) of the corresponding combination.

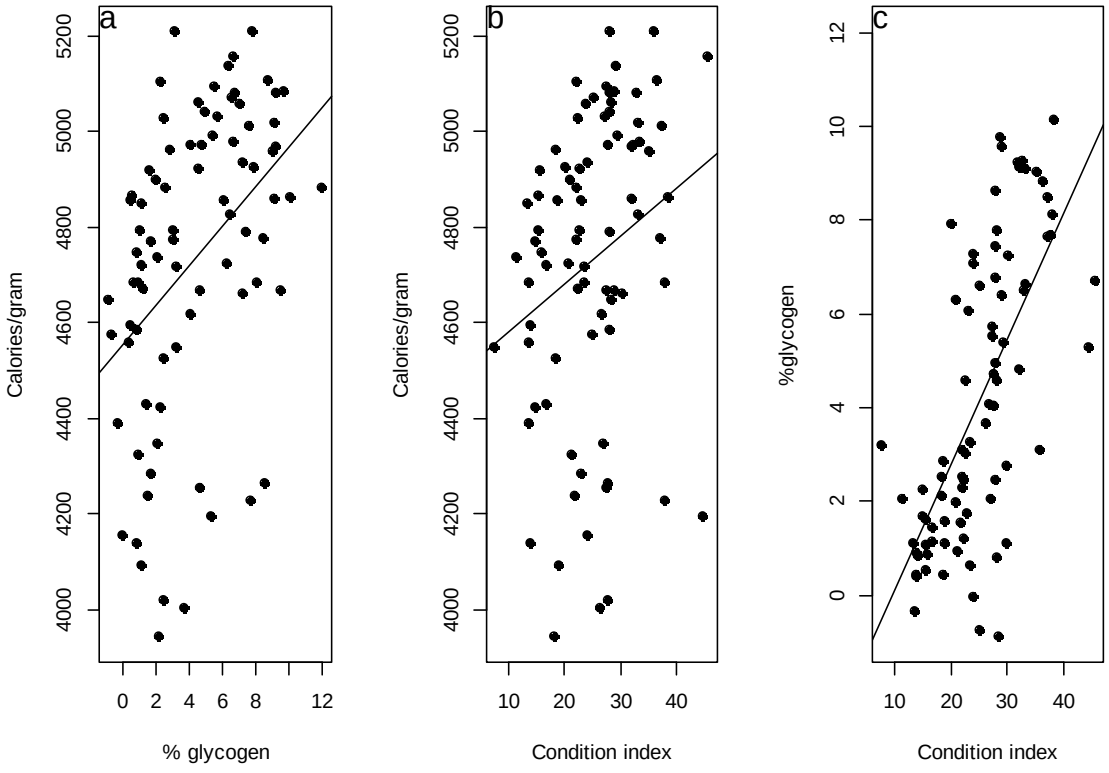

Figure 23. Comparison of various condition parameters determined on individual specimens of the bivalve *Ensis directus* collected in 2011 and 2012. All are significant with R-squared between 0.17 and 0.44 and pvalues <0.025.

Figure 24 gives an overview of the interrelationships of growth attributes and their relation to measured environmental factors as a pairplot. The terms on the diagonal represent the measured parameters (Chl-a, SPM, Ratio, Temp) and the average population response in terms of the change in length and condition (D.length, D.AFDW, D.cond, D.glyco and D.gonad). The xy plots in the panels below the diagonal are the graphic representation of these relationships between the datasets named on the diagonal. The upper panel (above the diagonal) gives the correlation coefficients and their significance of the corresponding graph of the lower panel.
The figure shows that the condition related attributes (D.glyco, D.cond, D.gonad) have the best relation to the observed weight changes (D.AFDW) and not so much to changes in average length (D.length). This is partially caused by the fact that the condition attributes are covariables. The difference between tissue and shell growth attributes suggests that both are at least partly decoupled. In the same figure the relationship between the main environmental factors which control growth are given (Temp, Chl-a, SPM, Ratio). Chl-a and SPM have a strong negative correlation (0.60) which is highly significant. Neither SPM nor Chl-a have a significant (linear) relationship to temperature (Temp).
There is a weak but significant relation between the change of shell lengths (D.length=shell growth) and water temperature in the preceding periods. The Chlorophyll concentration (Chl-a), the concentration of suspended matter (SPM) or the ratio between both do not seem to matter, none of them yielded significant correlations. This suggests that shell growth (calcification) is temperature driven. The correlation coefficient between shell growth and Temperature was 0.29 and just significant.
This in contrast to the change in soft tissue mass (D.AFDW) which does not show a significant relationship with temperature but is significantly positively related to the Chlorophyll-a concentration in the preceding period and negatively (significant) correlated with the silt concentration. SPM and Chlorophyll-a are covariates which makes it hard to separate their effects on growth in a field study like this. We therefore used the ratio between them to represent the quality aspect of the available food particles. This showed that the change in AFDW (D.AFDW) is positively related to the Ratio between Chlorophyll-a and SPM. This translates into similar relationships between these environmental variables and the change in the condition index or the change in the amount of glycogen stored in the soft tissue.
Gonad development is a spring event resulting in a statistically inverse relation to water temperature. The time series on gonad development show that it starts before the spring bloom. At the time that spring bloom peaks, the loss in gonadal tissue is maximal, i.e. the animals are spawning. The data furthermore show that the change in the amount of gonadal tissue is inversely related to the change in length and that shell growth and gonad development and spawning take place in different seasons. This timing also results in a negative correlation between the change in gonadal tissue and the concentration of Chlorophyll-a. The time lag between the development of gonads and increase in AFDW (Figure 25) suggests that gonad development relies at least partly on the reallocation of energy from within the animal before it has been able to recharge its energy reserves by feeding on fresh spring bloom algae and detritus. In Figure 25 the temporal development of the glycogen reserves has not been depicted as it actually mirrors the overall condition index (Figure 23). From above analyses it is evident that the seasonal cycle in gonad development, tissue growth shell growth and the resulting condition follow each other in time.

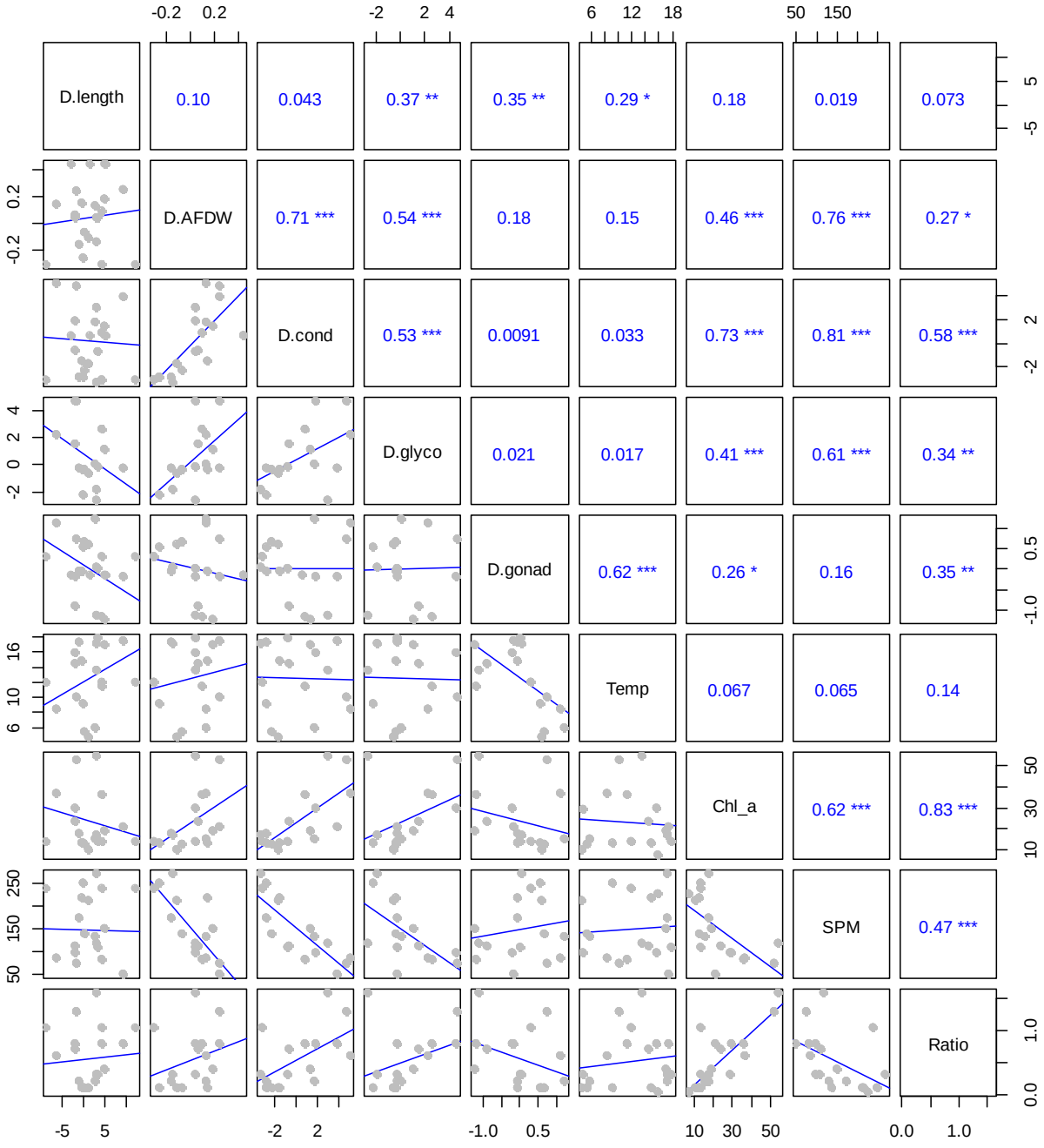

Figure 24. Pairplot of the change in averaged attributes of *Ensis directus* together with environmental conditions as measured in the preceding period. The lower panel (below the diagonal) gives the relation between the response and control variable together with a linear regression. The upper panel gives the associated absolute correlation coefficients and significance level (*P<0.05;**p<0.01;***p<0.001) of the corresponding response -control combination.

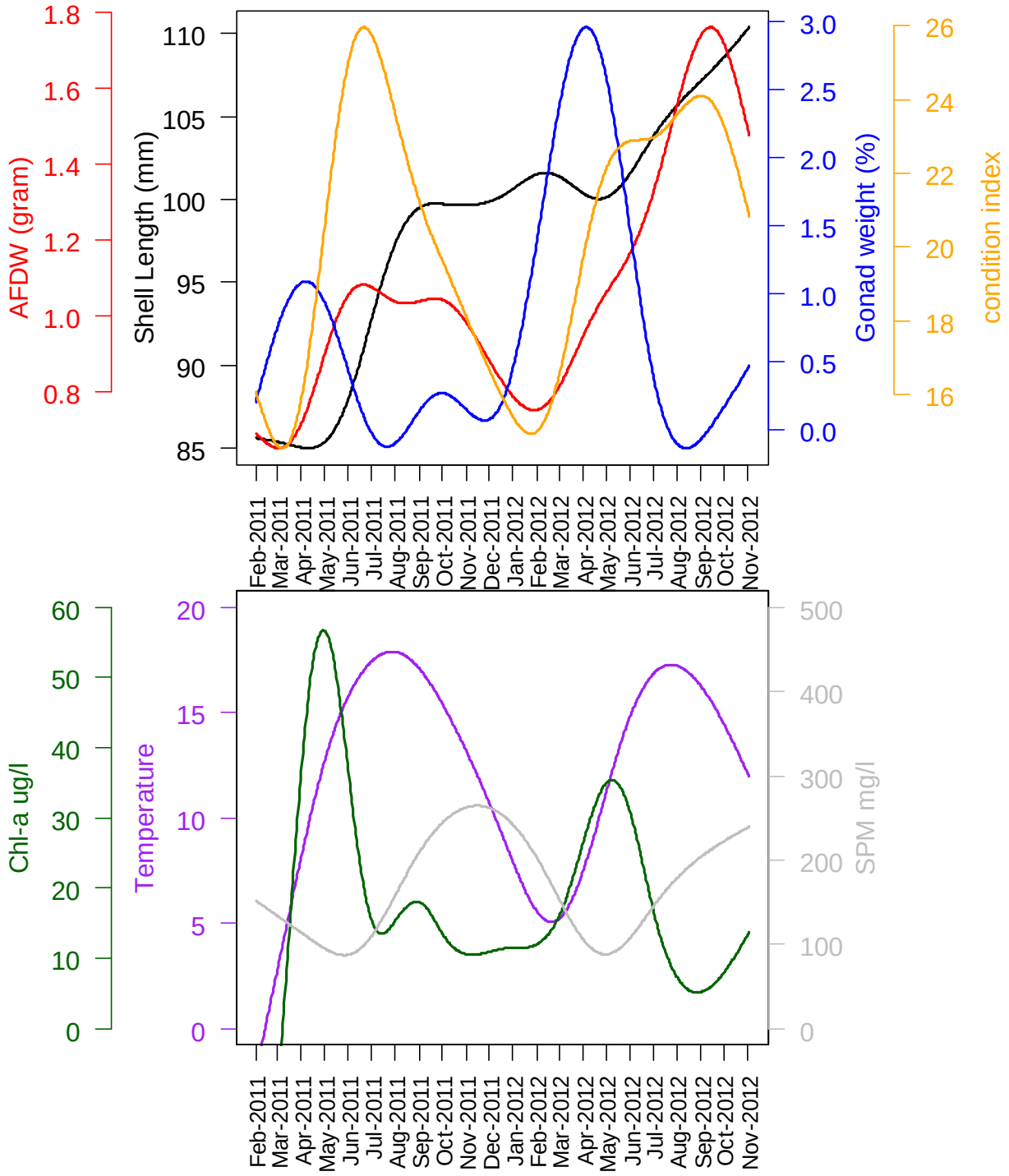

Figure 25. Gam curve fits showing the seasonal order of shell growth and condition parameters (AFDW, %gonad, shell lengths and Condition) (upper panel) together with gam fits of the seasonal change in Chlorophyll-a, SPM and Temperature.

The pair plot (Figure 24) gives all possible univariate relationships together with their correlations and shows that most are covariates of each other. The *condition* attributes of *Ensis directus* significantly correlate among each other (condition, glycogen, caloric content, gonads and AFDW) and also the measured environmentals (Chl-a and SPM) correlate with each other. This implies that there is a dependence among the response variables and among the controlling environmental variables which limits their use together in one multiple regression analyses as

that would give false estimates of the p-values of the regression models and might exclude significant explanatory variables as well. Therefore we only applied regression analyses between individual independent response variables (Shell growth, Tissue growth, Gonad growth and Condition change) against the Temperature in combination with the Chl-a/SPM Ratio. The ratio represents the interplay between the amount of Chlorophyll-a and the amount of inorganic suspended matter and thus gives how the quality of potential food relates to the change in the condition and growth of *Ensis directus*. The effect of an interaction between water temperature and food quality (Ratio) has been tested as well. For each of the four growth/condition parameters regression models of the form:

"Growth=a*Ratio + b*Temp + Intercept +(Temp*Ratio)"

have been tested and the results for the models without interaction are given in (Table 5). The relationships between environmentals and growth response not necessarily have a linear character. Therefore univariate gam models between above response variables and control variables have been given in the appendix (Figure 60 -Figure 63).

The regression analyses shows that shell growth is only weakly linearly related to temperature. Also when tested in an univariate model with only temperature as explanatory variable, about 10% of the variance is explained. This poor fit is caused by the negative growth rates caused by observed size selective mortality with as a consequence, negative back calculated shell growth rates. Another reason was that during the sampling in the winter 2011/2012 the sizes of the caught animals happened to be larger than those catched later in the year leading to "negative" growth rates. Without using these "negative" growth rates, temperature can explain 45% of variance in the observed change in shell length. Adding the interaction term between water temperature and Ratio (foodquality) gave further improvements of the model. The Gam model (Figure 60b) support the effect of temperature on shell growth and shows that for the temperature range up to 12-14°C the shell growth rate is low and extremely variable. Only when temperatures surpass 12-14°C, shell growth rates pick up and start to increase steadily. Figure 60c indicates that the shell growth is maximal at Chl-a/SPM Ratios between 0.4 and 0.7. This fit is however not significant. The fact that the relation between shell growth and Ratio or Chlorophyll is not one of a steady increase is caused by the fact that in spring when chlorophyll peaks and thus also the ratios peak, the water temperature is still too low to enable significant shell growth as the process of calcification is temperature dependent. Due to the low water temperature in spring, *Ensis directus* can not fully profit from the spring bloom in terms of shell growth.

For tissue related parameters a different pattern emerges. The change in AFDW and the Condition can both be significantly explained by the Chl-a/SPM ratio. The univariate gam analyses (Figure 61, Figure 62) furthermore suggest that a high SPM concentration has a negative effect on the AFDW and thus condition. The amount of chlorophyll has a positive effect on tissue growth and condition. This results in an almost linear increase with increasing Chl-a/SPM Ratios on tissue growth (Figure 61d) or condition (Figure 62). Thus food quality is an important determinant of tissue growth. The effect of temperature on tissue growth and condition is small or negative. A pattern emerges that tissue growth appears to be less dependent of water temperature and is strongly influenced by the interaction between the ratio and the water temperature. A linear model which includes such an interaction term gives a slightly, though significant, better fit than a model without such interaction term (r^2=0.44 and 0.39 respectively P< 0.001). This suggest that the interaction between the quality of available food and temperature is an important variable combination determining tissue growth. The same

holds for shell growth. Using an interaction term (Ratio*Temp) improves the regression model and increases the amount of explained variance from 10% to 44%.
The change in condition of the animals follows the same pattern as the change in AFDW. The univariate gam fit (Figure 62b) shows that optimum conditions are reached in the period that water temperatures are between 8 and 12 degrees which is the period of the spring phytoplankton bloom. The fit is however not significant but stresses the likely importance of the spring bloom for tissue build up. In the linear regression model (Table 5) the effect of temperature on the change in the condition index is slightly negative. The effect of the Chl-a/SPM Ratio is however strong. If an interaction term (Ratio*Temperature) is added, the amount of explained variance increases and again stresses that the quality of food in combination with the temperature is an important determinant for the increase in condition. The suggested (modelled) decrease of condition at the higher temperatures is possible if shell growth outpaces tissue growth. This is especially likely at the higher temperatures (Figure 55) in late summer when the quality of food is low (low ratios) and temperatures are high and thus favourable for shell growth (carbonate deposition) and less favourable for tissue growth. Higher temperatures cause higher metabolic rates. In case these extra energy expenditure is not matched by food intake, soft tissue mass is likely to decrease. This is illustrated by the fact that for the change in condition the interaction (Ratio*Temperature) term was highly significant. The regression model with such a term could explain 77% of the variance in the change of condition.
The regression coefficients of the linear model describing the change in the percentage of gonadal tissue in relation to temperature and the ratio are both negative but only the effect of temperature is significant and introduction of the interaction term hardly improves the regression model. Gonadal development starts in winter before there is a spring bloom and when the temperatures are still low. In spring, with increasing temperatures before the phyto plankton bloom, gonads build up. At about the time that the bloom peaks the animals start spawning. The change in gonadal tissue at that time is maximal (see Figure 19). After the spring bloom the percentage of gonadal tissue decreases steadily while with the progressing of time, the seawater temperature increases, explaining the inverse relationship with temperature.
In summary, shell growth seems to be controlled by temperature, while tissue growth and condition are strongly related to the amount of chlorophyll-a in relation to total SPM i.e. the quantity and quality of the potential food. The major development of the gonadal tissue precedes the spring bloom and at time of the spring bloom, spawning takes place. This makes that most of the gonadal cycle has an opposite trend when compared to the trend in water temperatures or food supply. The gonads thus respond differently to the seasonal change in growth conditions. This shows that the build up of gonadal tissue is to a large part driven by reallocation from energy reserves from within the animal.

Table 5. Overview of the regression coefficients of the various multiple regression models tested. D.AFDW= change in Ash free dry weight, D.length=Change in shell length, D. Condition=change in Condition index, D.Perc gonad, change in the percentage of gonadal tissue. Regression model had the general form of Growth=a*Ratio + b*avg. temperature + Intercept. R squared and p are given in the last column. for each coefficient level of significance is given.

	Intercept	Ratio	Temp	R^2	p
D.Length	-0.0938	0.050	0.0111**	0.10	0.02917
D.AFDW	-0.0367*	0.017***	0.00012	0.41	3.54e-8
D.Condition	-0.0503*	0.417 ***	-0.001851	0.70	<.2e-16
D.Percgonad	0.0393***	-0.0171	-0.0030***	0.29	1.52e-5

3.3 Valve gape

3.3.1 Valve gape Mytilus

In Figure 26 a pair plot of all *Mytilus* valve gape measurement (by the minute measurements) have been plotted together with the correlation coefficients for each of the combination of individual mussels. All records show a positive relationship (which becomes masked by the massive amount of datapoints) and the corresponding correlation coefficients are all significant (also because of the extreme length of the records).

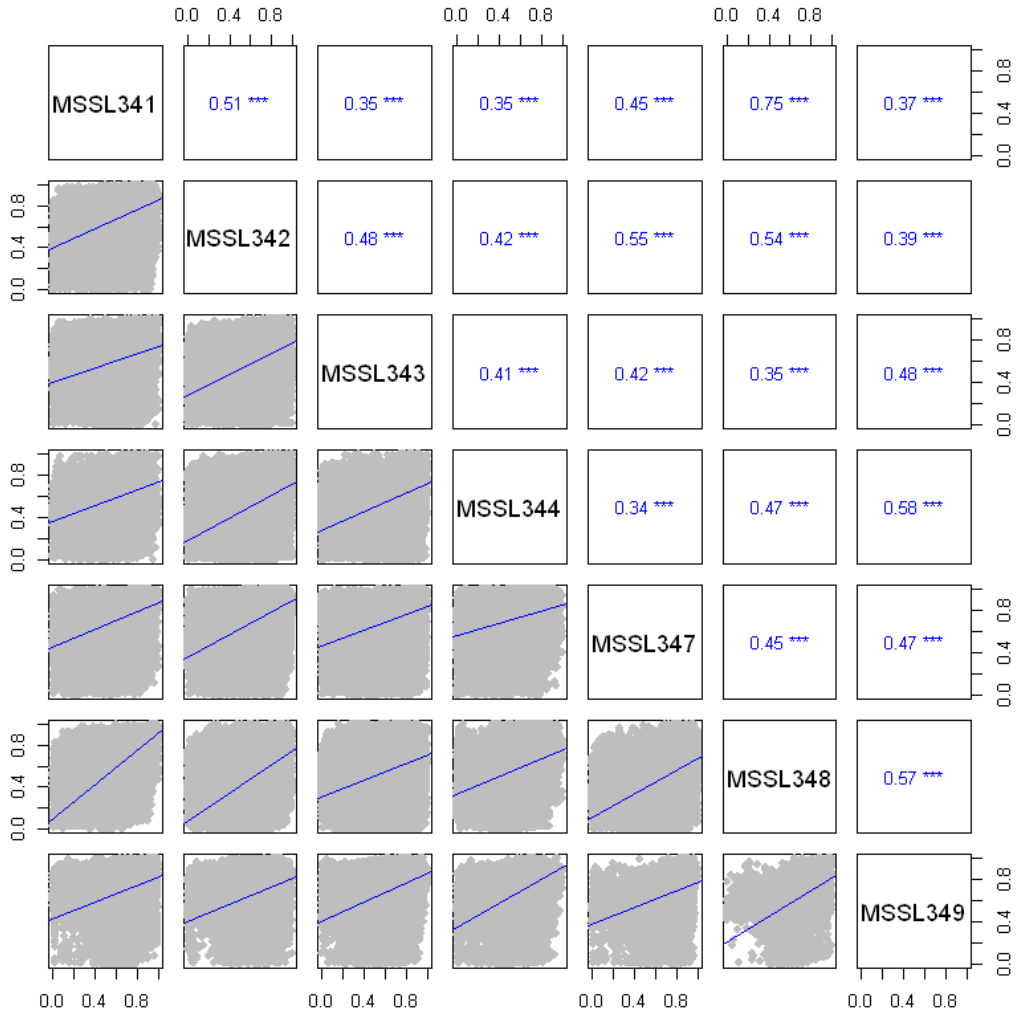

Figure 26. Pairplot of *Mytilus* valve gape, showing the synchrony between different individuals over the entire period of measurement (2011-2012). The lower panels give the x-y plot of the valve gape of two individuals given on the diagonal. The corresponding upper panel gives the associated absolute correlation coefficients and significance level (*P<0.05;**p<0.01;***p<0.001) of that animal combination.

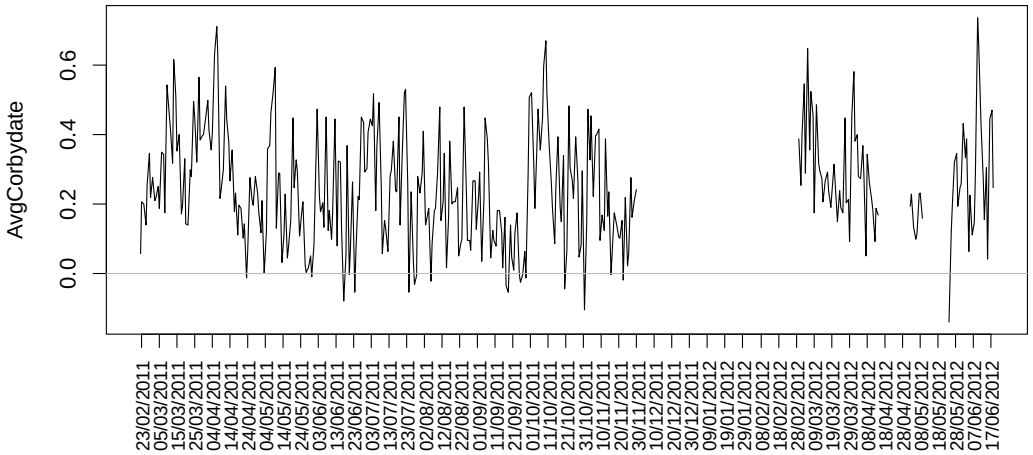

Figure 27.Average correlation between all possible *Mytilus* valve gape records. The correlation plotted is the average correlation of all gape records determined for that day.

For each day that valve gape records (measured by the minute) were available, the records were correlated to those of the other *Mytilus* specimens which were recorded during the same day at the same time. Thus for each day 1440 valve gape values (minutes) were correlated to similar values obtained at the same time for other mussels. After doing this a series of daily average correlation coefficients was calculated with the aim to see whether there is a temporal pattern in valve synchrony over time (seasons). The resulted in the time series which is plotted in Figure 27.

Between February 22nd 2011 and July 26th 2012 the average correlation of all possible combinations is 0.27. The graph illustrates that the range of correlation values varies between -0.14 and 0.74. Only a few instances show a negative correlation. For mussels mainly positive correlations were found and during all months the maximum daily correlations found, ranged between 0.71 and 0.93. Each of the specimens shows occasions of high correlations with other specimens. Thus synchrony is not coupled to a specific time of the year or to specific individuals.

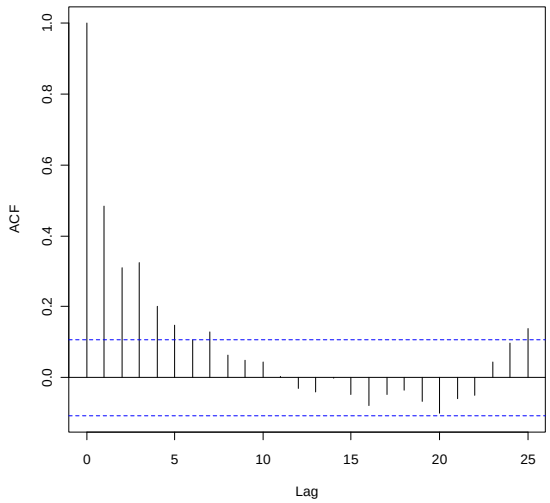

Figure 28. Autocorrelation of the average daily inter mussel correlations with a time lag given in days, as given in Figure 27

If an autocorrelation function is plotted over the maximum uninterrupted section of the time series of daily correlations (Figure 28) between mussels it becomes evident that there are periods of 5 to 6 days in which correlation is at maximum and gradually decreasing. After about 25 days significance in correlation returns indicating that the synchrony in valve gape is high again. This suggests that the valve gape in mussels might be related to a lunar cycle or variables directly coupled to the lunar cycle such as maximum tidal currents.

3.3.2 Valve gape *Ensis directus*

For *Ensis directus*, not all measurement periods yielded valve gape records for more than one specimen. Sometimes only one individual survived which implied that for these periods no "between" *specimen* correlation of the valve gape could be calculated. This makes the available data set much more limited then the Mussel valve gape dataset. In total 850 between-animal correlations could be calculated, covering 140 days. Mean average correlation =0.11 and ranging between -0.60 to 0.72. Correlations are not really skewed to positive values like in *Mytilus*, suggesting that synchrony is weak although for some selected periods real high correlations between specimens were found .

The synchrony of valve gape between *Ensis* specimens is lower than for *Mytilus*. An autocorrelation suggests that the time series depicted in Figure 30 contains a periodicity of 12 days, i.e. after 12 days the average correlation of valve gape between individuals (measured by day) peak again and surpasses the levels of insignificance. This is about half the periodicity observed in mussels and also points to a link with the tidal cycle.

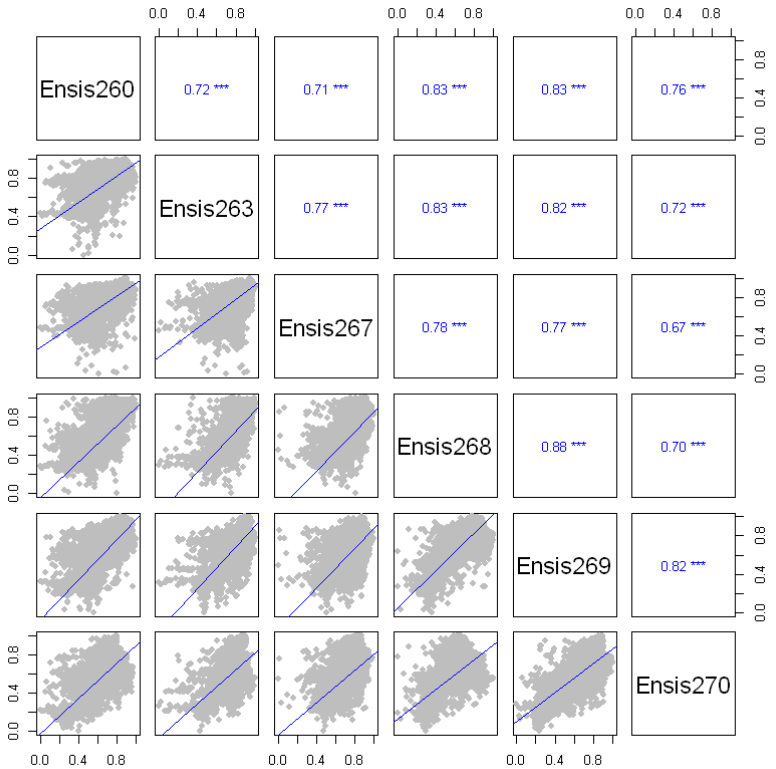

Figure 29. Pairplot of valve gape of *Ensis directus*, showing the synchrony between different individuals in week31 to week 34 in 2011. This appeared a period with the highest correlations found for this species. The lower panels give the x-y plot of the valve gape of two individuals given on the diagonal. The corresponding upper panel gives the associated absolute correlation coefficients and significance level (***p<0.001; **p<0.01; *P<0.05) of that animal combination.

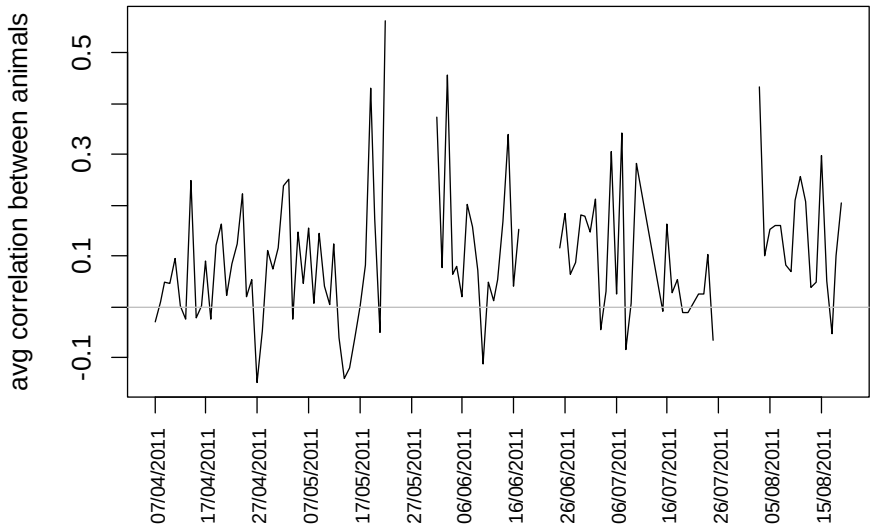

Figure 30. Averaged daily correlations of valve gape records for *Ensis directus* in 2011.

3.4 Valve gape *Ensis directus* versus *Mytilus edulis*

Over the period from the start of the field work in February 2011 until July 26th 2012 the matching daily valve gape records of both species were compared, i.e. for each possible shell combination the correlation between both gape records was calculated for each day (156 days). This involved 26 *E. directus* specimens and 13 *M.edulis* specimens. In total for 2093 animal-day combinations of correlations could be made. The correlation coefficients for these combinations ranged between -0.53 to 0.74. The average over all combinations was almost zero. No temporal patterns were found in the height of the correlation suggesting the absence of a well defined seasonal effect in the synchrony of valve movements between both species. The high correlations however indicate that at some days selected specimens of the two species behaved rather similarly. For most of the periods the correlations among the *Ensis directus* specimens is low. It is hard to judge whether this is an intrinsic aspect of their behaviour or whether this is an artefact. The correlations found for period week 31-34-2011 (Figure 29), suggests that also this species can show a high synchrony, similar to what is found in *Mytilus edulis*.

3.5 Valve gape and environmental factors.

3.5.1 Ensis directus

The correlation between valve gape of *Ensis directus* and measured water temperature is low and somewhat variable but mainly positive. Plotting does not suggest clear trends between valve gape and temperature or salinity.

The correlations of valve gape with Chl-a, SPM or the Ratio between Chl-a and SPM are also low and moreover highly variable, i.e. range between positive and negative effects. Hence as such the effect on the behaviour (over all specimens) is not significant (R_{Ratio}=0.0023,$R_{Chl\text{-}a}$=0.0067, R_{SPM}=-0.046). Neither a significant relationship was found between the valve gape of *Ensis directus* and current speed ($R_{speed)}$=-0.03 or wave height ($R_{waveheight}$=0.008).

Although no clear trend is visible in the average valve gape and any of the environmental variables, plots of the maximum valve gape against particle concentrations showed a decrease with concentrations. To describe and quantify this the SPM record was subdivided into concentration classes of 100mg/L each. For each class the mean SPM concentration was calculated and the maximum observed valve gape values measured in that concentration interval were determined. These have been plotted in Figure 31 which shows that valve gape decreases with increasing SPM concentrations. In all cases the regression between both is significant. Similar negative trend is found between valve gape and wave height which finds its origin in the relationship between increasing SPM concentrations with increasing wave heights. Chlorophyll concentrations are partially coupled to the SPM concentrations causing a negative trend between valve gape and Chl-a. The minimum valve gape of *Ensis* directus shows a positive relationship with the Ratio between Chl-a and total SPM. Although this might suggest this species reacts positively on an increasing quality of suspended matter, the maximum valve gape decreases at the same time. The mechanism behind this response in unclear but could direct to a behavioural response optimizing food intake.

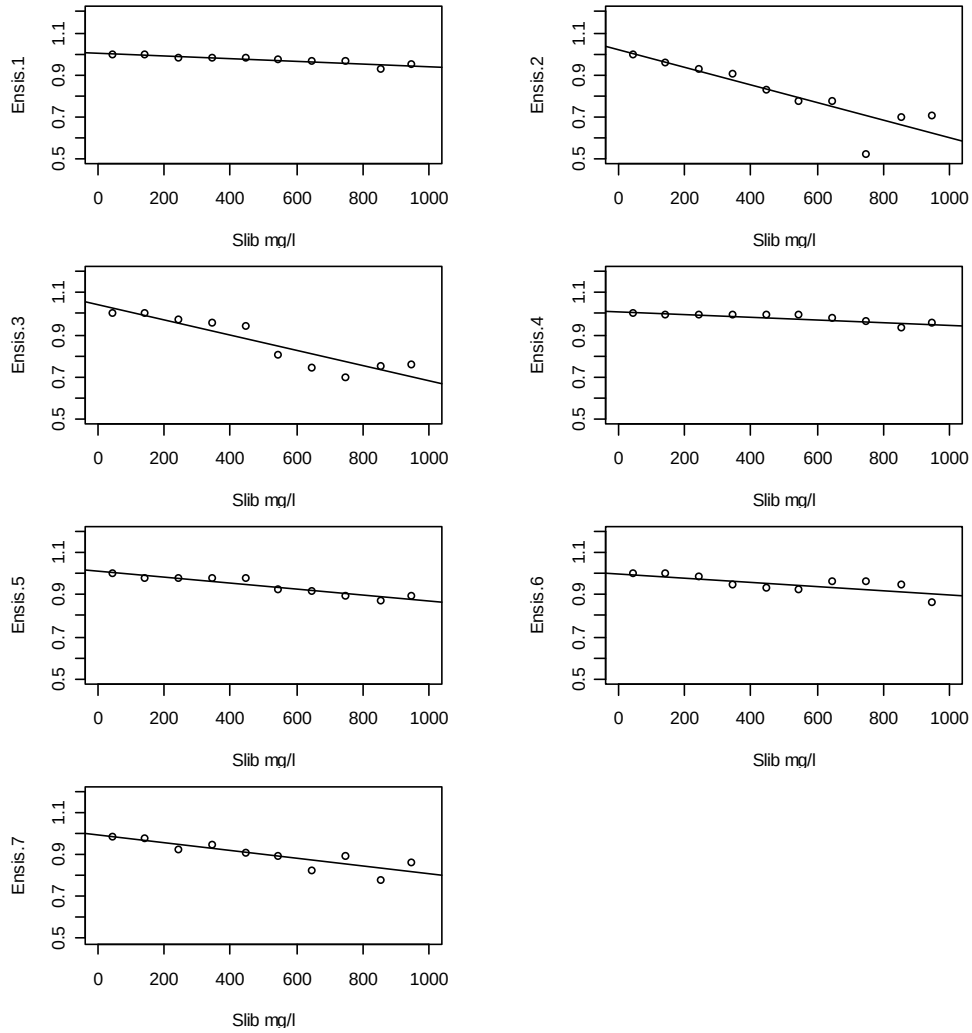

Figure 31. Maximum measured valve gape for 100mg/L concentration classes. All data, pooled over channels (several individuals) have been used. All channels (Ensis.1-Ensis.7) show that maximum valve gape decreases with increasing SPM concentrations. plotted regression are all significant at p<=0.01. In most cases there is no clear trend in relation between the residuals and fitted values

3.5.2 Mytilus edulis

The relationships between valve gape of *Mytilus edulis* and environmental conditions are similar to those found for *Ensis directus*. The correlation between *Mytilus* valve gape and temperature over the entire period is variable and insignificant (R_{Temp}=-0.124).

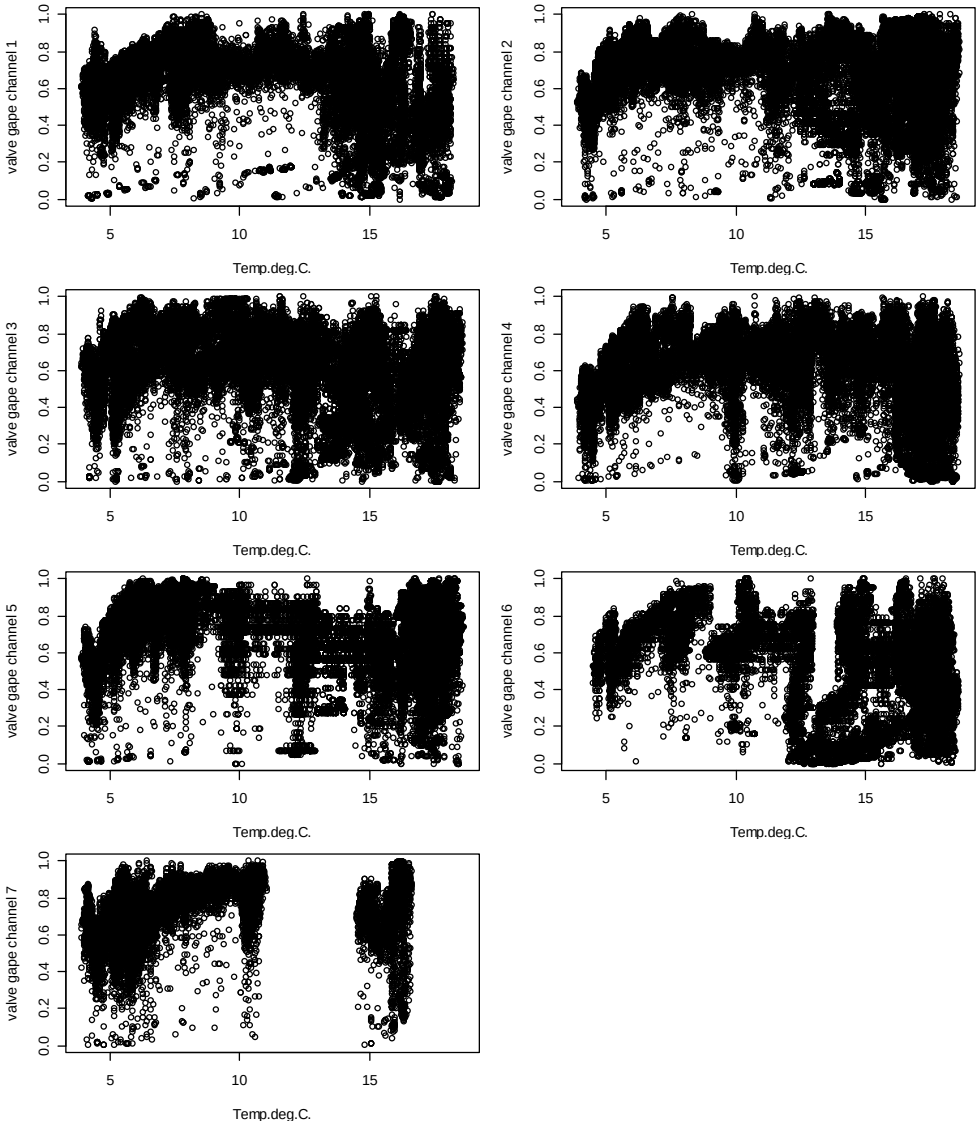

Figure 32. Plot of *Mytilus* valve gape over the Temperature range at which is measured. For each "channel" at which is measured a seperate graphs has been made. It is evident that all 7 records show a steady increase in valve gape over the first part of the temperature range. The significance of this increase has to be explored in more detail.

It must however be mentioned that maximum valve gape in the lower temperature range (3-7 C°) shows an gradual increase suggesting that temperature controls the degree to which the valves are opened. This has to be tested in more detail by looking at individual records seperately. Increasing chlorophyll concentrations due to the development of a spring bloom acts however as a covariate. Further analyses is needed to estimate the significance of the observed trend between valve gape and temperature. The overall correlation with Chl-a is 0.083 and the correlation with the Ratio between Chl-a and SPM is on 0.166.

All mussels show negative correlations with SPM (Figure 33). The correlation with the Ratio is poorly defined, unless one looks at the minimum valve gape as dependent of the ratio. In *Mytilus* the minimum valve gape increases with increasing Ratios of the SPM. At the same time the decrease in maximum gape is limited. Because the trend between SPM concentration and

Mytilus valve gape seems so evident the height of these correlation coefficients was tested for significance. All correlation coefficients appeared to be significant. (n ranges from 16643 to 50744 measurements.

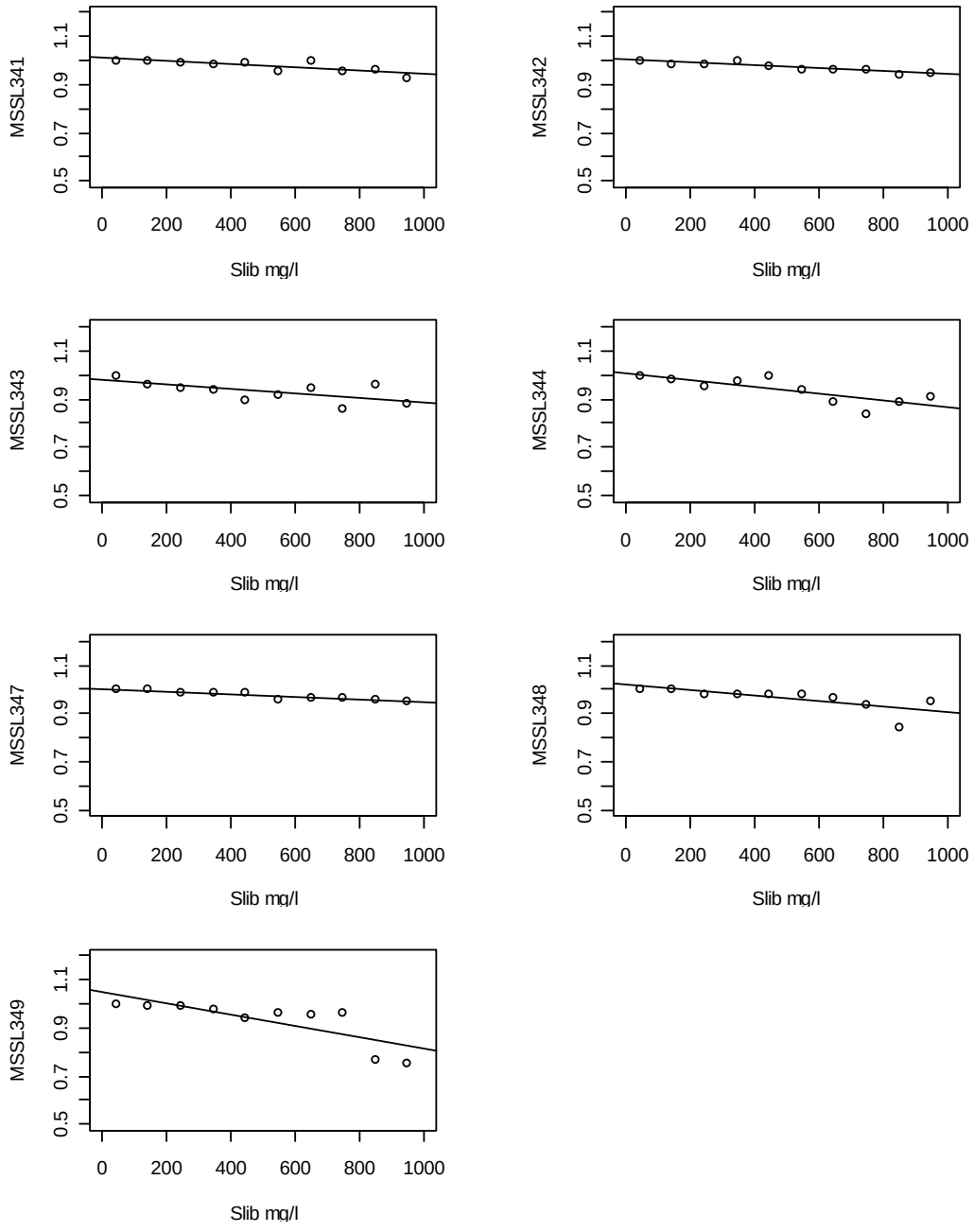

Figure 33. Maximum measured valve gape for 100mg/L concentration classes. All data, pooled over channels (several individuals) have been used. All channels (Mytilus342-Mytilus349) show that maximum valve gape decreases with increasing SPM concentrations.

3.6 Environmental Data

3.6.1 Temperature and Salinity

Figure 34 gives the temperature and salinity measured at 10 minute intervals over the experimental period between February 2011 and October 2012. Temperature ranged between 1.7 and 20.5 deg °C. Salinity ranged between 24.5 and 32.7 ‰ . Both parameters show a well defined tidal cycle (
Figure 35) which is present all through the measurement period. The summary table (Table 6) shows that the a-biotic conditions in terms of these two parameters are rather constant despite the near coastal environment. There seems to exist a salinity minimum in spring and autumn but the amplitude of this seasonal mean is of the same order of magnitude as the variation in salinity over a tidal cycle (Figure 35). The data also suggest that there is an effect of the spring – neap tide tidal cycle.

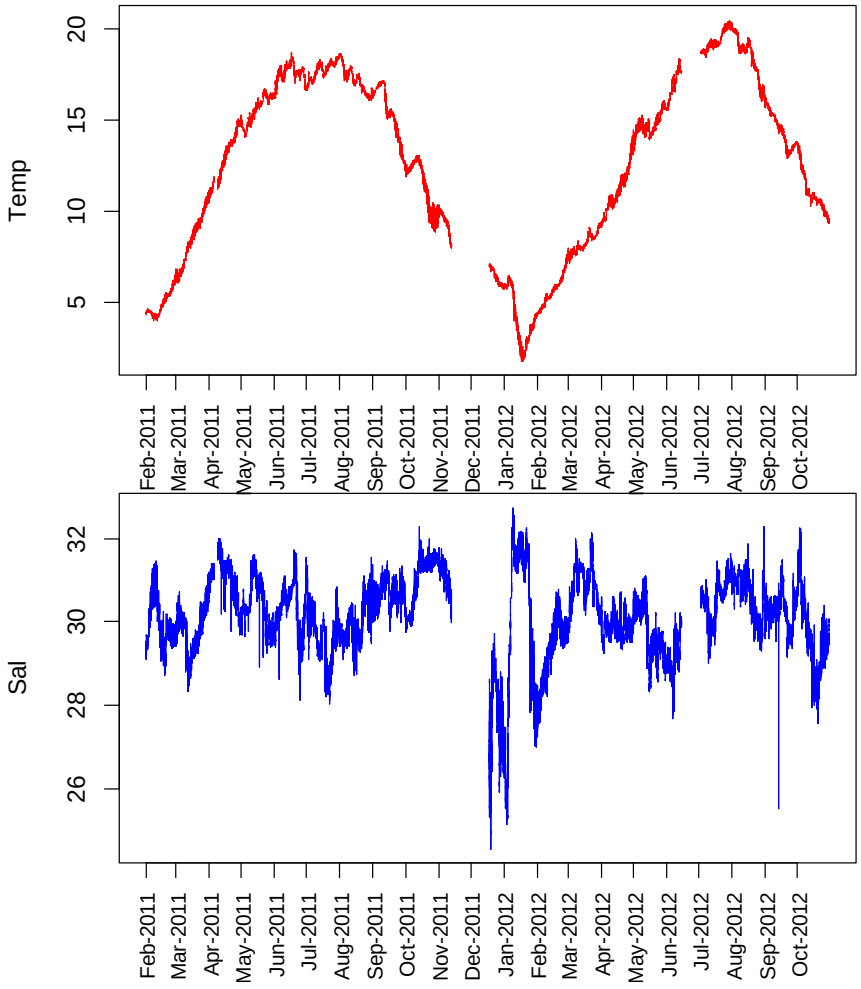

Figure 34. Seasonal change of Water temperature and salinity at the location off the coast of Egmond measured at 140 cm above the seafloor..

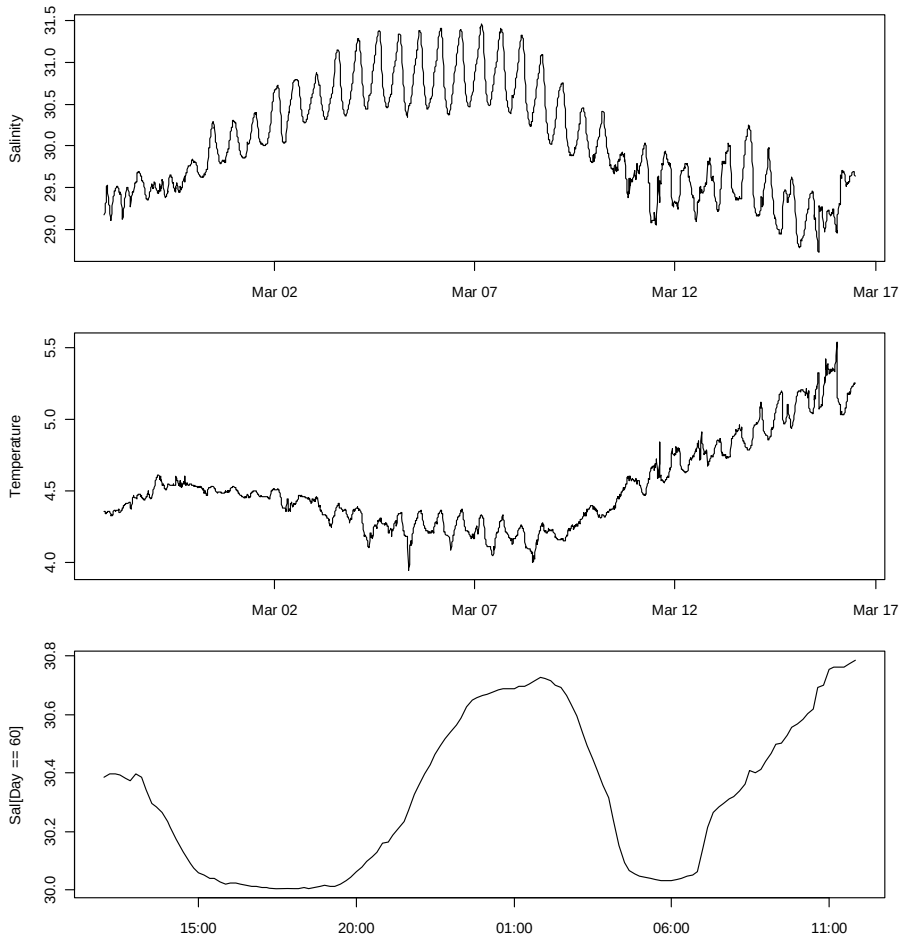

Figure 35. Illustration of the tidal changes in salinity and temperature at the lander location in spring. Showing that there is a spring neap tide cycle in the salinity as well as an effect of the daily tidal cycle.

Table 6 Monthly means and standard deviation of temperature (°C) and salinity (‰) at the lander location near Egmond at 11 meter depth in 2011 and 2012.

Month	Temp. °C.	STDev	Sal permil	STDev
Jan	6.26	0.4	27.62	1.17
Feb	3.8	1.06	30.24	1.63
March	5.71	1.02	29.83	0.64
April	8.95	1.07	30.34	0.78
Mei	12.81	1.51	30.4	0.65
June	15.72	0.85	30.1	0.74
July	17.63	0.5	30.25	0.69
Aug	18.72	0.91	30.05	0.77
Sept	17.28	1.06	30.31	0.55
Okt	14.21	1.39	30.49	0.4
Nov	10.79	1.08	30.39	1.12
Dec	9.02	0.52	30.94	0.29

3.6.2 Currents.

Table 7 gives key values for the current velocities in m/s for each month and averaged over 2011 and 2012. Figure 36 and Figure 37 summarize these data as a series of vector plots. The main current has an almost northward direction, although in selected months the residual current might be completely opposite, i.e. flow to the south like in February and March 2011. Maximum current speeds of over 1 m/s are sometimes measured during storms.

Table 7. Key values (speed in m/s) of the current vector measured at 140 cm above the seafloor. Given are minimum and maximum and current components as well as the average in each month Averaged over 2011 and 2012.

Month	Min North	Max North	Avg North	SD North	Min East	Max East	Avg East	SD East
Jan	-0.733	0.990	-0.010	0.312	-0.403	0.433	0.001	0.076
Feb	-0.536	0.816	-0.014	0.295	-0.429	0.172	0.014	0.057
March	-0.552	0.853	-0.032	0.296	-0.209	0.173	-0.013	0.046
April	-0.461	0.891	0.027	0.291	-0.169	0.192	-0.001	0.054
May	-0.566	0.827	0.034	0.318	-0.250	0.198	0.012	0.059
June	-0.532	1.190	0.017	0.294	-0.285	0.542	0.026	0.106
July	-0.646	0.867	0.018	0.295	-0.233	0.250	0.002	0.061
Aug	-0.765	0.865	0.023	0.308	-0.206	0.350	0.021	0.065
Sept	-0.558	1.213	0.034	0.285	-0.165	0.266	0.028	0.055
Okt	-0.698	0.972	0.020	0.341	-0.251	0.214	0.022	0.045
Nov	-0.731	0.773	-0.002	0.326	-0.161	0.334	0.023	0.045
Dec	-0.744	1.031	-0.004	0.281	-0.497	0.418	0.035	0.112

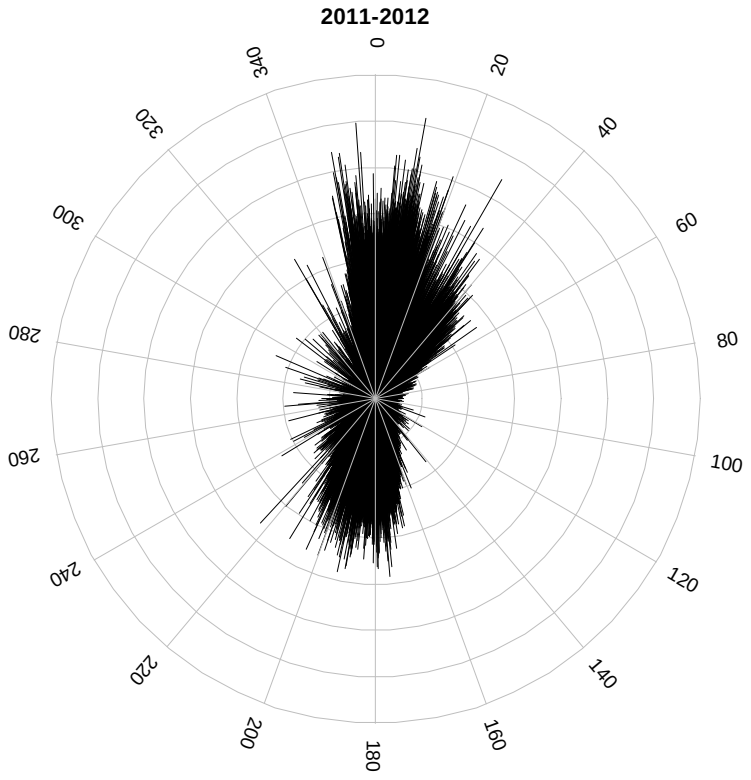

Figure 36. Vector plots of current direction and strength at 140cm above the bottom for the period between February 2011 and November 2012.. Radial grid steps reflects current speed in steps of 0.2 m/s. Outer circle is maximum speed of 1.4 m/s. Labels around outer circle is current direction in degrees.

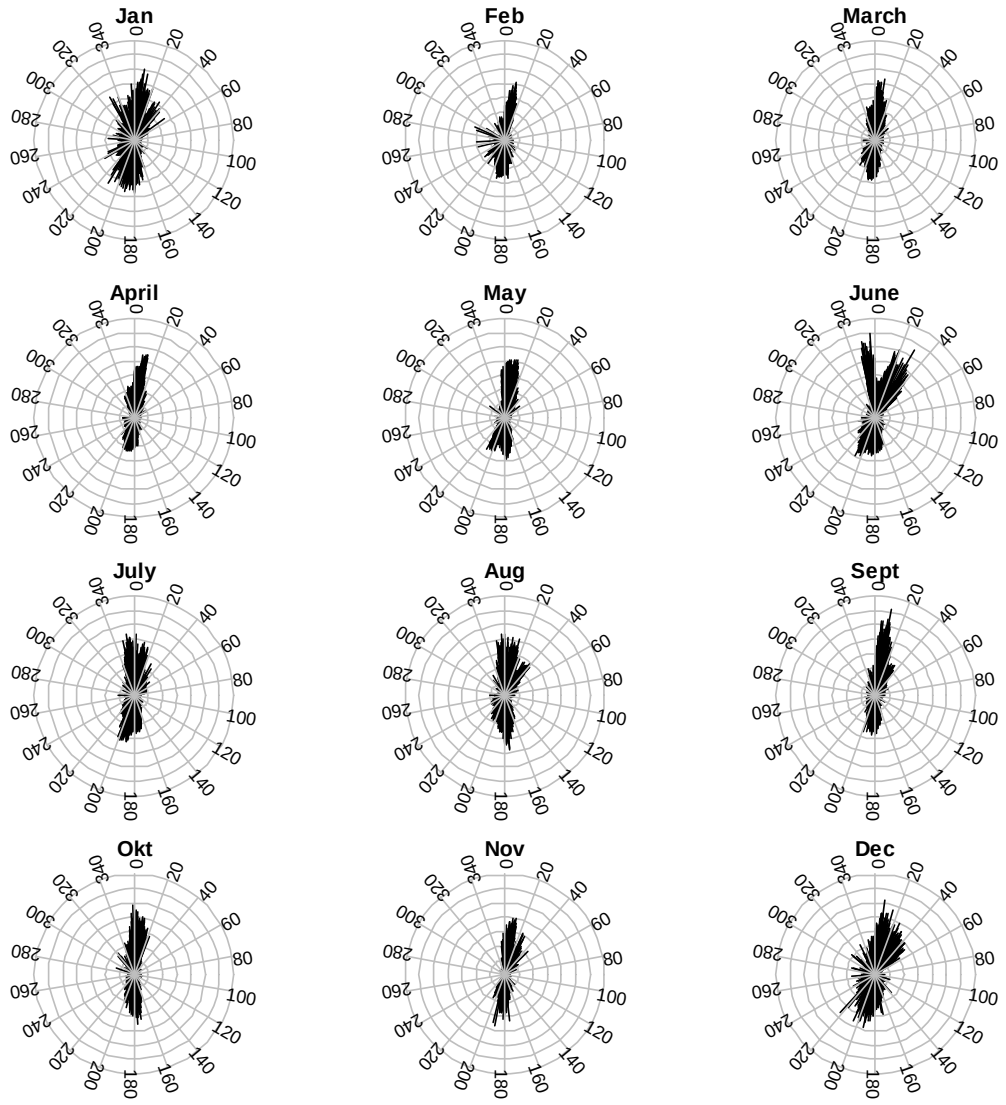

Figure 37 Vector plots of current direction and strength by month in 2011 and 2012 at 140 cm above the bottom . Radial grid steps reflects current speed in steps of 0.2 m/s. Outer circle is maximum speed of 1.4 m/s. Labels around outer circle is current direction in degrees.

The absolute current strength at 140 cm is higher than the current measured at 30 cm above the bottom (Figure 38). Especially during storm events (Figure 39). In some deployment periods we however observed that the difference between the current speeds at the two heights was dependent on the tide. Most likely this is caused by the fact the physical construction of the lander caused a lee side for one of the two current meters. In this stage it is unclear which one. This effect is most likely linked to the orientation of the lander in relation to the main current direction.

Because the Vektor current meter measured in 2 minute long burst with a frequency of 1 measurement per second, the minimum and maximum pressure measured during that interval could be used to obtain the amplitude of the pressure difference. This gives in indication of wave heights and the occurrence of storm events (Figure 40).

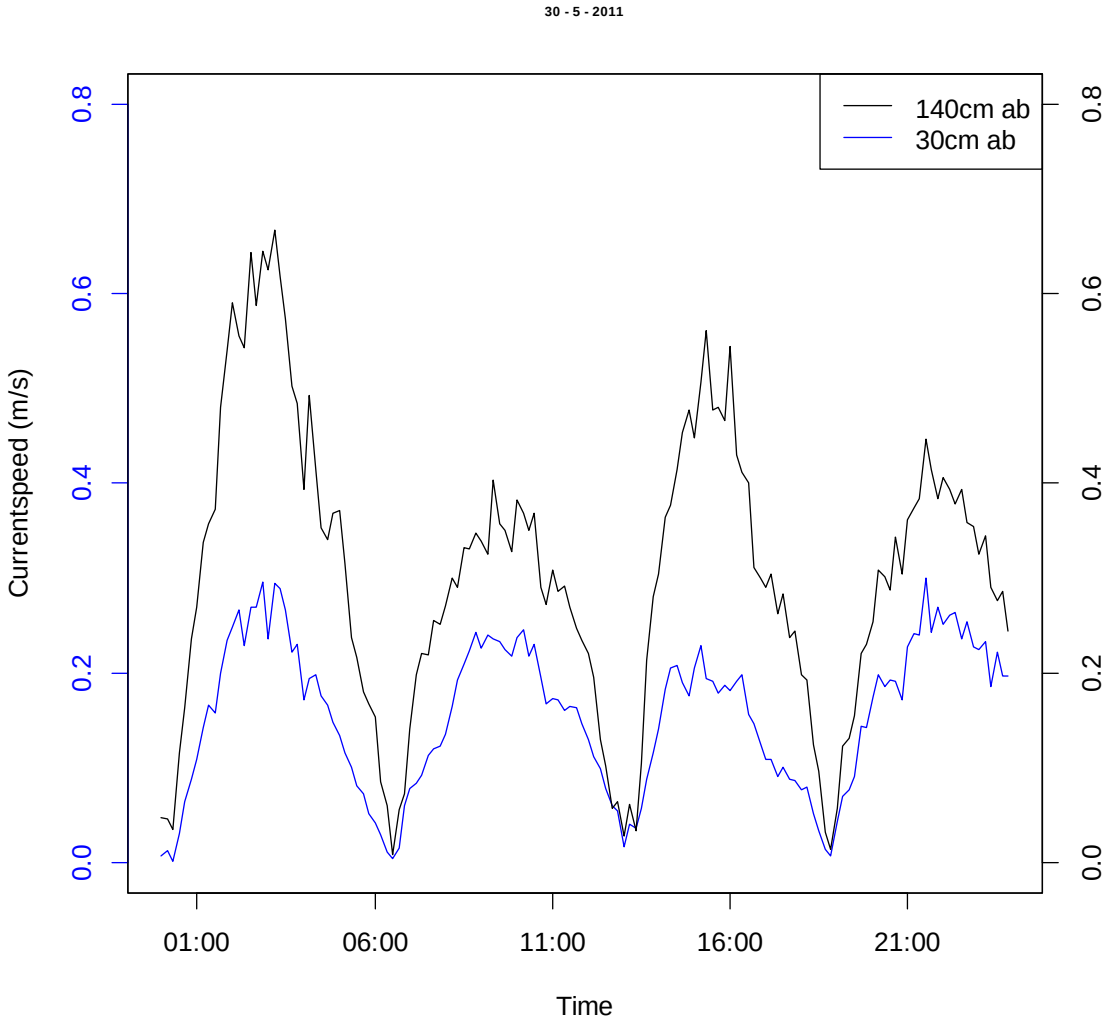

Figure 38 The measured currentspeeds at 140 cm above the bottom (Aquadop) and at 30 cm above the bottom (Vector) for 1 day i.e. May 30th 2011.

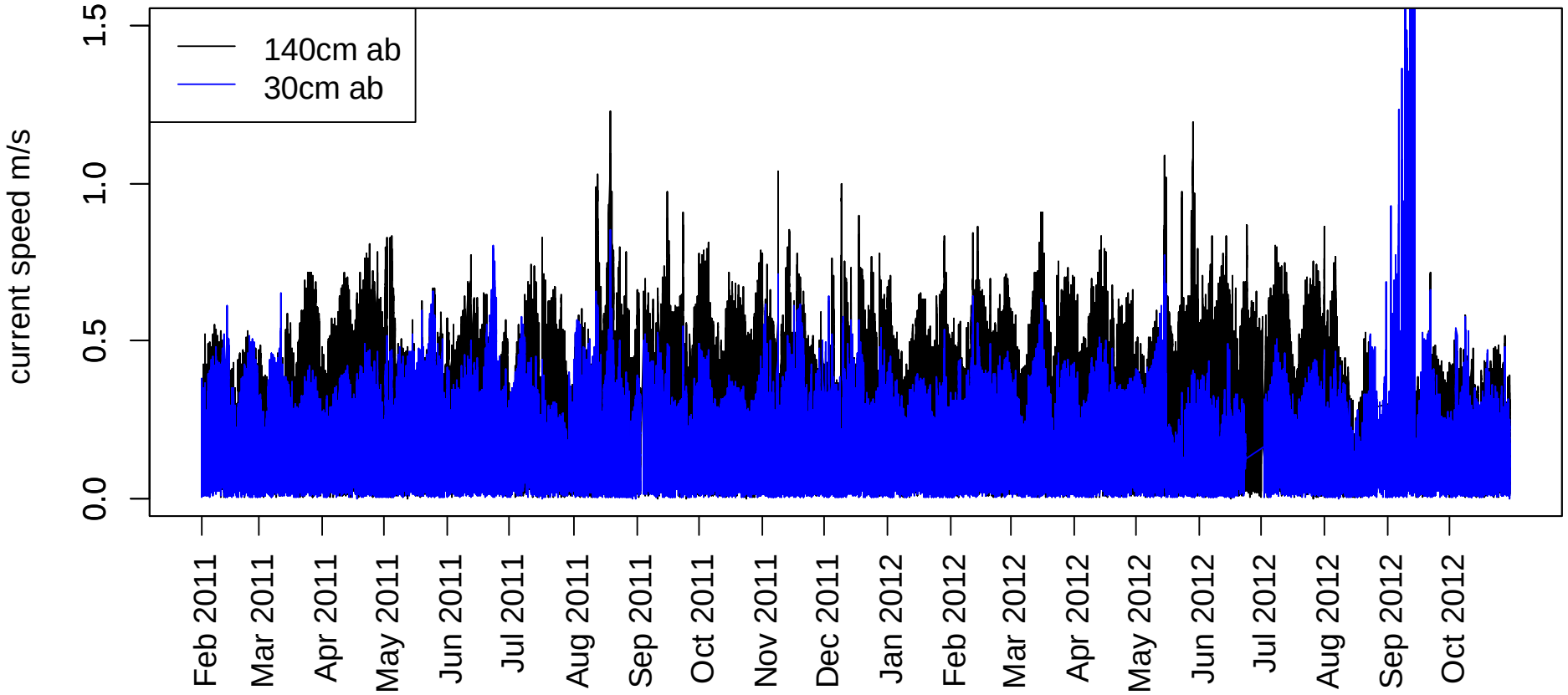

Figure 39. The measured currentspeeds at 140 cm above the bottom (Aquadop) and at 30 cm above the bottom (Vector) for the entire measurement period. The peak current speeds measured in September 2012 at 30cm above the seafloor probably relate to a measurement error of which its cause could not be resolved at the time of publication of this report.

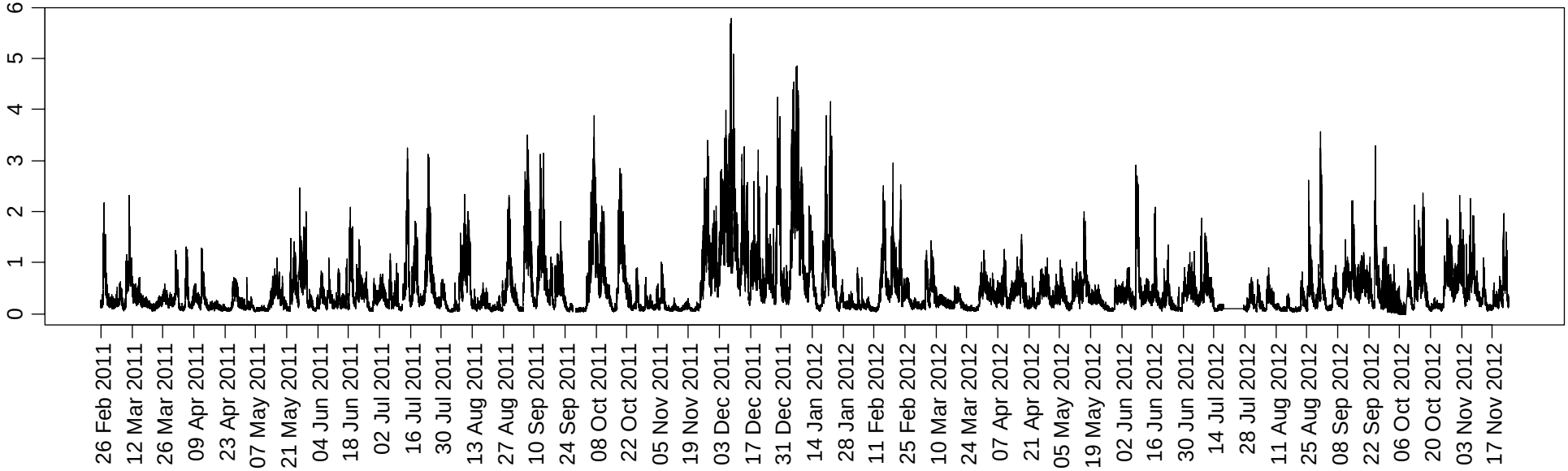

Figure 40. Maximum observed wave induced pressure variations, determined on basis of the difference between minimum and maximum measured pressure within one burst measurement period of 2 minutes length.

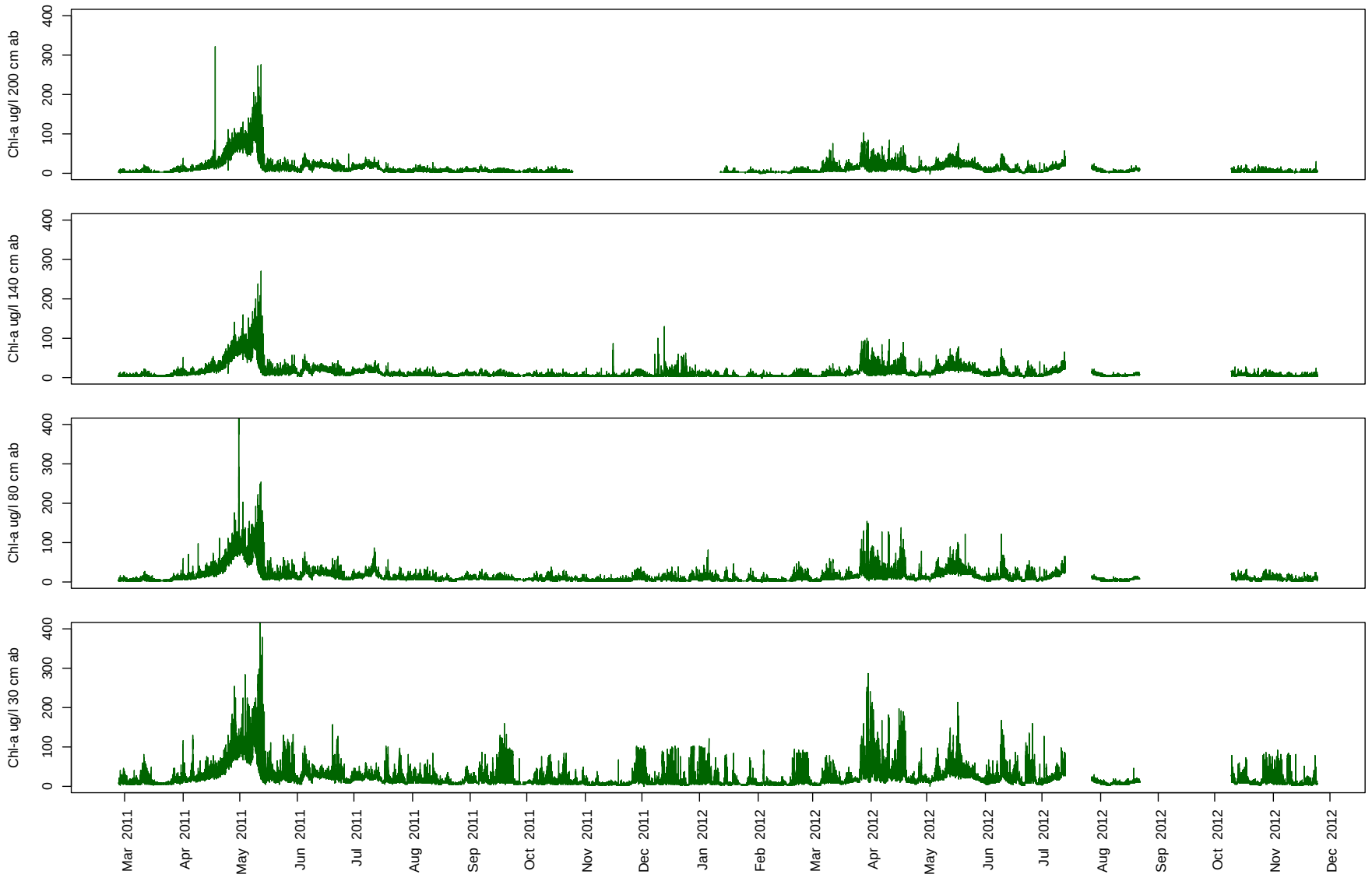

Figure 41 Record of the chlorophyll-a concentration measured off the coast of Egmond at four heights above the bottom.

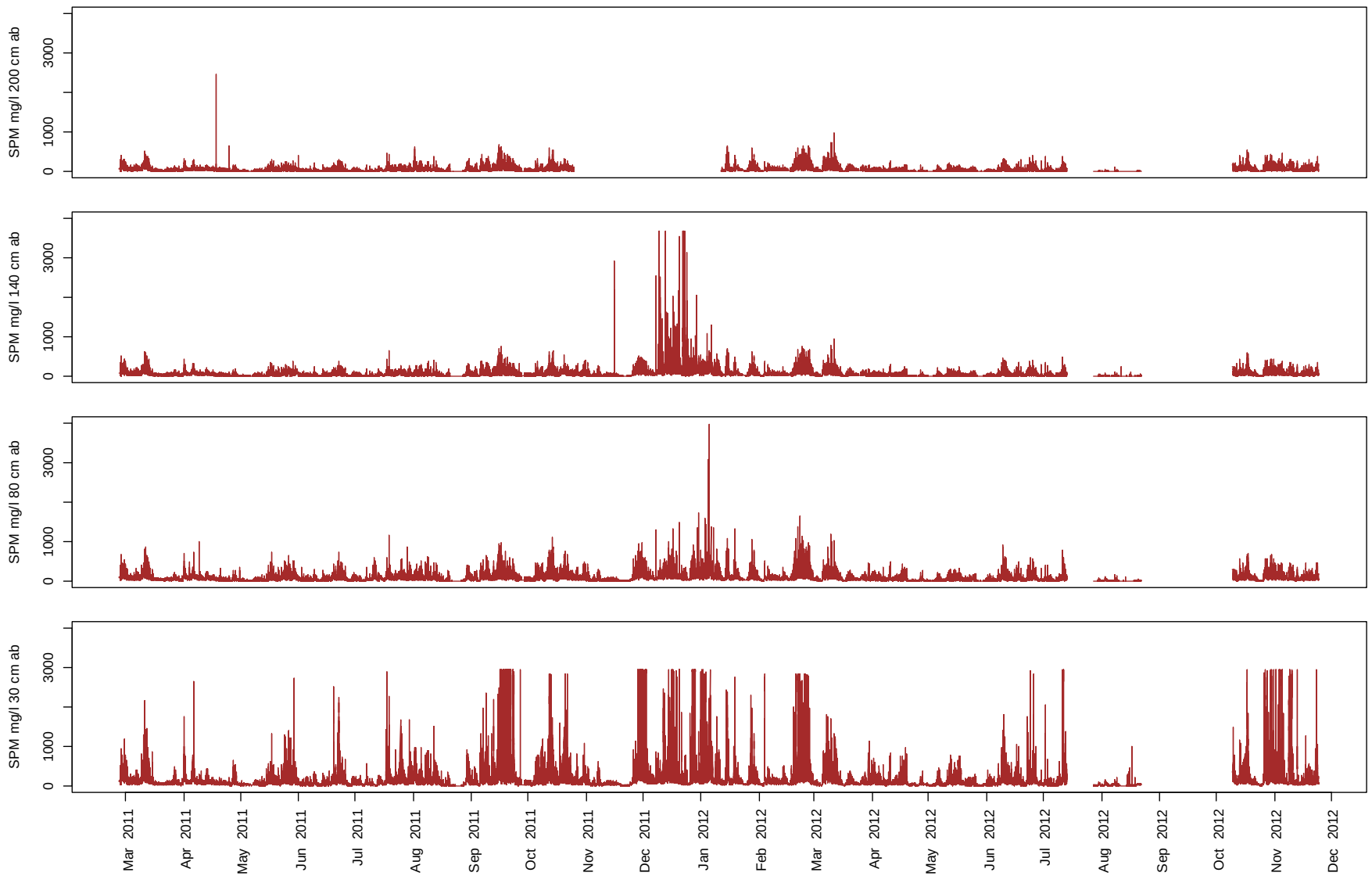

Figure 42. Record of total suspended matter measured off the coast of Egmond at four heights above the bottom.

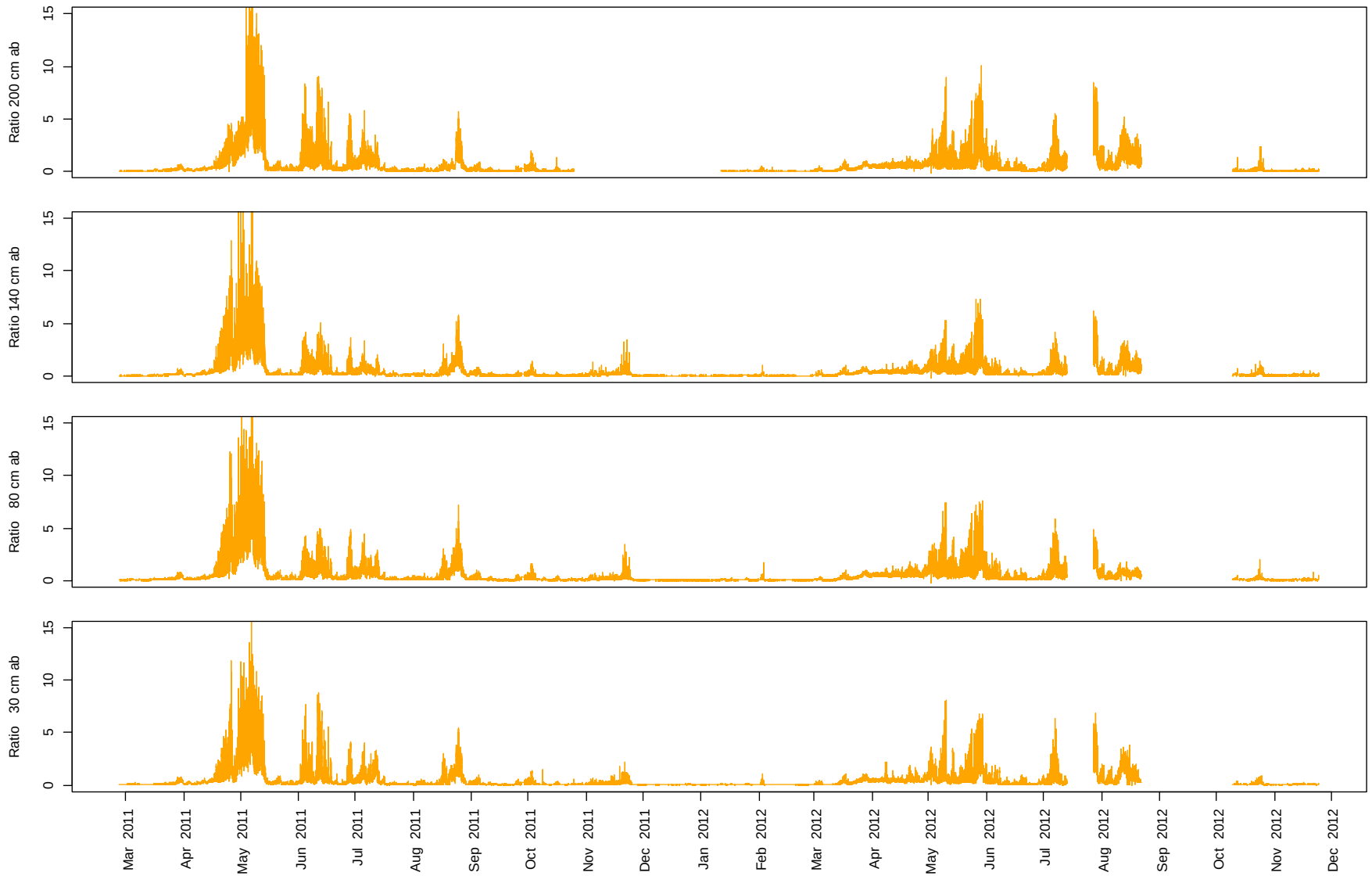

Figure 43 Time series of the Ratio (ugr Chl-a/mg SPM) between chlorophyll (µgr/l) and SPM (mg/l) off the coast of Egmond at four heights above the bottom

3.6.3 Suspended matter and Chlorophyll.

Fluorescence and turbidity has been measured at four heights above the bottom. These data have been summarized in Figure 41- Figure 42, Figure 54 and in Table 9.

Maximum Chl-a concentrations are measured in April and May during the spring phytoplankton bloom and the highest Chl-a and SPM concentrations were mostly measured closest to the seafloor. It is obvious that the spring bloom in 2011 was much more intense and more time constrained than in 2012. On average, the concentrations of Chl-a is a factor of 2 higher in the near bottom layer when compared to the concentrations at 200 cm above the bottom. The animals living at the seafloor thus experience higher concentrations then what is measured higher up in the water column.

Although there is a seasonal variation in the concentration of SPM, it is less distinct than the seasonal trend in Chl-a. Highest concentrations are generally found during the winter months and these can be as high as 3-3.5 grams/litre. On average the concentration at 30 cm above the bottom is about 2.5 times higher when compared with the concentrations at 200cm above the bottom.

The ratio between the Chl-a concentration and the concentration of SPM is an indicator of the quality of the material available as food for benthos. A plot of this parameter over time more clearly defines the bloom periods in the remainder of the year in terms of potential food availability and quality. This plot also shows that especially in 2011 there are several short period during the summer with phytoplankton blooms leading to short-term increases in the Ratio between Chl-a and total SPM (Figure 43).

The seasonal development of the phytoplankton with a spring bloom causes that the qualitative characteristics of the material differs markedly between seasons. This is most evident from Figure 44 where the Chl-a concentrations have been plotted against turbidity for each month separately. This figure shows that during the spring bloom (April – May) the ratio between both dramatically increases, visualized as increasing slopes, ultimately resulting in the presence of two clusters of material in May. After May this separation gradually disappears and merges in material with a more uniform composition in terms of the Ratio.

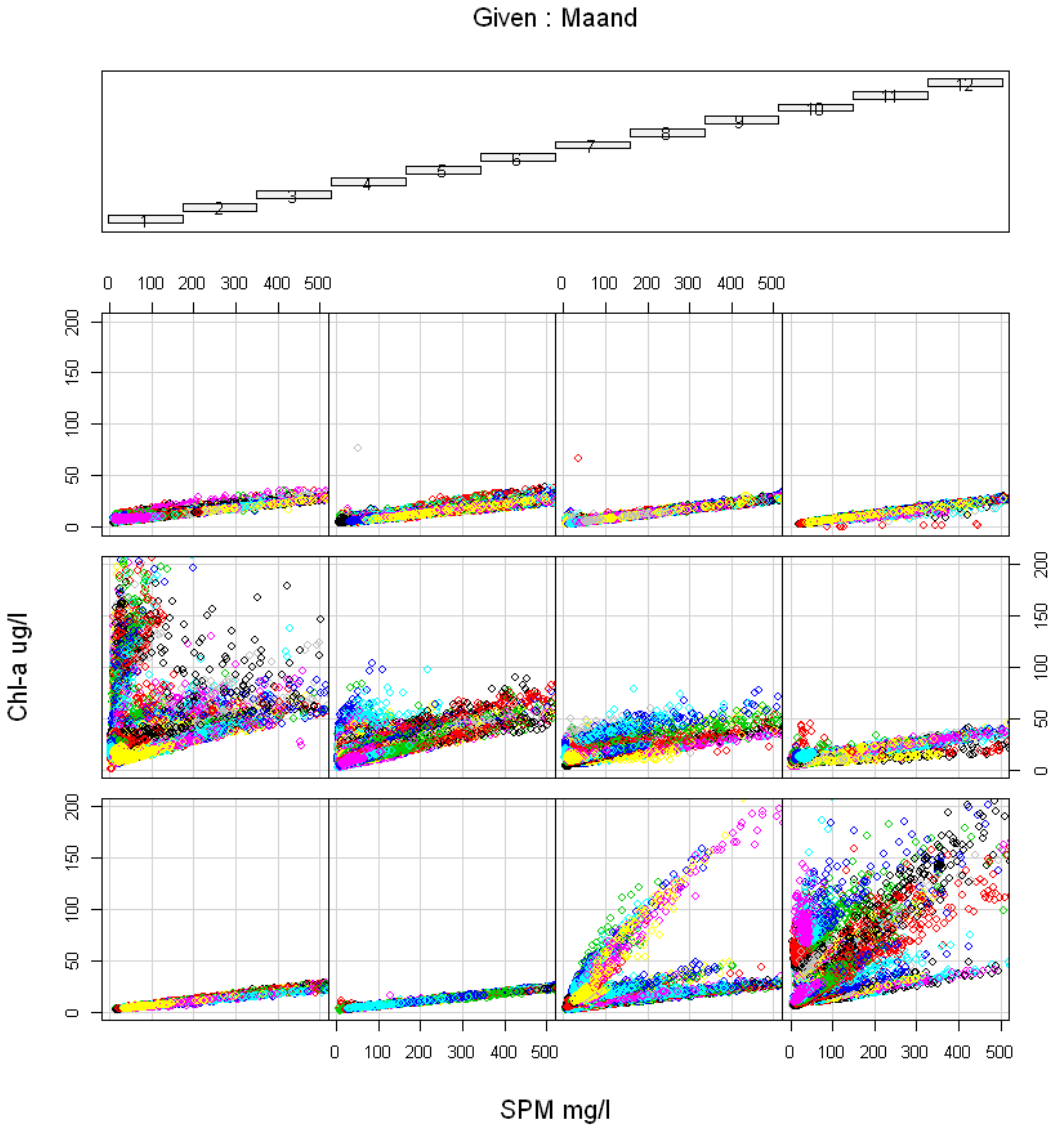

Figure 44. Monthly change in the ratio between Chl-a and SPM over the years 2011 and 2012. Lowest row is January to April, Middle row is May to July and top row denotes the month September to December. Similar symbol colours within each panel indicates values measured at the same day. It is clear that in April there is a gradual change from a low ratio SPM material to a double peaked spectrum in May. In the months following the spring bloom the spectrum becomes narrower suggesting that the chlorophyll rich part of the SPM gradually disappears.

There is not only a seasonal difference in the amounts and quality of the suspended material, but also differences at different heights above the seafloor. These differences in the vertical have been explored in more detail by plotting the Chl-a and the SPM concentrations at the different depths against those measured at the other depths, together with the 1:1 diagonal line indicating equal concentrations. Thus the positioning of the data points, relative to that line, gives information to what extent the observed concentrations of suspended material at both heights are equal and correspond to each other. The figure shows that the concentration of SPM at 30cm and at 80 cm is always higher than the concentration at the other depths. Only the SPM concentrations at 140 and 200 cm height match and fall around the 1:1 line. For Chl-a this already happens with the concentrations measured at 80 cm and 140cm (and higher). This suggests that there is a strong vertical gradient in the amount and quality of the material above the seafloor and furthermore that SPM and Chlorophyll behave differently in terms of sedimentation and resuspension (Figure 45).

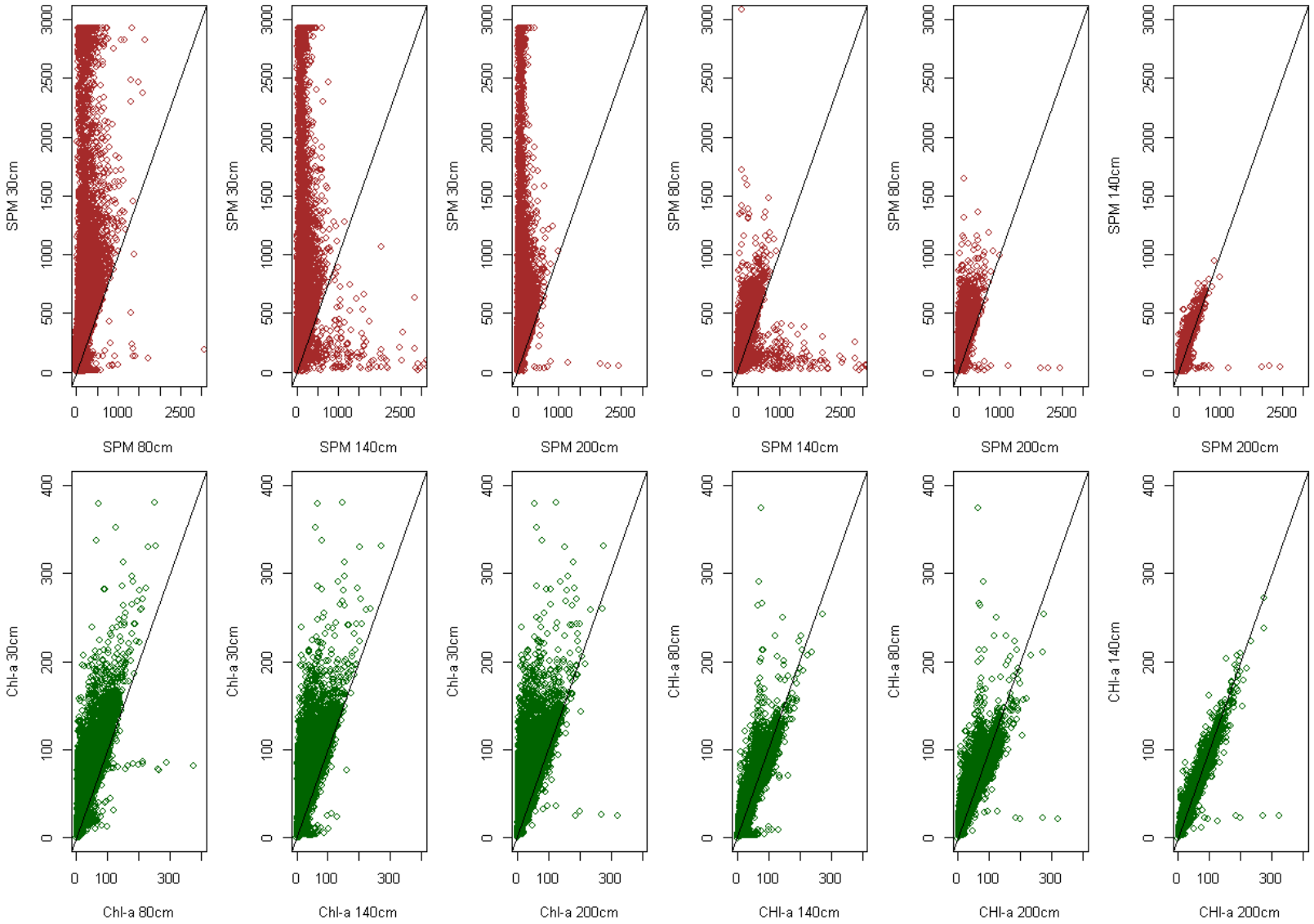

Figure 45. Comparison of the concentrations of SPM and Chlorophyll at the different depths. If the concentrations are equal, the points should fall on the 1:1 diagonal line. The figure illustrates that there is a difference in settling rate between SPM and Chl-a thus causing quality difference at different heights above the bottom.

Table 8. Average SPM concentration (mg/l) at the four depths above the seafloor off the coast of Egmond in the period that the lander was deployed. In August and September 2012 no or only some data were collected. The average value, based on incomplete series of measurement is annotated with *

Year	Month	SPM 30cm	SPM 80cm	SPM 140cm	SPM 200cm
2011	Feb	247	162	138	117
2011	March	117	78	67	60
2011	April	102	72	59	64
2011	May	112	72	54	46
2011	June	92	59	43	38
2011	July	115	81	52	49
2011	Aug	115	69	50	52
2011	Sept	309	115	92	90
2011	Okt	217	123	86	74
2011	Nov	143	62	53	-
2011	Dec	333	137	181	-
2012	Jan	236	131	100	75
2012	Feb	247	124	95	90
2012	March	131	90	76	79
2012	April	84	51	36	34
2012	May	65	40	30	28
2012	June	150	81	57	50
2012	July	103	44	33	32
2012	Aug	22*	12*	13*	9*
2012	Sept	-	-	-	-
2012	Okt	245	106	88	86
2012	Nov	234	94	79	76

The effects of different resuspension and settling behaviour of SPM and chlorophyll rich particles is especially evident during spring periods with lots of fresh and light weight organic material present during quiet weather conditions. In such conditions wind induced wave and current effects are minimized. Observations on selected days suggest that during such circumstances a “blanket” of suspended material settles during slack tide. The time difference between the time of recording the peak concentrations of settling material between the top two sensors (200 & 140cm) and the bottom two sensors (30 & 80cm) is evident (Figure 46). This observation suggests a sequential settling of material of different densities. It also suggest that above the bottom layers with different particle properties and densities are present. This is also suggested by the results presented in Figure 45. and most likely implies that the chlorophyll rich particles and the inorganic SPM are only partially linked. This aspect should be analysed in more detail as it might give a clue to settling velocities of the various categories of suspended materials.

Table 9. Average Chl-a concentration (ug/l) at the four depths above the seafloor off the coast of Egmond in the period that the lander was deployed. In August and September 2012 no or only some data were collected. The average value, based on incomplete series of measurement is annotated with *

Year	Month	Chl-a 30cm	Chl-a 80cm	Chl-a 140cm	Chl-a 200cm
2011	Feb	12	6	6	5
2011	March	11	6	7	6
2011	April	42	36	30	31
2011	May	58	42	42	42
2011	June	27	20	18	17
2011	July	20	15	13	13
2011	August	13	9	8	8
2011	Sept	18	9	8	7
2011	Okt	13	7	7	6
2011	Nov	9	6	5	-
2011	Dec	16	7	7	-
2012	Jan	12	7	6	4
2012	Feb	11	6	5	4
2012	March	21	15	13	15
2012	April	35	19	18	17
2012	May	31	23	21	21
2012	June	22	12	10	9
2012	July	22	16	15	14
2012	Aug	8*	6*	6*	6*
2012	Sept	-	-	-	-
2012	Okt	15	9	7	7
2012	Nov	12	7	5	5

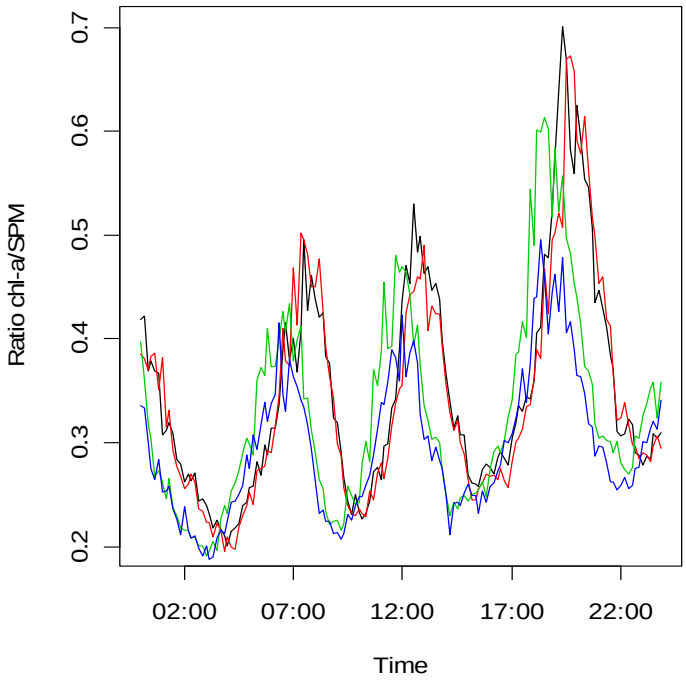

Figure 46. The tidal induced temporal variation of the Ratio of Chl-a/SPM in the bottom 2 meters as measured with turbidity fluorescence sensors at four heights above the seafloor on April 11th, 2011. Black line 30cm above the bottom, redline, 80cm above bottom, blue line 140cm above bottom and green line 200 cm above bottom. Note for 11 April 2011 the time lag at which the peak values are measured between the two highest and two lowest height levels.

The seasonal effect on the Chl-a/SPM ratio is in all seasons modified by current speeds and wave action. In Figure 47 a plot of the relation between current speed and ratio for each month demonstrates the strong seasonal effect caused by the abundant presence of light organic particles in spring and early summer.

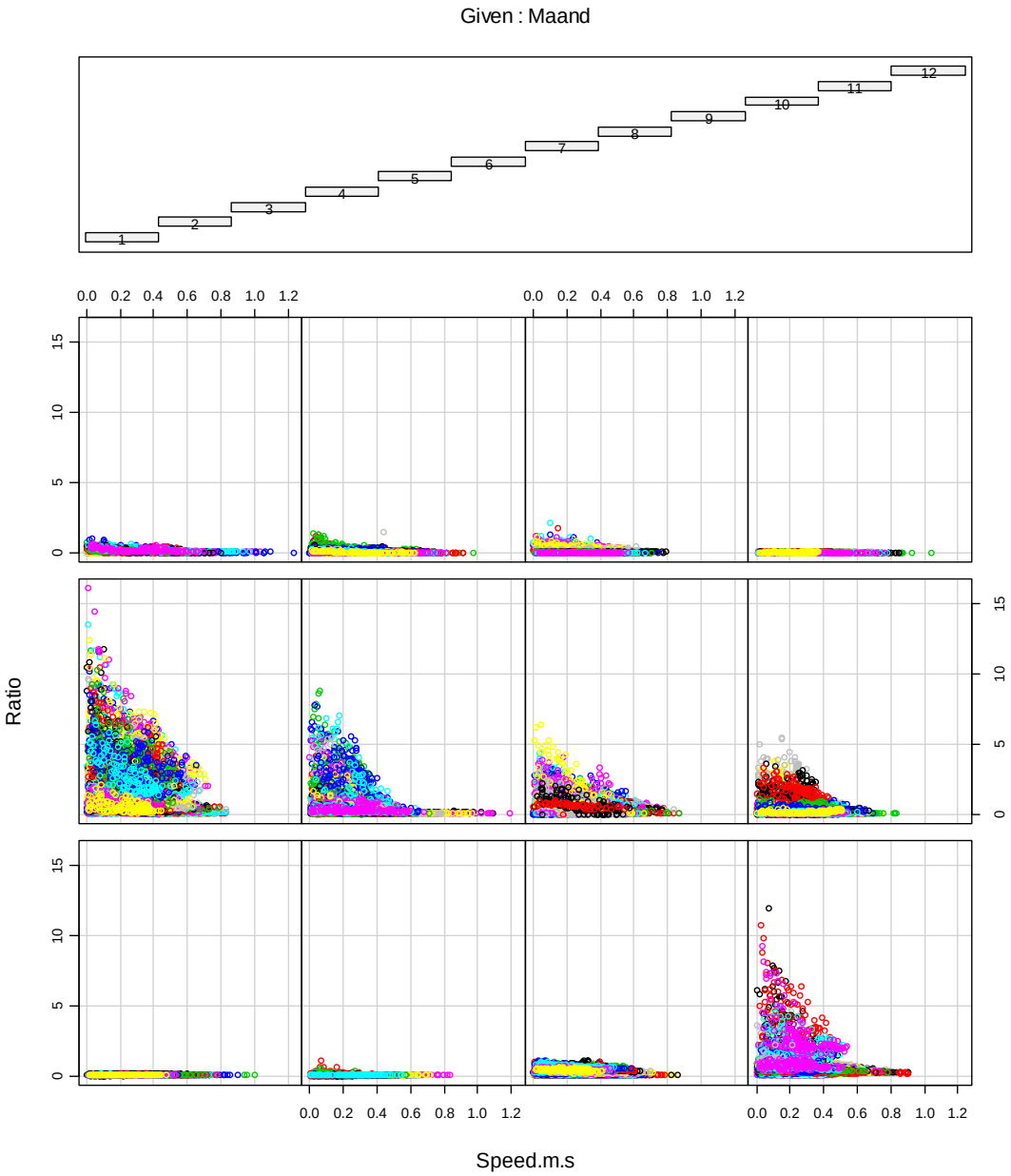

Figure 47. Relation between the Chl-a/SPM ratio at 30cm above the bottom, plotted against current speed, for each month in the year. 2011 and 2012(up to July 2012). starting with January in the left down corner and ending with December in the top right corner.

The limited water depth at the deployment location makes the bottom “vulnerable” to effects of waves. This is best illustrated when the record of suspended matter and wave heights are plotted against each other (Figure 48) or plotted as superimposed time series (Figure 51) . At increasing wave amplitudes the minimum concentrations of suspended material significantly increase. Close inspection of the time series of SPM and wave height suggests that there is a time lag before material gets resuspended and that it might take several days before material has settled again. During the resuspension events also an increase in the concentration of Chl-a is recorded. Apparently fine particles with attached chlorophyll are released from the sediments

and that this fraction may potentially act as a “food bank” for the local fauna. The exact origin of this "fresh" material is unclear. It might represent freshly buried pelagic phytoplankton which is sequestered in the bottom where it is preserved under anoxic conditions before it is released by a storm. Alternatively it can point to a local source in the form of epi-phytobenthos brought into the water column during severe wind events. Microscopic analyses of aggregates caught confirm the presence of benthic diatoms (BWN, 2011 unpublished results). Especially the shallower fore shore parts (less then 10 meter) might host such a epi-phyto-benthic community. In this zone, light penetration is potentially high enough to promote primary production at the seafloor. Subsequent release and export of this material might likewise explain the high concentrations of Chl-a in the bottom layer during and shortly after storms. It might also contain the clue why densities of *Ensis directus* are highest so close to the coast (BWN 2011, unpublished results).

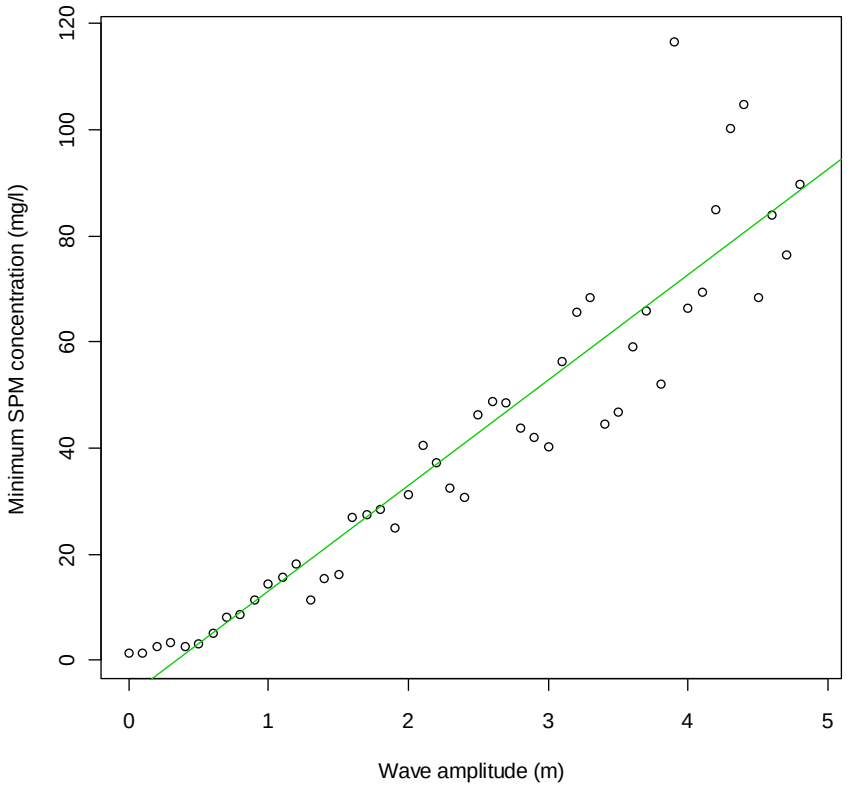

Figure 48. Quantile regression between the minimum SPM concentrations (0.1 quantile) and measured wave amplitude, measured at 30cm above the seafloor over the entire experimental period. Mass of points lying above the line are not plotted.

During a cruise in the same area for the Building with Nature program, there was a beach nourishment taking place at a location close to the lander at a distance of only approximately 500 meter. We documented the approximate (visual observation) times at which the two ships (IJsseldelta & Amazone) were dumping their loads. In Figure 49 the near bottom SPM concentrations have been plotted together with these records. The figure shows that most of the dumping actions (grey bars) are followed by a small peak in SPM at 30cm above the bottom. During this day weather conditions were calm (3-5 Bft south westerly wind) and the maximum wave height amplitude varied between 0.3 and 0.5 meter. Figure 48 shows that at these wave heights the minimum SPM concentrations close to the bottom remain constant, which makes it likely that the observed peaks in SPM are due to the dumping actions.

On June 24th the beach nourishment was still ongoing and in Figure 50 the frequency distribution for the Ln(SPM) concentrations for that day, the entire month of June and the entire year (2011) are plotted for 30cm and for 200 cm above the bottom . This figure shows that during that day the near bottom concentrations (30cm ab) were skewed towards the higher concentrations classes when compared to the monthly average or the remainder of the year without the month of June. Since the concentration classes have a natural logarithm as base it means that concentrations were approximately 3 times higher. At an height of 200 cm above the bottom the concentrations on June 24th are only slightly higher than in the rest of the month or entire year. The difference between both heights suggests that the SPM which is released in the water column because of the nourishment, rapidly settles and apparently tends to spread over the bottom as a "blanket".

The observations made on June 24 it suggest that the increase in the load of suspended matter at 30 cm above the seafloor and close to the area of dumping is significant. Absolute concentrations (54 and 729 mg/L) are however still relatively small when compared to those measured during storms (>3000mg/L) causing resuspension because of waves (Figure 51 and Figure 52).

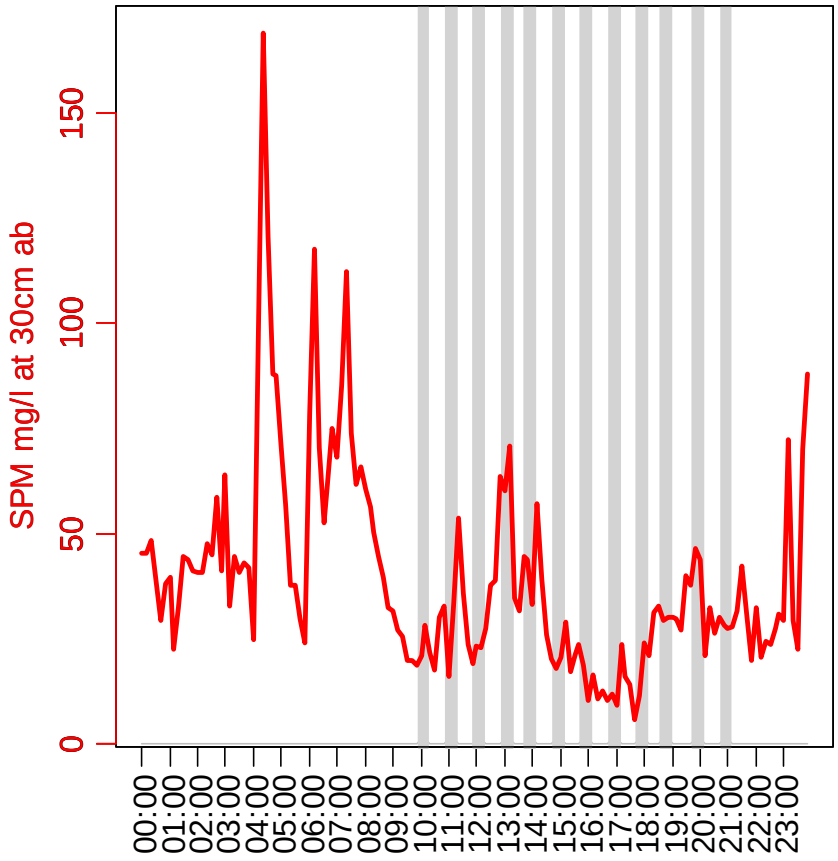

Figure 49. The measured SPM load at 30 cm above the bottom over time on June 6th 2011 when two ships were working actively on a beach nourishment at an approximate distance of 500 meter from the measurement platform. The grey vertical bars indicate the time frames at which the ships dumped their loads. Many of these grey bars are followed by slightly elevated SPM concentrations.

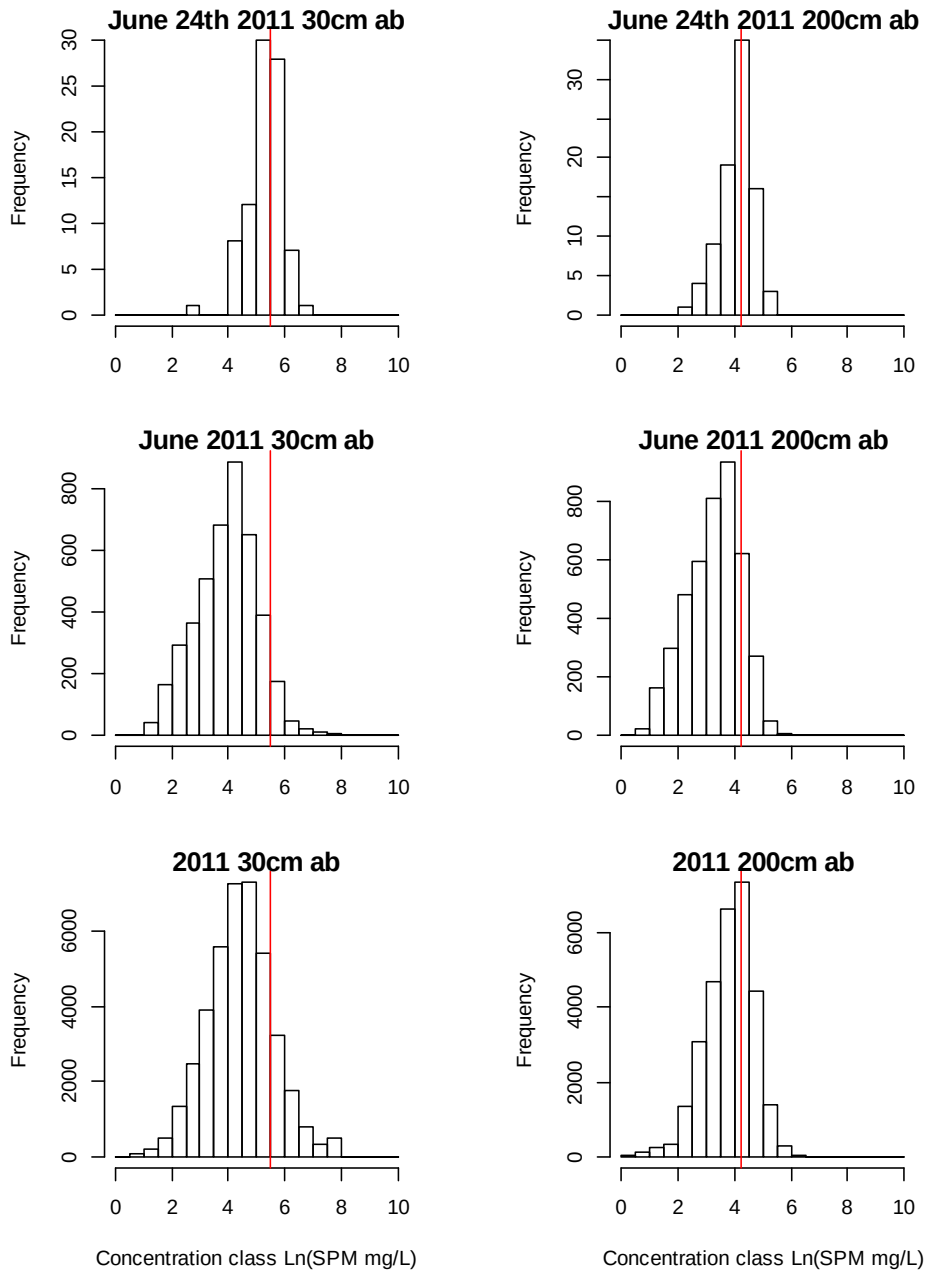

Figure 50. Comparison of the frequency of occurrence of SPM concentrations at 30 cm above the bottom. SPM in Ln(concentration). Measurement frequency was 1 burst measurement per 10 minutes. The red line gives the most common frequency on June 24th at 30 cm and 200 cm above the bottom.

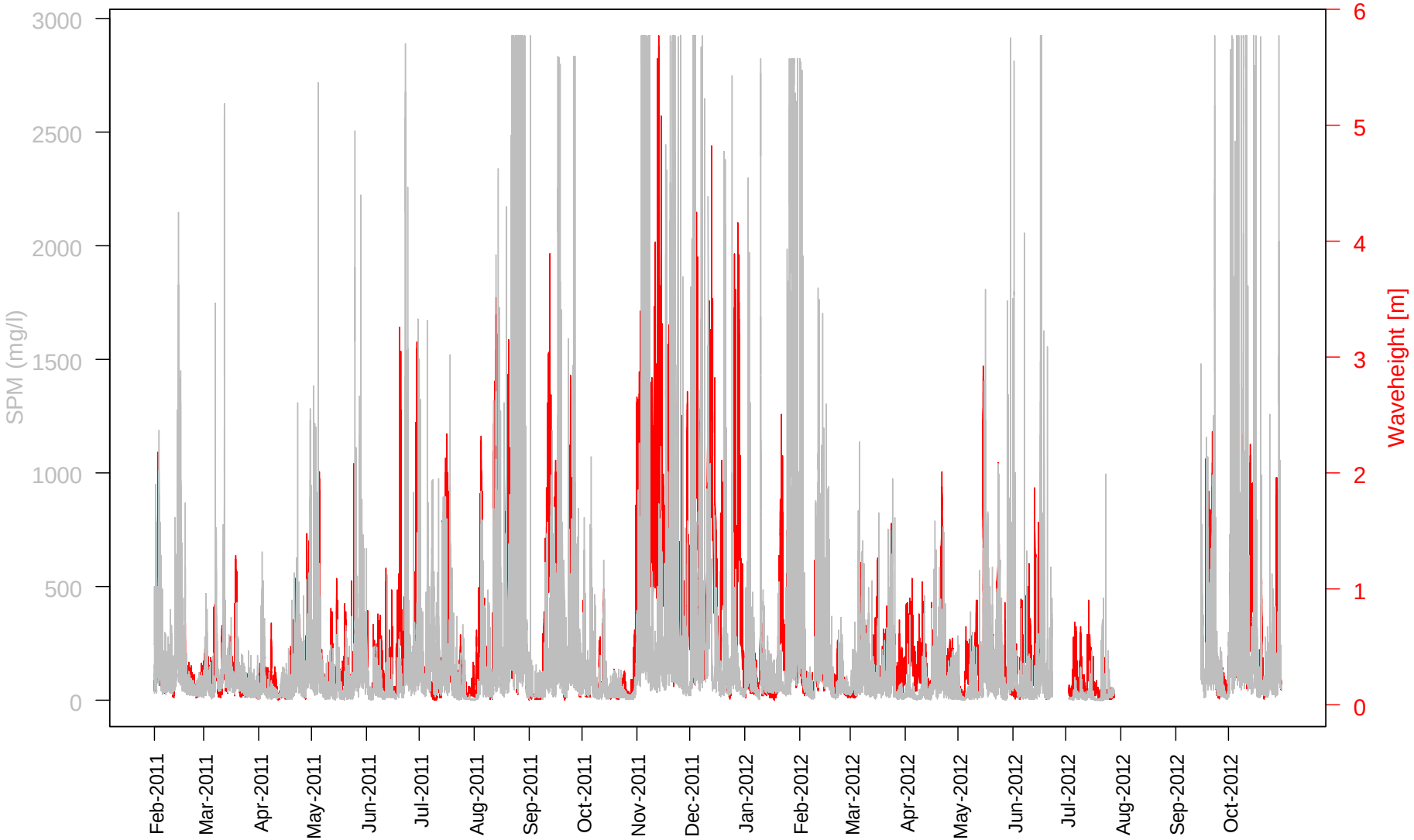

Figure 51. The SPM concentration and the wave heights measured at 10 minute intervals. The alignment of “wave events” and increases in the concentration of suspended material at a height of 30 cm above the bottom is evident.

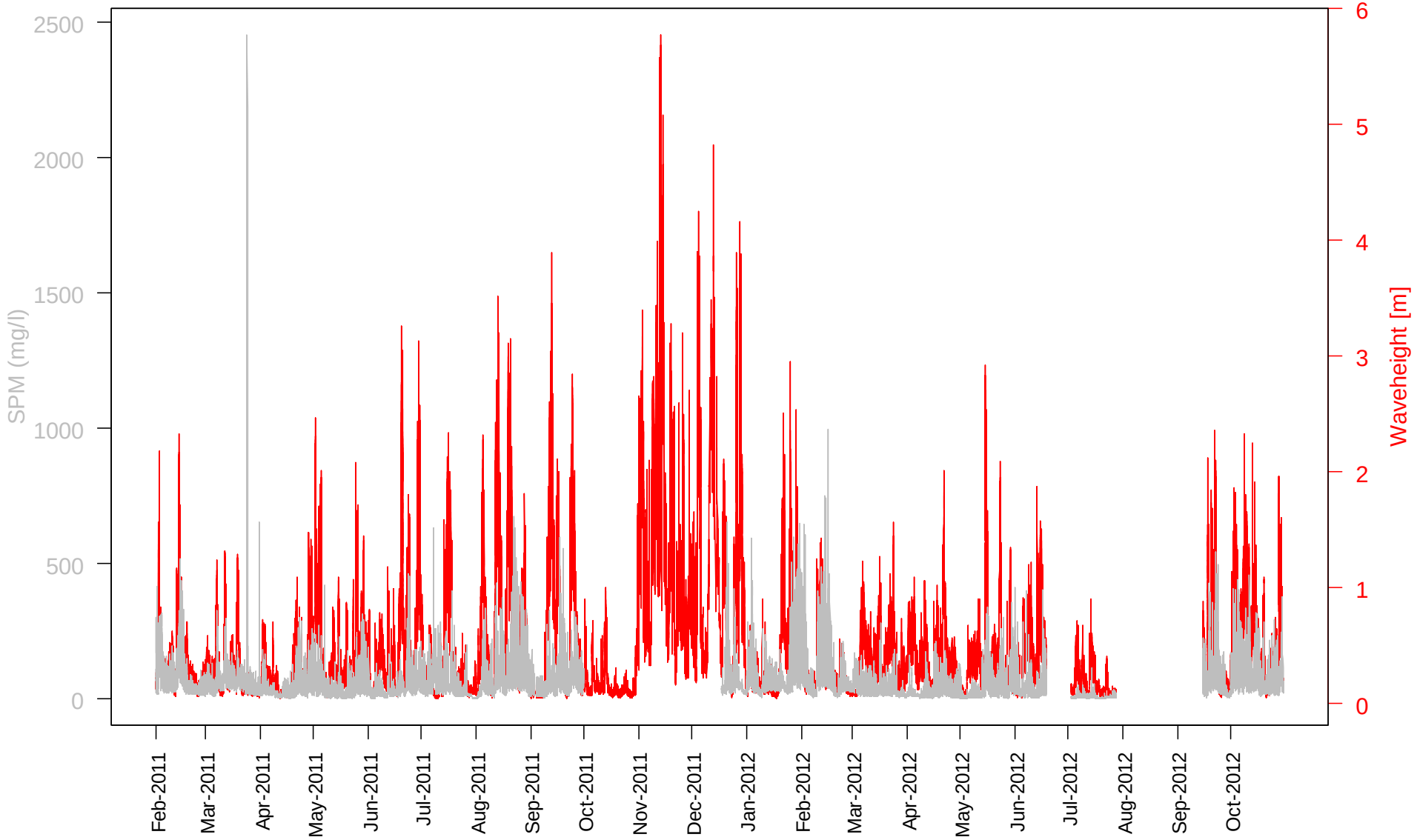

Figure 52 The SPM concentration and the wave heights measured at 10 minute intervals at an height of 200 cm above the bottom. The alignment of “wave events” and increases in the concentration of suspended material at a height of 200 cm above the bottom is evident.and shows the same pattern as measured at 30cm ab but the maximum SPM concentrations are lower than at 30 cm above the bottom.

3.6.4 Sediments.

During each lander service operation sediment samples were taken from the boxcores. These samples have been analysed for mud content and median grainsize. From every boxcore one sub core was taken. Thus for each station and date, two sediment samples were available. Average mud content over all samples (<63um) was 5.3%. Median grain size was 190 µm. The percentage of mud at station LSW (mean=7.9) is marginally significantly different when compared to the two eastern stations (LSE & LNE). The median grain size at the southern stations (188-186µm) tends to be lower than the northern stations (196-191µm)
Plotting the measured median grain size and the percentage of mud shows that there is a huge variation between the different samples taken at each date. There is a weak but insignificant trend of increasing median grain size in the winter months and increasing mud contents in the summer months (Figure 53).

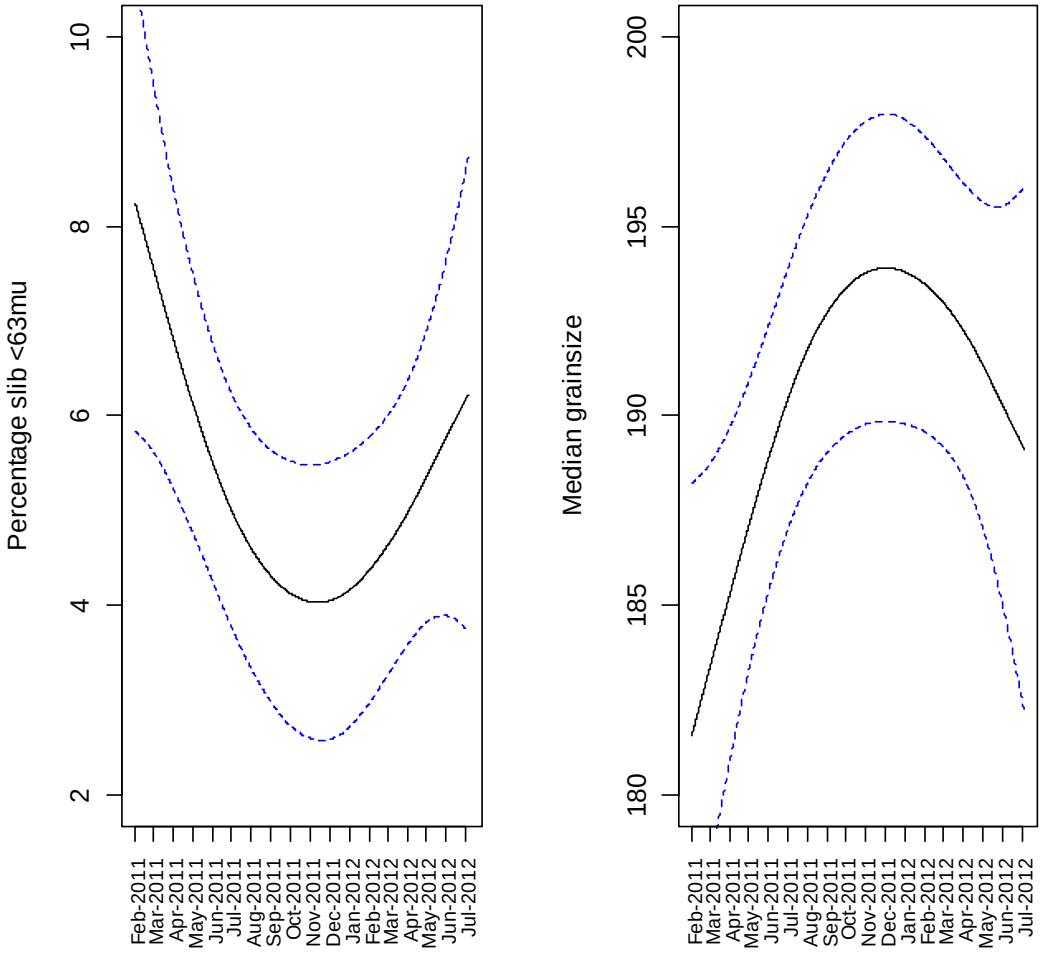

Figure 53. Tentative seasonal trends in median grain size and mud content of the top 5 cm bottom layer of the sediment samples collected from the four stations around the lander (LNE, LNW, LSE, LSW). Fitted smoother models are non significant but suggest a seasonal trend.

4 DISCUSSION

The dominant seasonal cycles as measured over the two years of monitoring are plotted in Figure 54. These appear to be the main environmental conditions against which the seasonal trends in growth and condition of *Ensis directus* relates to (Figure 25).

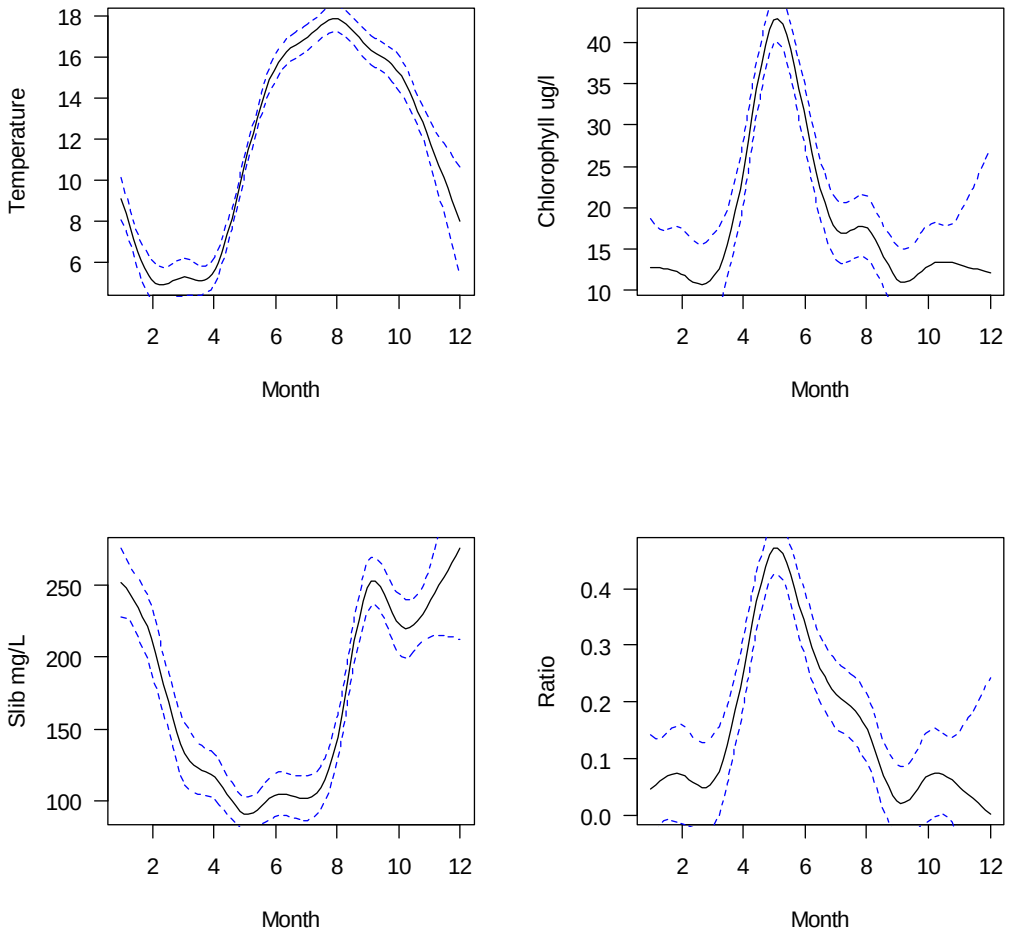

Figure 54. The average seasonal cycles in Temperature, Chlorophyll, SPM and the Ratio between Chlorophyll and SPM, all measured over the period February 2011-November 2012

The seasonal trends in somatic and gonadal growth correspond closely to those found by Cardoso et al (2009) who followed an *Ensis directus* population from the western Wadden Sea between 2001 and 2003. They found that maximum gonadal mass being only 2.5% of the somatic mass, was low. The population which we followed off the coast of Egmond had a similarly low (maximum) percentage of gonadal tissue. In 2012 the maximum percentage was about 3.5%. Like in the Wadden Sea the amount of gonadal tissue peaks in the period of the spring bloom. For the Egmond location no clear evidence of a second period of spawning could be detected. We observed that the increase in gonadal mass precedes the spring bloom and with that also the increase in body condition. This suggests that early in the process, the development of gonadal mass is at the expense of the somatic mass. Growth of the AFDW and with that, the condition mainly takes place in the period of the spring bloom or shortly after that.

After the summer months *Ensis directus* starts to loose condition most likely because the quantity and quality of the food particles decrease in combination with high water temperatures which are still high, causing increased metabolic rates.
An important determinant of food quality appears to be the amount of suspended inorganic particles (SPM). Kamermans & Witbaard (2009) determined a threshold of approximately 200 mg/l above which clearance rate of *Ensis directus* is reduced. This would mean that between September and March of the following year SPM concentrations are likely to reduce the clearance rate and with that, limit food uptake, irrespective of whether particle quality in the field is sufficient to promote growth. Applying the 200 mg/l concentration threshold also implies that during storm events in the main growth season (April-August) the amount of inorganic suspended matter is likely to hamper food uptake. Especially if is realised that also in this period the average monthly concentrations close to the bottom are just below this value. Analyses show that over the monitoring period (516 days), 20% of the time the SPM records have values above 200 mg/L. Knowing this makes clear that calm periods during the spring bloom form the most important period of the year for feeding and soft tissue growth of *Ensis directus* in this part of the coastal zone. Whether high SPM concentrations really lead to depressed growth rates is unclear as laboratory experiments showed that high kaolinite concentrations (300mg/l) not necessarily lead to depressed laboratory growth rates in small *Ensis directus* (Kamermans & Dedert, 2012). One of the reasons for this observed difference is that natural aggregates and flocs are big and irregularly shaped which directly interfere with uptake and filtration while kaolinite as used in experiments remains suspended as small clay minerals and are possibly easier to deal with in the filtration apparatus of shellfish.

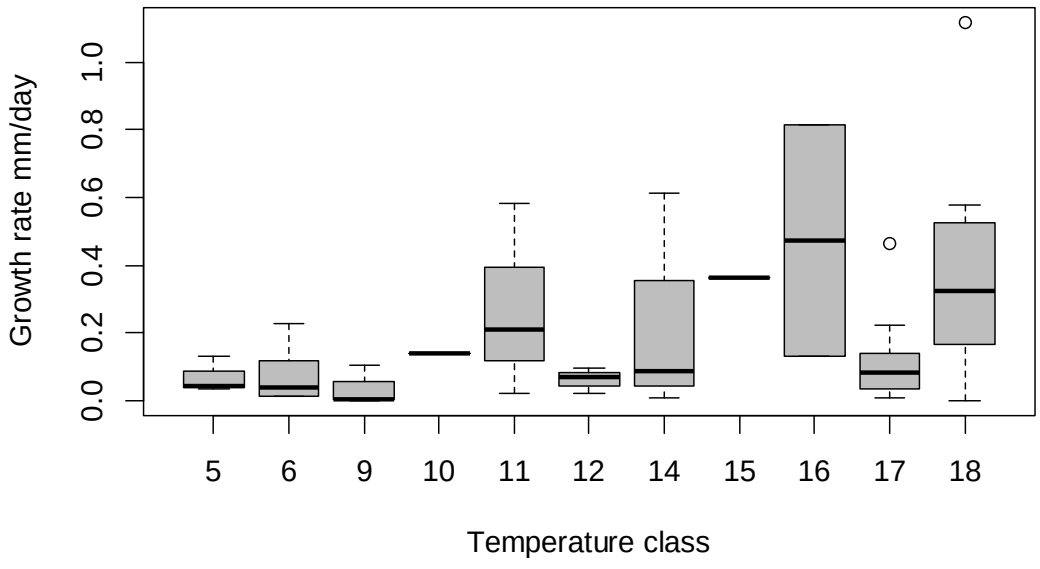

Figure 55. Boxplot of population average shell growth rates plotted against water temperatures in the preceding period.

The shell growth rate determinations are based on sample averages obtained from the four stations around the lander. It appeared that in 1/3 of the cases a negative shell growth rate was obtained. One of the reasons for this are the low shell growth rates in spring and winter in combination with the inaccuracy of shell length measurements (sd measurement=0.34 mm). In

addition to this, we observed in the spring months that especially bigger/older animals were dying (shells with rotten flesh), causing the average size to decrease. From the negative growth rates (which are theoretically impossible in cases of shell length) a standard deviation of 0.22 was calculated. This value can be taken as an estimate for the errors of shell growth rates based on population shell length averages. If the magnitude of this measurement error is taken into account, a weak but significant linear relation between shell growth and water temperature is found. Figure 55 suggests that the optimum temperature for shell growth lies in the upper temperature limit i.e. 16-18 °C although a well defined decrease in shell growth rates in this upper temperature range is not evident. Maximum calculated growth rates which outreach the estimated standard deviation (0.22) are found for temperatures above temperatures of 10°C suggesting that below this temperature shell growth is small, insignificant and below the measurement error. This observation fits well with the back calculated temperature range for shell growth on basis of stable oxygen isotopes by Cardoso et al (2011). They reconstructed water temperatures ranging between 6 and 20°C, and at the same time observed that most of the reconstructed temperature values (as well as most detail) was found for temperatures at 14.5°C or higher. This evidently suggests that shell growth rates are highest at or above that temperature which corresponds to the field measurements presented here.

Ensis directus from the near coastal environment off Egmond also seem to face a large mismatch between the optimal conditions for shell growth and tissue growth. In Figure 56 a tentative optimum curve describing the change in condition in relation to temperature is given. Plotting AFDW against temperature would yield a similar graph as given in Figure 55 because the change in weight is coupled to the change in shell size. Therefore we plotted the change in condition index against temperature because this gives a "size corrected" weight. The graph shows that condition change is largest at temperatures around 10 degrees. Tissue growth thus clearly precedes shell growth in view of the seasonal temperature cycle. Fastest increase in condition coincides with the phytoplankton peak in spring.

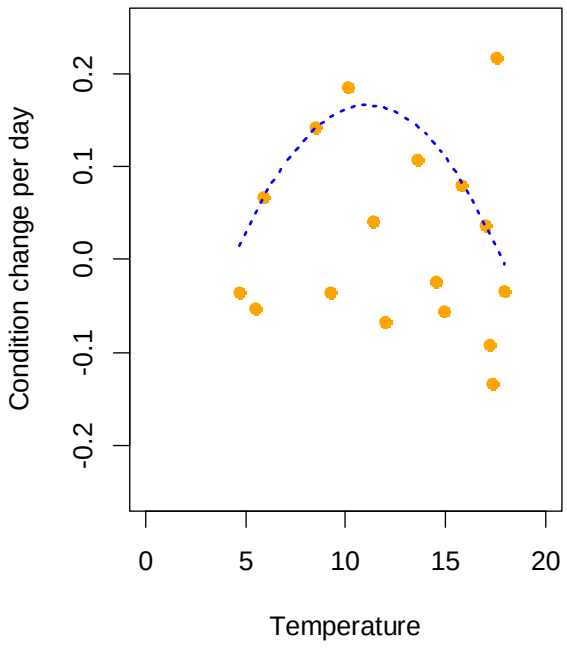

Figure 56. The standardized change in weight (condition index) plotted against the temperature together with a tentative (non significant) 0.75 quantile regression parabolic function.

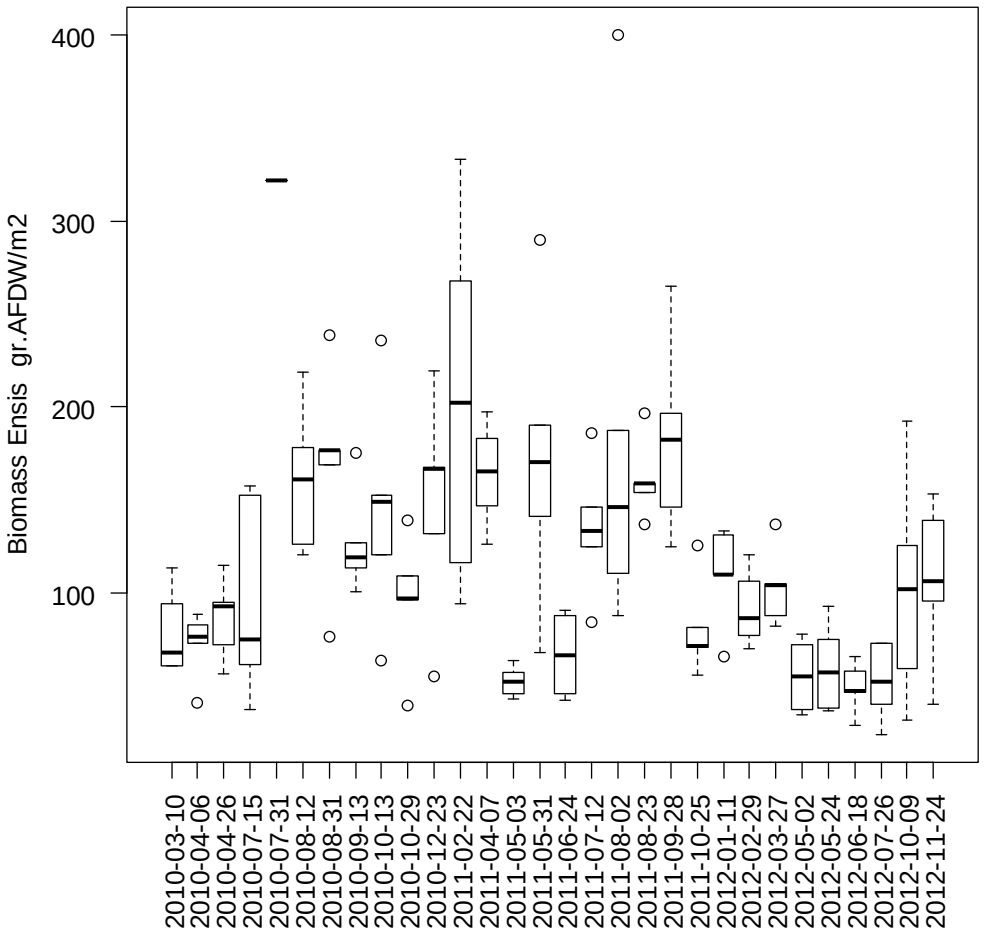

Figure 57. Biomass of *Ensis directus* (gr AFDW) population per m^2 between 2010 and 2012 off the coast of Egmond

One of the questions which remains is whether secondary production by *Ensis directus* is limited by food supply. In 2011 we observed that the stations south of the lander had the highest densities but that average shell size at these stations was lowest (Figure 8; Figure 10). This might indeed indicate that there is a density dependent control on shell growth and fits with the observations made by Palmer (2004). Palmer who worked studied growth in a patch with densities of 2000/m² observed that growth was much lower than what Beukema & Dekker (1995) found at densities of 6/m². On basis of data collected since 1982 Dekker & Beukema (2012) come to the conclusion that variability in production by *Ensis directus* could largely be explained by the initial densities of the 0-group individuals at the end of their first winter and production seems to be maximal in the second year of life (Dekker & Beukema, 2012). This is supported by Figure 57 for which we calculated the average biomass/m^2 for each sampling date (on basis of average length and average density) and plotted this against time (Figure 57). The cohort which settled in 2009 shows a steady increase in biomass during 2010 and a decrease in total population biomass since the end of 2011. Peak biomass values were found in 2011 when the average size was about 90 mm and the animals were 2 years old (settled end 2009). The existence of this peak in biomass in 2011 also suggests that the area can support an higher biomass than what is found later. It is unclear to what extent the observed inter annual biomass trend is related to inter annual differences in primary production or whether intra specific competition plays a role or changes with the average body size of *Ensis directus*.

The field data collected in this project have been used in the validation of a DEB model (Schellekens & Witbaard, 2012) to see whether the use of DEB_{Ensis} for predictive purposes of the model on the effects of silt, temperature and chlorophyll is justified within the study on the effects of sand mining. It appeared that the unadjusted form of the model describes maximum growth over the years rather well, but that predicted average sizes are too high. Close inspection of the model results showed that the model is unable to describe the seasonal loss in tissue weight (loss in condition) in autumn and winter, while in the field data growth and condition show a marked seasonal cycle with minima in autumn and winter. The absence of such a decrease in the model prediction means that in the model a larger proportion of the energy uptake is used for growth while in reality that part of the energy uptake is used for recovery of internal reserves, and thus is not seen/measured as growth.

This mismatch between model and field data also might imply that in the field other factors which have not been incorporated within the DEB model, in reality modify growth rates. For instance disturbance. Freudendahl et al. (2006) showed that *Ensis directus* under threat of predation by birds, buried themselves more often and for longer periods of time, leading to a decrease in condition. Other factors causing differences between model outcomes and field data might relate to small spatial scaled differences in topography, sediment composition which can modify food supply on very local scales (Yager et al, 1993). From the results obtained in this field study, such small scaled spatial effects can however never be resolved.

To answer the question to what extent growth of *Ensis directus* is negatively influenced by high loads of suspended matter is hard to answer on basis of the field measurement presented here. The for growth important controlling variables (Temperature, SPM and Chl-a) all have strong seasonal trends which turns them into covariates of which the individual effects on shell growth or tissue growth are hard to separate and are overshadowed by the seasonal effect on all of these control variables. The valve gape data however suggest that at high SPM concentrations valves close. This has been observed for both Mytilus *edulis* and *Ensis directus*. Also the reduced clearance rate with increasing kaolinite concentrations (Kamermans & Witbaard, 2009) suggest the existence of an effect of clay particles on filtration. It is however unclear how such a behavioural response translates to shell and tissue growth as Kamermans and Dedert did not observe reduced growth at high silt concentrations in laboratory experiments. Their observation might even suggest that if high quality food is available in combination with high SPM levels, the animals are still capable to grow, despite relative high concentrations of clay particles. These observations however contradict the observations of faster shell growth of *Mytilus* higher up in the water column when compared to growth near the bottom (Witbaard unpublished, Saraiva et al, 2012) or negative effects of elevated levels of SPM on growth in *Pecten maximus* as observed by Szostek et al (2013).

Inorganic particles in the field are available as large aggregates or flocs. Such aggregates tend to scavenge organic material when moving through the water column and sinking to the bottom. This in itself already might decrease their suitability and availability as food item. Furthermore the size of the aggregates make them also useless in terms of food as most bivalve species have limited size range of particles which they can handle. Thus quality aspects of the available food particles in the field are likely to control growth as suggested by the strong positive relationships between the Ratio of Chl-a/SPM and AFDW growth or conditions change (Fig 23). Determination of the relation between valve gape and filtration or clearance rate might be the clue to give a more definite answer to that question.

5 CONCLUSIONS.

Ensis directus nowadays plays an important ecological role in the “protected” coastal zone. In this zone continuous shoreface and beach nourishments take place to protect the coast from flooding. These activities might influence growth and production of the coastal *Ensis directus* population and with that form a threat to the functioning of the entire coastal ecosystem including its role as foraging area for higher trophic levels
The research presented here is meant to give basic insight into the seasonal variability of environmental processes and how these control the ecology and growth dynamics of *Ensis directus* in this near coastal zone.
Five questions were to be answered

1. What is the natural variation in silt concentrations close to the seabed
2. What is the forcing factor of this variation (erosion, advection, season)
3. Is the valve gape of *Ensis directus* related to the silt concentration and how (linear, stepwise) if not which other factors control the gape of *Ensis*.
4. Describe the growth of Ensis *directus* in terms of DEB variables.
5. What factors correlate the best with DEB growth variables of *Ensis directus*

It was anticipated that with finding the answers on these questions the significance of the ecological effects of sand extraction and beach nourishment can be better estimated and understood.
Following the growth and development of *Ensis directus* gave insight in the seasonal timing of shell, tissue and gonadal growth for this species. The attention focussed on collecting data about the most important parameters needed for DEB (Dynamic Energy Budget) modelling. These data were used to validate the DEB model (Schellekens & Witbaard, 2012) which was constructed for this species and on basis of this validation, detailed insight in the model's behaviour and outcomes increased its applicability for the estimation of the effects of increased SPM concentrations in relation to sand extraction and beach nourishment in the future (question 4 & 5).
The research also focussed on directly measuring the valve gape of *Ensis directus*. Because of the large set of environmental data which were collected simultaneously, relationships with these control variables could be used to estimate the effects of varying levels of SPM on the behaviour. This together with lab experiments (Witbaard & Kamermans, 2011, Kamermans & Dedert, 2012) gave a further theoretical quantification of effects of increased loads of suspended matter as well as an indication a maximum concentration above which filtration is influenced (question 3).
The almost two year lasting deployment yielded a wealth of data about the near bottom processes and conditions in all kinds of weather conditions. This gives new insights in the natural variation of SPM concentrations and Chl-a concentrations close to the seabed and showed that there are strong seasonal components causing resuspension and sedimentation. On the local scale of where the measurement platform was positioned a fairly good idea of environmental forcing factors was obtained by which the man induced increases in SPM (dredging beach nourishment) can be seen in the perspective of "natural" variations (question 1 & 2).

The combined results of the environmental monitoring and the monitoring of the growth and production of the local *Ensis directus* population showed that high loads of SPM affect the valve gape of both *species* negatively. Negative relationships between total SPM and tissue growth or condition of *Ensis directus* also suggest adverse effects of high loads of SPM but with the existing dataset this effect can not be separated from the seasonal trends in both SPM and Chl-a. Therefore the Ratio of Chl-a to total amount of SPM (Ratio) was used as indication of the quality of food. This ratio also undergoes a seasonal cycle but has the advantage that it incorporates both parameters into one. Tissue growth indeed responds strongly to this parameter and an almost linear relationship was found (Figure 61d).which supports the idea that the quality of the available food is an important determinant for soft tissue growth. Quality in this context is determined by the relative amount which Chl-a contributes to total suspended matter.
The long time series of measurements on SPM off Egmond showed that waves and currents are determinants of near bottom SPM concentrations. Near bottom SPM measurements during two occasions when beach nourishments were undertaken in close proximity of the measurement platform suggests that under the then prevailing weather conditions the increase in SPM load near the bottom was relatively small when seen in comparison to the levels measured during storms in the same season or during other times of the year.

Below a bulleted list of the main conclusions on basis of the field measurements described in this report is given.

- The data show that there is a marked seasonal variation in the concentrations of Chl-a and suspended particulate matter. Peak concentrations of SPM at 30 cm above the bottom exceed 2500 mg/L during storm events. Such events have been observed to occur throughout the year.
- Chl-a peak concentrations are mainly linked to the spring phytoplanton bloom and are observed in April and May.
- The measurement of SPM at four heights above the seafloor suggests that a “blanket” of suspended material above the bottom is present. The dynamics and composition of this blanket is moderated by the seasonal variations in primary production and short term hydrodynamics under influence of wind, waves and tidal currents.
- There appears to be vertical separation in the amount and quality of material in this "blanket" at a height between 80 and 140cm illustrating that the Chl-a rich and SPM "behave" differently. This is an important factor which determines the quantity and quality of available food for the benthic filterfeeders, such as *Ensis directus*.
- Tidal and wind induced currents and waves cause resuspension and mixing of organic and inorganic light particles which causes the concentrations and quality of suspended material to vary from tidal to seasonal timescales. The measurement of SPM and Chl-a show that both particle types are only partly linked which results in a strong quality gradient in the water column up to 2 meters above the seafloor.
- Variations in the levels of suspended mud over the year show that these variations are mainly controlled by wind induced waves and currents. Increasing wave heights and increasing current speeds make minimum SPM concentration rise from less than 20 mg/l in calm weather conditions to 200 mg/l in rough conditions. About 20 % of the time concentrations close to the seafloor surpass 200 mg/l.

- Measurements taken during ongoing beach nourishments in June 6th, 2011 show that near bottom SPM concentrations double at or shortly after ships dumped their loads. The shift in concentrations on June 24th suggest that under the then prevailing calm weather conditions the suspended inorganic concentration at 30cm above the bottom were about three times higher compared to the other days in June or the rest of the year. Despite these large increases the absolute concentrations remain relatively low when compared to the change in concentrations measured during storm events later in the year. Similar effects at a height of 2 meter above the bottom are less clear.
- The fact that some of the turbidity peaks are strongly delayed in relation to waves caused by storms suggests that they are the result of lateral transport and only partly evolved from local resuspension.
- Data on the valve movements of both *Mytilus edulis* and *Ensis directus* under varying SPM concentrations suggests that maximum valve opening decreases with increasing SPM concentrations. This indicates that SPM concentrations are critical and are likely to limit feeding behaviour.
- No well-defined relationships between valve gape and salinity, temperature or currents could be detected in an analyses in which all data over the entire period were used. The observed autocorrelation lags however suggest that tidal (lunar) cycles are important.
- Significant shell growth of *Ensis directus* starts late during the year. The data suggest a minimum temperature between 12 and 14°C.
- Soft tissue growth (AFDW) and the increase in condition starts with the spring bloom peak and continues into the summer. In late summer, autumn and winter the condition of the animals rapidly decrease. The loss in condition is also evident as decrease in percentage of glycogen reserves in the tissue as well as in the total caloric content of the tissues. The short period of increasing condition parameters suggests that after the spring bloom food quality or quantity is insufficient to maintain the body condition high.
- The growth of gonads in *Ensis directus* starts long before the spring bloom and precedes tissue growth. This observation suggests that gonad development is based on the reallocation of internal energy reserves.
- The spring bloom peak is mainly used for soft tissue growth and most likely the ripening of the gonads. The main spawning of *Ensis directus* in 2011 and 2012 took place at and shortly after the spring bloom.

6 REFERENCES

Anonymous, 2002. Noordzee-atlas voor zwevend stof op basis van satellietbeelden in 2000. Rapport RIKZ/IT/2002.102: 33pp.

Alphen van, J.S.L.J. (1990) A mud balance for the Belgian-Dutch coastal waters between 1969 and 1986. Neth. J. Sea Research 25, 19-30.

Archambault M.-C, Bricelj V.M., Grant J., Anderson D.M., 2004. Effects of suspended and sedimented clays on juvenile hard clams, *Mercenaria mercenaria*, within the context of harmful algal bloom mitigation. Marine Biology 144: 553-565.

Beukema, J.J. & Dekker, R., 1995. Dynamics and growth of a recent invader of European coastal waters: the American razor clam, Ensis directus. J.Mar. Biol. Ass. UK 75, 351-362.

Cardoso J.F.M.F, Nieuwland G., Wijsman J., Witbaard R., Van der Veer H.W., 2011. Validation of a method for age determination in the razor clam *Ensis directus*, with a review on available data on growth, reproduction and physiology. NIOZ-Report 2011-9: 33 pp.

Cardoso, J.F.M.F.,H,W. van der Veer, S.A.L.M. Kooijman, 2006. Body-size scaling relationships in bivalve species: A comparison of field data with predictions by the Dynamic Energy Budget (DEB) theory. Journ. Sea Res, 56(2):125-139.

Cardoso, J.F.M.F, Witte, IJ, Veer van der, H.W., 2009. Reproductive investment of the American razor clam *Ensis americanus* in the Dutch Wadden Sea. Journal of Sea Research, 62 (4) 295–298.

Dekker, R.; Beukema, J. J. (2012). Long-term dynamics and productivity of a successful invader: The first three decades of the bivalve Ensis directus in the western Wadden Sea. Journal of Sea Research, Volume 71, p. 31-40.

Duin C.F. van Gotjé ,W., Jaspers C.J. & Kreft M., 2007. MER Winning suppletiezand Noordzee 2008 t/m 2012. Grontmij Hoofdrapport, Definitief. 13/99080995/CD, revisie D1 242 pp, Grontmij, Houten.

Ellerbroek, G., M.J.C. Rozemeijer, J.M. de Kok, J. de Ronde, 2008. Monitoring and Evaluation Programme Sand mining RWS LaMER, part B5 of the evaluation programme Sand mining. Ministerie van verkeer en waterstaat, Noord holland.

Kok,de J. M., 2004. Slibtransport langs de Nederlandse kust. Bronnen, fluxen en concentraties. Rapport RIKZ/OS/2004.148w: 31pp.

Goudswaard, P.C.; Kesteloo, J.J.; Perdon, K.J.; Jansen, J.M., 2008.
Mesheften (*Ensis directus*), halfgeknotte strandschelpen (*Spisula subtruncata*), kokkels (*Cerastoderma edule*) en otterschelpen (*Lutraria lutraria*) in de Nederlandse kustwateren in 2008. Yerseke : IMARES, (Rapport / IMARES C069/08)

Goudswaard P.C., K.J. Perdon, J.Jol, J.J. Kesteloo, C. van Zweeden & K. Troost, 2011. Schelpdieren in de Nederlandse kustwateren Bestandsopname 2011. Imares rapport c094/11 78pp.

Kamermans, P., Brummelhuis, E. & Wijsman, J., 2011. First pioneering laboratory experiments on filtration, respiration and growth of the razor clam (*Ensis directus*, Conrad) IMARES Rapport C115/11, 48pp.

Keppler, D,& K.Decker, 1970. Glykogen. Bestimmung mit amylogucosidase. In; Bergmeyer, methoden der enzymatischen analyses, Verlag chemie Weinheim.

Keppler, D,& K.Decker, 1974. Glycogen. Determination with Amylogulcosidase. In; Bergmeyer H. U., Methods of enzymatic analysis., Verlag chemie Wennheim/Berlin.

Palmer, 2004. Growth of the razor clam Ensis directus, an alien species in theWash on the east coast of England. J. Mar. Biol. Ass. U.K. (2004), 84, 1075-1076

S. Saraiva, J. van der Meer, S. A. L. M. Kooijman, R. Witbaard, C. J. M. Philippart, D. Hippler, R. Parker, 2012. Validation of a Dynamic Energy Budget (DEB) model for the blue mussel Mytilus edulis. Mar. Ecol. Prog. Ser. 463: 141–158, 2012

Schellekens, T. & R. Witbaard, 2012. DEBensis vs. data.Imares report C155/12. 30pp

Szostek, C.L., A.J. Davies & H. Hinz, 2013. Effects of elevated levels of suspended particulate matter and burial on juvenile king scallops Pecten maximus. Mar. Ecol. Prog. Ser 474:155-165.

Wilber D.H., Clarke D.G., Rees S.I., 2007. Responses of benthic macroinvertebrates to thin-layer disposal of dredged material in Mississippi Sound, USA. Marine Pollution Bulletin 54: 42-52.

Wijsman, J.W.M.,2011. Dynamic Energy Budget (DEB) parameters for *Ensis directus.* Yerseke: IMARES, (Report C116/11). 39pp.

Witbaard, R. & P. Kamermans, 2011. De bruikbaarheid van de klepstandmonitor op *Ensis directus* ten behoeve van de monitoring van aan zandwinning gerelateerde effecten.NIOZ rapport 2009-10, 44 pp

Yager, P. L., A.R.M Nowell and P.A. Jumars (1993). "Enhanced deposition to pits: a local food source for benthos. J. mar res 51: 209-236.

7 APPENDIX

7.1 Data integrity

The location where the lander platform has been deployed is a site which is about 1 km off shore at a water depth of 11 meter. Apart from human activities such as fisheries and recreation, extreme wave heights and current speeds and associated sediment scour and sedimentation might seriously impose negative effects on the integrety of the data. These problems have an stochastic character, while the problem of overgrowth by sessile organisms such as barnacles, hydrozoa and sedimentation of large amounts of SPM have a more seasonal character.
In the selection of the instruments used for this project, in combination with the tight maintenance schedule and prophylactic measures we managed to minimise the loss of data due to fouling.
The Turbidity and Fluorescence measures have been made with the wiped version of the JFE – ALEC data loggers. The wiper appeared to be a sufficient means to keep fouling under control (Figure 58)

Figure 58. Overgrown Alec Turbidity sensor. The wiped area is perfectly clean while the surrounding area is heavily over grown by barnacles.

The CTD we used is a pumped version and the pumped interior is protected from fouling by a TBT resin tablet, preventing overgrowth of fouling organisms in the flow circuit and on the sensors.
Both Nortek current meters work acoustically. The acoustic screens are protected by a veneer of udder ointment, preventing fouling, without influencing the sensitivity of the acoustic signal. The pressure sensor might however suffer from ongrowth/ingrowth of epifauna as well, resulting in a gradually change of the pressure signal.

One of the aspects which is hard to control are the physical conditions. In some periods, effects of sediment scour, high currents and waves got “grip” on the lander platform, resulting in movements and replacement. At the end of the winter period (January 11th) the lander platform had moved 150 meter to the south in relation to its deployment position.
Both the Nortek current meters, log such movements by storing “Heading”, “Tilt” and “Roll”. From these records insight into the occurrence of potential measurement errors can be obtained. Errors themselves are also given in special error and status messages stored with the data.

From these messages the times at which the data are suspect can be determined. In Figure 59 a time record with of such measurement errors, as being logged by the Vektor current meters, is given for the year 2011. The green line gives the period of the year in which fouling potentially can have had an influence on the obtained data quality. The red, vertical bars/spikes give the times/dates that the current meter data are known to be unreliable. The observed errordays in July probably deal with disturbance caused by fishing. The other spikes/bars in the record are related to bad weather. Serious bad weather started on December 7th . At that moment also a (linked?) clock error of the vektor current meter occurred, i.e. the instrument clock was not in line more with actual time. The observed time difference at the end of this measurement period is used to realign the measurements with a linear interpolation of time over the measurement bursts. A comparison between the pressure data from the ctd and the vektor current meter showed that up to December 7th time alignment was right.

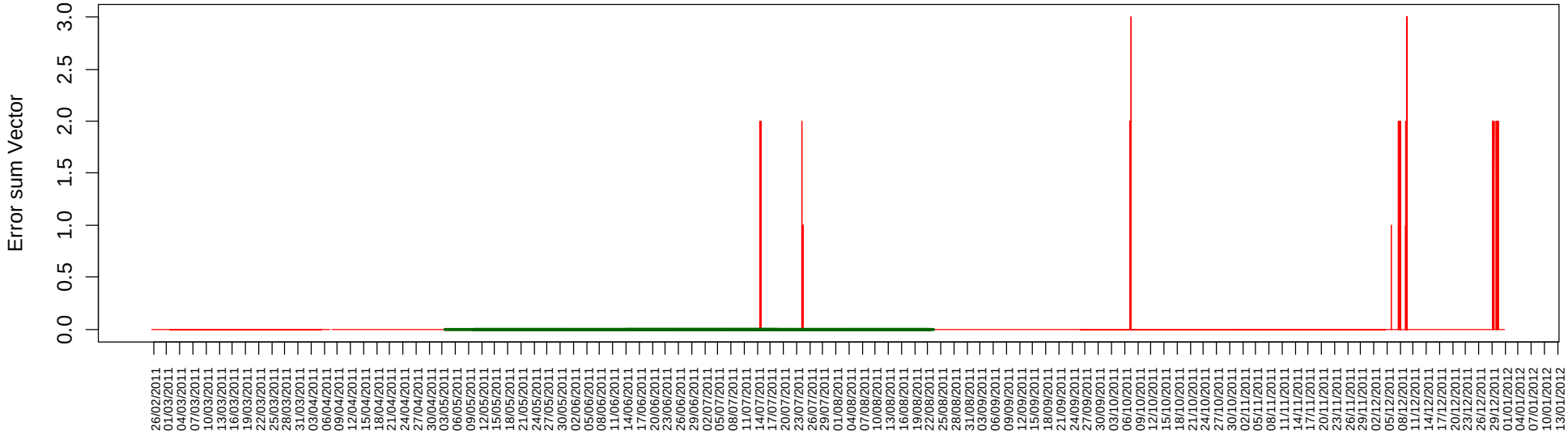

Figure 59. Fouling record of the lander and error record of the Nortek Vektor current meter. The green horizontal bar indicates the period in which significant fouling (mainly barnacles) was present. The red spikes indicate cumulative recorded measurement errors of the Vektor current meter. At the spike times, tilt, Roll and Heading changed beyond the levels that measurements were reliable. Over the 11 month measurement period there were 5 moments at which the errors indicate that the data are unreliable.

7.2 Gams Shell growth X environment

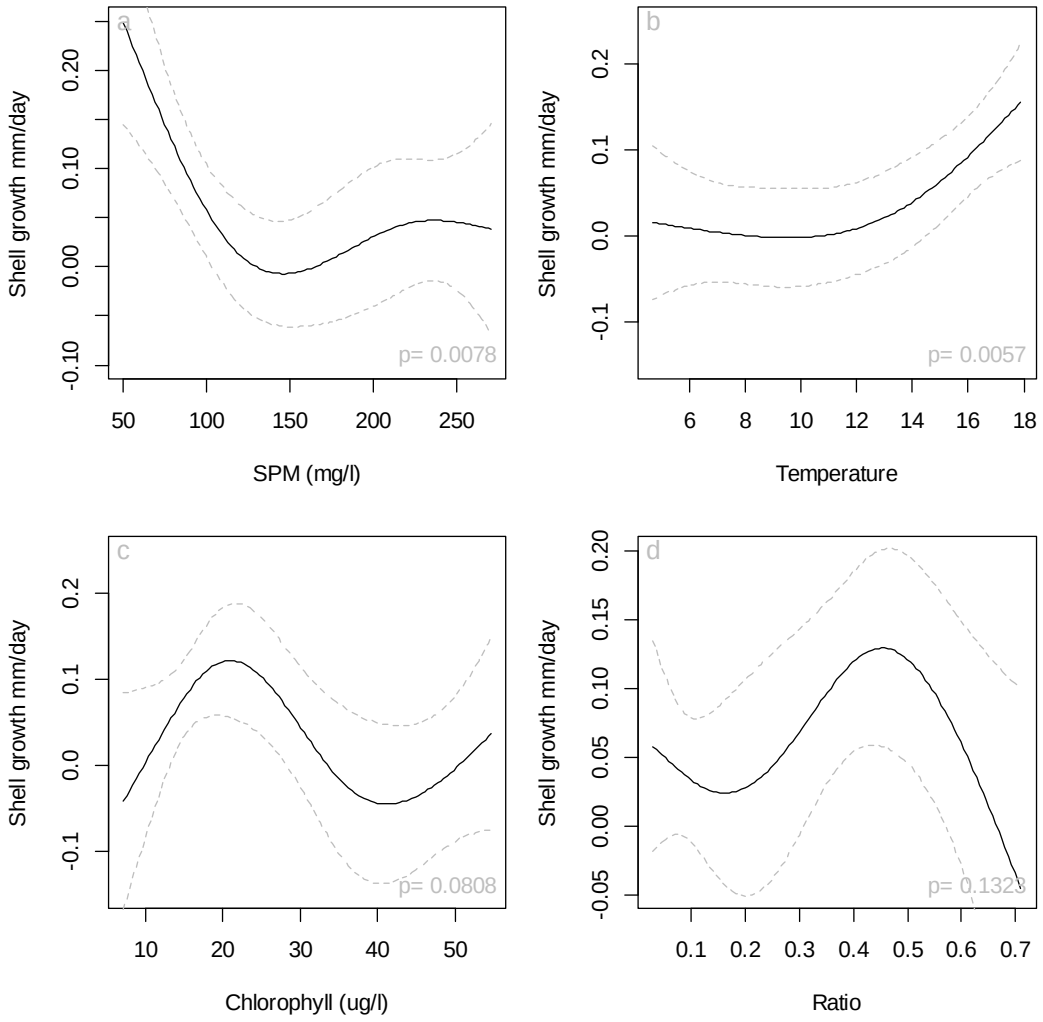

Figure 60. Gam models showing the shell growth rates being dependent of average concentrations of SPM, Chlorophyll, average Temperature and the Ratio between Chlorophyll and SPM. In the lower right corner of each graph the significance of the model fit is given

7.3 Gams AFDW X environment

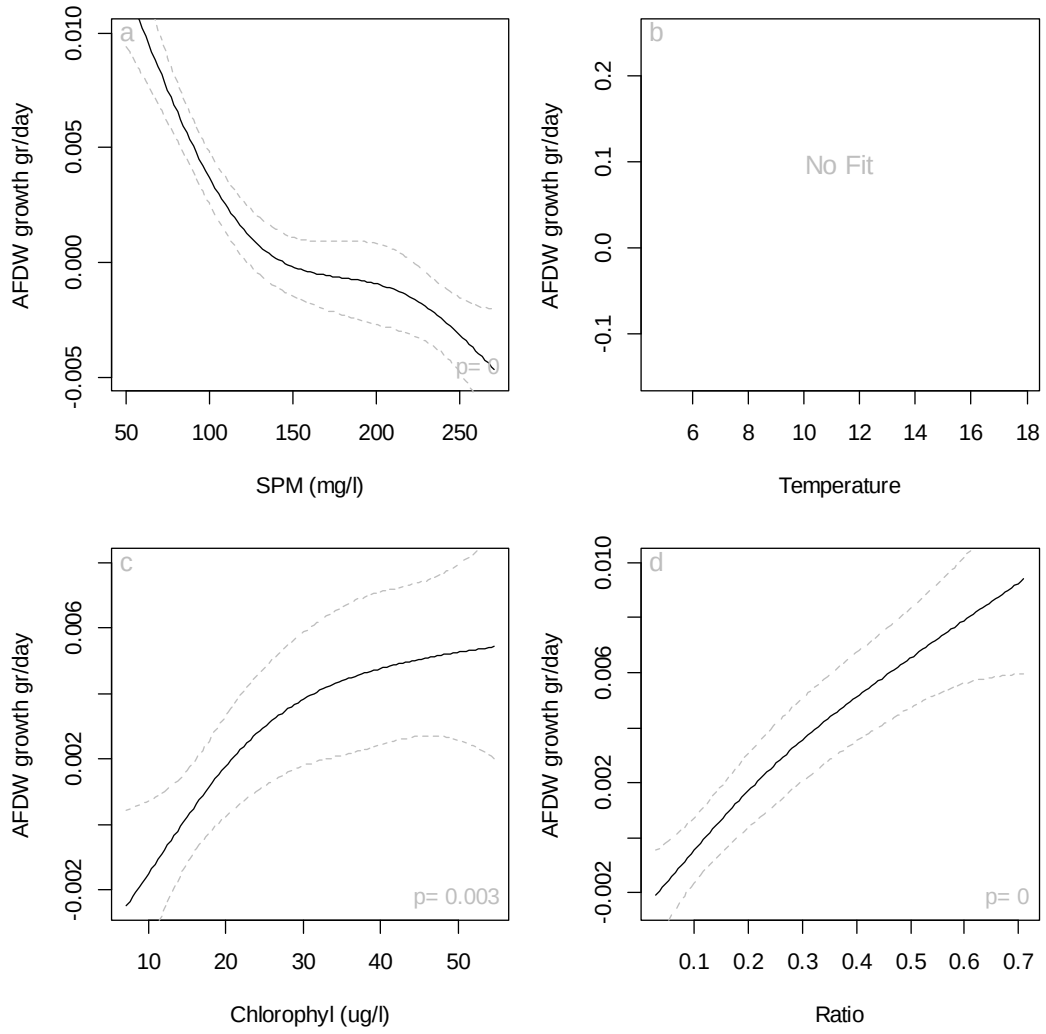

Figure 61 Gam models showing the Tissue growth rates being dependent of average concentrations of SPM, Chlorophyll, average Temperature and the Ratio between Chlorophyll and SPM. In the lower right corner of each graph the significance of the model fit is given

7.4 Gams Condition X envrironment

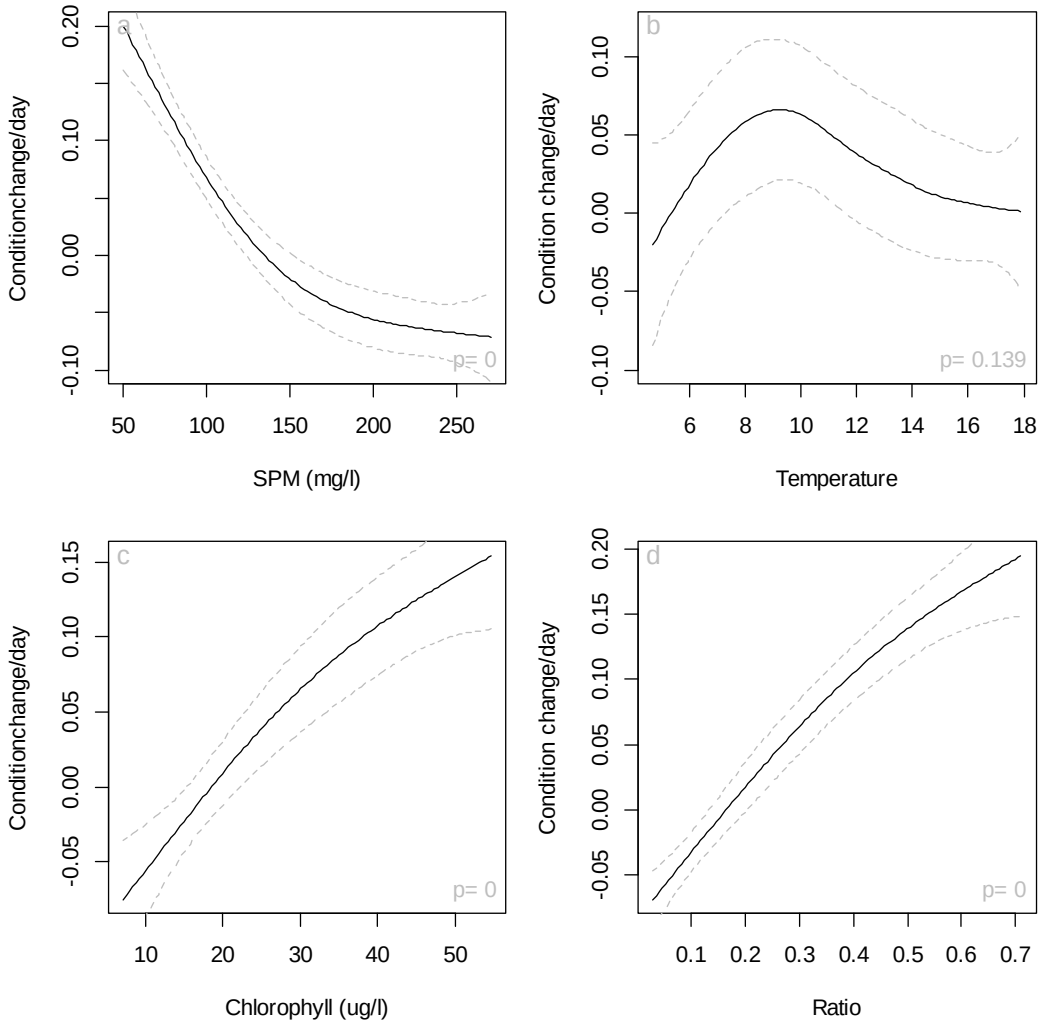

Figure 62 Gam models showing the condition index being dependent of average concentrations of SPM, Chlorophyll, average Temperature and the Ratio between Chlorophyll and SPM. In the lower right corner of each graph the significance of the model fit is given

7.5 Gams Gonad X environment

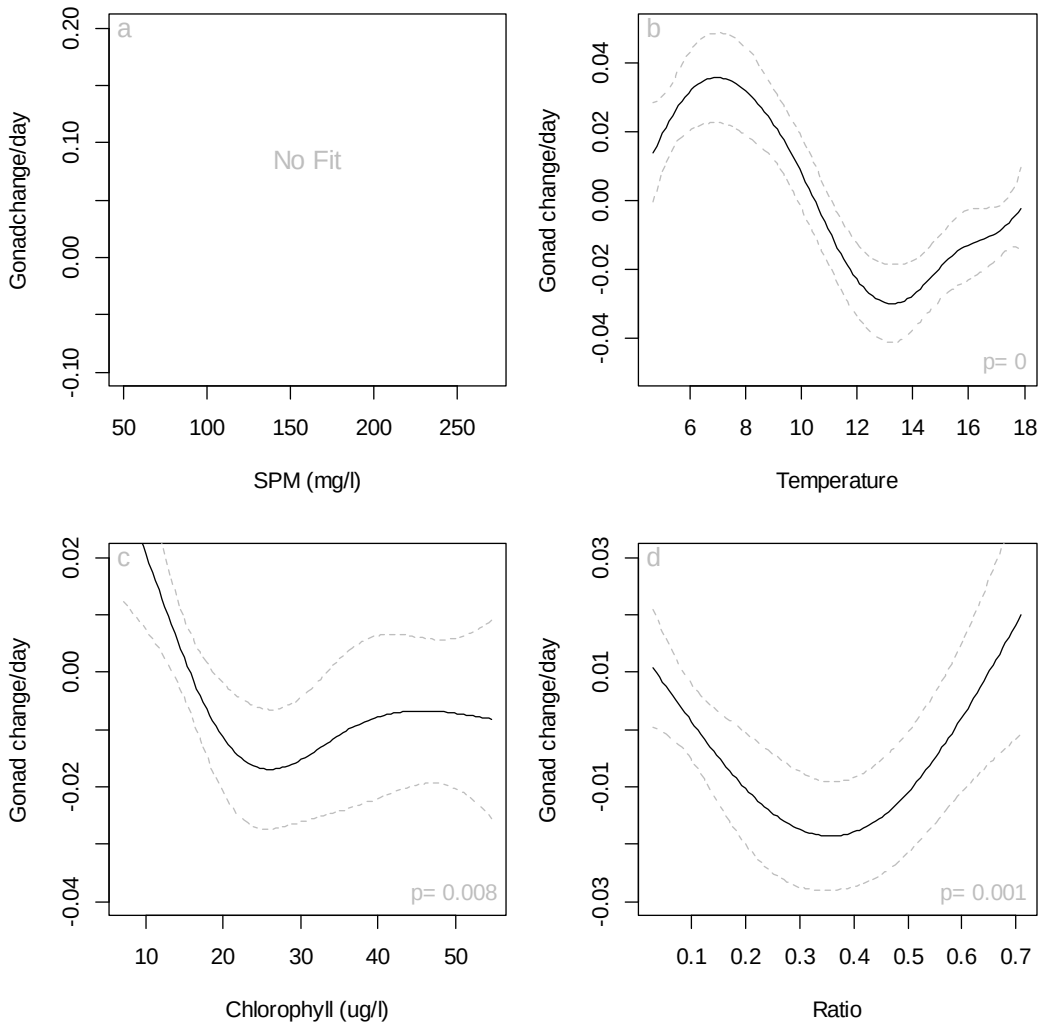

Figure 63 Gam models showing the change in the percentage of gonadal tissue being dependent of average concentrations of SPM, Chlorophyll, average Temperature and the Ratio between Chlorophyll and SPM. In the lower right corner of each graph the significance of the model fit is given